

A FUNCTIONAL IMMOBILIZATION MATRIX BASED ON A CONDUCTING  
POLYMER MODIFIED WITH PMMA/CLAY NANOCOMPOSITES AND GOLD  
NANOPARTICLES: APPLICATIONS TO AMPEROMETRIC GLUCOSE  
BIOSENSORS

A THESIS SUBMITTED TO  
THE GRADUATE SCHOOL OF NATURAL AND APPLIED SCIENCES  
OF  
MIDDLE EAST TECHNICAL UNIVERSITY

BY  
MELİS KESİK

IN PARTIAL FULFILLMENT OF THE REQUIREMENTS  
FOR  
THE DEGREE OF MASTER OF SCIENCE  
IN  
CHEMISTRY

FEBRUARY 2014



Approval of the thesis:

**A FUNCTIONAL IMMOBILIZATION MATRIX BASED ON A CONDUCTING  
POLYMER MODIFIED WITH PMMA/CLAY NANOCOMPOSITES AND  
GOLD NANOPARTICLES: APPLICATIONS TO AMPEROMETRIC  
GLUCOSE BIOSENSORS**

submitted by **MELİS KESİK** in partial fulfillment of the requirements for the degree  
of **Master of Science in Chemistry Department, Middle East Technical University**  
by,

Prof. Dr. Canan Özgen  
Dean, Graduate School of **Natural and Applied Sciences**

---

Prof. Dr. İlker Özkan  
Head of Department, **Chemistry**

---

Prof. Dr. Levent Toppare  
Supervisor, **Chemistry Dept., METU**

---

**Examining Committee Members:**

Prof. Dr. Suna Timur  
Biochemistry Dept., Ege University

---

Prof. Dr. Levent Toppare  
Chemistry Dept., METU

---

Assoc. Prof. Dr. Ali Çırpan  
Chemistry Dept., METU

---

Assist. Prof. Dr. Emren Nalbant Esentürk  
Chemistry Dept., METU

---

Dr. Senem Kırpalp Kayahan  
Yalçiner Patent ve Danışmanlık Ltd. Şti.

---

**Date:**

05.02.2014

**I hereby declare that all information in this document has been obtained and presented in accordance with academic rules and ethical conduct. I also declare that, as required by these rules and conduct, I have fully cited and referenced all material and results that are not original to this work.**

Name, Last name: Melis KESİK

Signature

## **ABSTRACT**

### **A FUNCTIONAL IMMOBILIZATION MATRIX BASED ON A CONDUCTING POLYMER MODIFIED WITH PMMA/CLAY NANOCOMPOSITES AND GOLD NANOPARTICLES: APPLICATIONS TO AMPEROMETRIC GLUCOSE BIOSENSORS**

Kesik, Melis

M. Sc., Department of Chemistry

Supervisor: Prof. Dr. Levent Toppare

February 2014, 97 pages

Designing biosensors for detection of target species in any test solution has attracted keen interest throughout the world. Over the conventional methods biosensors have several advantages which are specific, rapid, and simple to operate, and ease of fabrication with minimal sample pretreatment involved. However, reproducibility and stability are still major drawbacks. To overcome these problems, a suitable immobilization method must be chosen. Conducting polymers serve excellent immobilization platform for biomolecule depositions owing to their biocompatibility, ease of preparation and ability to modify structural properties. Besides, combination of conducting polymers and nanostructures attracted considerable attention in biosensing applications. Modification of the electrode surface with nanostructures leads to increase rate of electron transfer between biomolecules and support material. By this way, effective and stable biosensor design is achieved. In this thesis, a functional polymer,

poly(6-(4,7-bis(2,3-dihydrothieno[3,4-b][1,4]dioxin-5-yl)-2H-benzo[d][1,2,3]triazol-2-yl)hexan-1-amine) poly(BEDOA-6), was utilized as an immobilization matrix for glucose oxidase biosensor construction. Moreover, conducting polymer surface was modified with PMMA/clay nanocomposite material and modified gold nanoparticles to develop two different glucose biosensors. After successful electrochemical deposition of the polymer; poly(BEDOA-6) on the graphite electrode, immobilization of glucose oxidase was carried out. During immobilization, nanostructures were used in biosensor fabrication to achieve the most effective surface design for target biosensors. By applying constant potential, consumption of oxygen concentration in bulk solution was followed using amperometric technique. Surface features of the biosensors were characterized using several techniques like SEM, XPS, TEM, Fluorescence Microscopy. The designed biosensors showed wide linear ranges with low detection limits. Also, kinetic parameters, operational and storage stabilities were determined. Finally, the biosensors were tested on real samples.

**Keywords:** Conducting Polymers, Glucose biosensors, Enzyme Based Amperometric Biosensors, Gold Nanoparticles, Clay Nanocomposites, Glucose Oxidase.

## ÖZ

# PMMA / KİL NANOKOMPOZİTLER VE ALTIN NANOPARTİKÜLLER İLE MODİFİYE EDİLEN İLETKEN POLİMER BAZLI FONKSİYONEL İMMOBİLİZASYON MATRİSLER: AMPEROMETRİK GLUKOZ BIYOSENSÖR UYGULAMALARI

Kesik, Melis

Yüksek Lisans, Kimya Bölümü

Tez Yöneticisi: Prof. Dr. Levent Toppare

Şubat 2014, 97 sayfa

Herhangi bir test solüsyonunda hedef analit tayininde biyosensör dizaynı tüm dünya tarafından oldukça ilgi çekmektedir. Geleneksel yöntemlere göre, biyosensörlerin kendine özgü, hızlı ve kolay çalışma ve en az örnek hazırlama işlemi ile kolay üretilebilme gibi birçok avantajı vardır. Fakat tekrarlanabilirlikleri ve kararlılıkları hala önemli sorunlardır. Bu sorunları çözmek için, uygun immobilizasyon metodu seçilmelidir. İletken polimerlerin biyoyuumlulukları, kolay hazırlanmaları ve modifiye edilebilir yapısal özellikleri sayesinde biyomoleküller için uygun immobilizasyon platformu olarak hizmet verirler. Bunun yanı sıra, iletken polimerlerin nanoyapılarla birlikte biyosensör uygulamalarında kullanımı hayli ilgi çekmektedir. Elektrot yüzeyini nanoyapılarla modifiye etmek biyomolekül ile destek malzemesi arasındaki elektron transfer hızının artmasına sebep olmaktadır. Bu sayede, etkili ve kararlı biyosensör dizaynı elde edilmektedir. Bu tezde, sentezlenmiş fonksiyonel bir polimer olan poly(6-(4,7-bis(2,3-dihidrotiyeno[3,4-b][1,4]dioksin-5-il)-2H-benzo[d][1,2,3]triazol-2-

il)hekzan-1-amin) (poly(BEDOA-6) glikoz oksidaz enzimi immobilizasyonunda immobilizasyon matrisi olarak kullanılmıştır. Ayrıca, iki farklı glikoz biyosensörü geliştirmek için, iletken polimer yüzeyi PMMA/kil nanokompozit ve modifiye edilmiş altın nanopartikül ile modifiye edilmiştir. Polimerin grafit elektrot yüzeyinde başarılı bir şekilde biriktirilmesinden sonra, glikoz oksidaz enziminin immobilizasyonu yapılmıştır. Bu immobilizasyon hedeflenen biyosensörler için en etkili yüzey dizaynını elde etmek için nanoyapılar kullanılmıştır. Sabit uygulanan potansiyel altında, çözeltideki oksijen konsantrasyonu tüketimi amperometrik teknik kullanılarak izlenmiştir. SEM, XPS, TEM ve Floresans mikroskop gibi bazı teknikler kullanılarak yüzey özellikleri karakterize edilmiştir. Dizayn edilen bu biyosensörler düşük saptama sınırı olan geniş lineer aralıklar göstermektedir. İlâveten, biyosensörlerin çeşitli kinetik parametreleri, operasyonel ve depo kararlılıkları tayin edilmiştir. Son olarak, hazırlanan bu biyosensörler farklı numunelerde test edilmiştir.

**Anahtar kelimeler:** İletken Polimerler, Glukoz Biyosensörleri, Enzim Esaslı Amperometrik Biyosensörler, Altın Nanoparçacıklar, Kil Nanokompozitleri, Glikoz Oksidaz.

**To my precious family....**

## ACKNOWLEDGMENTS

I would like to express my appreciation to my supervisor Prof. Dr. Levent Toppare for his guidance, support, encouragement, patience, valuable advices. Words cannot express my gratitude. It is feeling beyond words that I know he always support me during my whole life.

I would like to express my sincere thanks Prof. Dr. Suna Timur for her valuable discussions, endless support and help throughout this study.

I would like to express my thanks Assoc. Prof. Yasemin Arslan Udum for her assistance, endless help and patience for my countless phone calls.

I would like to express my appreciation to Assist. Prof. Dr. Emren Nalbant Esentürk for her valuable collaboration, partnership and providing me deep knowledge about Inorganic chemistry.

I would like to give my special thanks Assoc. Prof. Dr. Ali Çırpan for the nice working environment and his moral support. I will always be a playmate for cute baby Melis.

I wish to thank all the past and present members of Toppare and Çırpan Research Group for the nice working environment and their friendship.

I would like to express my appreciation to Fulya Ekiz Kanık for everything throughout my thesis study. I appreciate for her extraordinary support, endless help, motivation and her kind friendship.

I owe great thanks Gönül Hızalan Özsoy for teaching me organic synthesis with every details, kind friendship and endless help whenever I need her.

I would like to give my special thanks Seza Göker, Merve İleri, Sinem Toksabay and Saniye Söylemez for their endless support, real friendship, providing me excellent

working environment and spending time with me during my experiments until middle of the night. They make these years unforgettable for me.

I would like to express my deepest sense of gratitude to Nehir Utku, Bke Mihı, Esra gn, Esra zdemir for their real friendship, support and motivation. For 7 years, they are always with me whenever I feel blue or happy. I am one of the luckiest person in the World for being their friend.

I would like to thank Hande nay, Ozan Erlik, Emre Ataođlu, Ebru Iık, Janset Turan for their frienship, moral support and encouragement. I am deeply sorry not meeting with them before.

I would like to thank Berfu Esen for being a second sister to me and always being there for me, her true friendship. Since 2003, she believes in me and makes me feel happy.

I would like to thank Aye Gndođdu, Burhan Őentrk, Burak etinkaya, Orun Elitez and ilem iek for their frienship, spending wonderful time with me. The memories which they are involved always make me happy.

I would like to express my gratitude to Ali Mancar for his great love, continuous support, understanding and encouraging me. I could not achieve anything without his love and trust. I appreciate for every moment that we spend together.

I would like to express my special thanks and appreciation to my family for believing in me and giving me endless support. I am the luckiest person in the world being their daughter and sister. I would not be possible to achieve anything throughout my all life without them.

## TABLE OF CONTENTS

ABSTRACT.....	v
ÖZ .....	vii
ACKNOWLEDGMENTS.....	x
TABLE OF CONTENTS .....	xii
LIST OF TABLES .....	xvi
LIST OF FIGURES.....	xvii
LIST OF ABBREVIATIONS .....	xxi
CHAPTERS .....	1
1. INTRODUCTION .....	1
1.1. Conducting Polymers .....	1
1.1.1. History of Conducting Polymers.....	1
1.1.2. Theory of Conducting Polymers .....	3
1.1.3. Syntheses of Conducting Polymers.....	7
1.1.3.1. Chemical Polymerization .....	7
1.1.3.2. Electrochemical Polymerization.....	8
1.1.4. Applications of Conducting Polymers .....	11
1.2. Biosensors.....	11
1.2.1. Electrochemical Biosensors .....	13
1.2.1.1. Conductometric Biosensors.....	13
1.2.1.2. Potentiometric Biosensors .....	14
1.2.1.3. Amperometric Biosensors .....	14
1.2.2. Immobilization Techniques.....	17
1.2.2.1. Physical Adsorption.....	19
1.2.2.2. Entrapment .....	20
1.2.2.3. Covalent Bonding.....	21

1.2.2.4.	Intermolecular Crosslinking .....	22
1.2.3.	Applications of Biosensors .....	23
1.2.4.	Glucose Biosensors .....	25
1.2.5.	Conducting Polymers in Biosensing Design .....	26
1.2.6.	Nanostructures in Biosensing Design .....	28
2.	EXPERIMENTAL .....	33
2.1.	Materials .....	33
2.2.	Instrumentations .....	34
2.2.1.	Electrochemical measurements .....	34
2.2.2.	Characterization studies .....	34
2.2.2.1.	Nuclear Magnetic Resonance Spectrometer (NMR) .....	34
2.2.2.2.	High Resolution Mass Spectrometer (HRMS) .....	34
2.2.2.3.	Scanning electron microscope (SEM) .....	35
2.2.2.4.	Fluorescence microscope .....	35
2.2.2.5.	Transmission electron microscope (TEM) .....	35
2.2.2.6.	X-ray photoelectron spectroscope (XPS) .....	35
2.2.2.7.	UV-vis-NIR spectrophotometer .....	36
2.2.2.8.	Fourier Transform Infrared Spectrophotometry (FTIR) .....	36
2.3.	Synthesis of the Monomer .....	36
2.4.	Electrochemical Polymerization of the Monomer .....	38
2.5.	Construction of Biosensors .....	39
2.5.1.	PMMA/laponite nanocomposite/ poly(BEDO A-6)/GOx Biosensor .....	39
2.5.2.	Au NPs/MPA/ poly(BEDO A-6)/GOx Biosensor .....	40
2.6.	Amperometric Measurements .....	41
2.7.	Effect of nanostructure addition on biosensor responses .....	43
2.7.1.	PMMA/laponite nanocomposite/ poly(BEDO A-6)/GOx Biosensor .....	43
2.7.2.	Au NPs/MPA/ poly(BEDO A-6)/GOx Biosensor .....	43
2.8.	Optimization of Biosensor Performance .....	43
2.8.1.	Optimization of Conducting Polymer Thickness .....	43
2.8.2.	Optimization of Enzyme Amount .....	44

2.8.3.	Effect of pH.....	44
2.8.4.	Optimization of Nanostructures Amounts .....	44
2.9.	Analytical characterization of Biosensors .....	45
2.10.	Sample Application.....	46
2.10.1.	PMMA/laponite nanocomposite/ poly(BEDOA-6)/GOx Biosensor .....	46
2.10.2.	Au NPs/MPA/ poly(BEDOA-6)/GOx Biosensor.....	46
3.	RESULTS AND DISCUSSION.....	49
3.1.	Electrochemical Studies .....	49
3.1.1.	Electrochemical Polymerization of the Monomer .....	49
3.1.2.	Electrochemical Behavior of the Conducting Polymer.....	50
3.2.	PMMA/laponite nanocomposite/ poly(BEDOA-6)/GOx Biosensor.....	52
3.2.1.	Investigation of biosensor construction method .....	52
3.2.2.	Effect of PMMA/Laponite Nanocomposite dispersion for biosensor construction.....	53
3.2.3.	Effect of PMMA/Laponite Nanocomposite Introduction .....	54
3.2.4.	Optimization of Biosensor Performance .....	55
3.2.4.1.	Optimization of Conducting Polymer Thickness .....	55
3.2.4.2.	Optimization of enzyme amount .....	57
3.2.4.3.	Optimization of crosslinker (glutaraldehyde) amount.....	58
3.2.4.4.	Optimization of pH.....	59
3.2.4.5.	Optimization of nanocomposite amounts .....	60
3.2.5.	Surface Characterization of the biosensor design .....	61
3.2.5.1.	X-ray photoelectron spectroscopy (XPS).....	61
3.2.5.2.	Scanning electron microscope (SEM) .....	62
3.2.6.	Analytical characterization of the proposed biosensor .....	63
3.2.7.	Sample Application .....	66
3.3.	Au NPs/MPA/ poly(BEDOA-6)/GOx Biosensor .....	67
3.3.1.	Characterization of Modified Gold Nanoparticles .....	67
3.3.2.	Effect of Au NPs/MPA in Biosensor Fabrication .....	70
3.3.3.	Optimization Studies .....	72

3.3.3.1.	Optimization of Conducting polymer thickness.....	72
3.3.3.2.	Optimization of enzyme amount .....	73
3.3.3.3.	Optimization of Au NPs/MPA amount .....	75
3.3.4.	Characterizations of the proposed biosensor .....	76
3.3.4.1.	Fourier Transform Infrared Spectrophotometry (FTIR) .....	76
3.3.4.2.	Scanning electron microscope (SEM).....	77
3.3.4.3.	Fluorescence microscopy .....	79
3.3.5.	Analytical characterization of Biosensors.....	80
3.3.6.	Sample Application.....	82
4.	CONCLUSION .....	85
	REFERENCES .....	89

## LIST OF TABLES

### TABLES

Table 1.1. Immobilization procedures. ....	18
Table 1.2. Applications of biosensors .....	24
Table 3.1. Analytical characteristics of the biosensors. ....	65
Table 3.2. Glucose analyses in the serum samples. ....	66
Table 3.3. Results of glucose analyses in beverages.....	83

## LIST OF FIGURES

### FIGURES

Figure 1.1. Common conjugating polymer structures .....	3
Figure 1.2. Band structure for an insulator, a semiconductor and a metal. ....	5
Figure 1.3. Structural representation of bipolaron formation in polypyrrole and its corresponding energy bands in the mid gap .....	6
Figure 1.4. Synthetic routes of polyheterocycles for chemical polymerization.....	7
Figure 1.5. Proposed mechanism of the electropolymerization of pyrrole.....	10
Figure 1.6. Simple representation of a biosensor.....	12
Figure 1.7. Schematic representation of three generations of amperometric biosensors	17
Figure 1.8. Schematic representation of physical adsorption method. ....	20
Figure 1.9. Schematic representation of entrapment method.....	21
Figure 1.10. Schematic representation of (a) covalent immobilization method. ....	22
Figure 1.11. Schematic representation of intermolecular crosslinking immobilization method.....	23
Figure 1.12. Representation of Reaction mechanism of glucose oxidase.....	26
Figure 1.13. Representation of clay and polymer/clay nanocomposite. ....	30
Figure 1.14. Representation of self-assembled gold nanoparticles functionalized with MPA.....	31
Figure 2.1. Synthetic route to BEDOA-6.....	38
Figure 2.2. Schematic representation of PMMA/laponite nanocomposite/poly(BEDOA- 6)/GOx Biosensor .....	40
Figure 2.3. Schematic representation of Au NPs/MPA/ poly(BEDOA-6)/GOx biosensor .....	41
Figure 2.4. Representation of amperometric measurement procedure .....	42

Figure 3.1. Repeated potential scan electropolymerization of monomer at 100 mV/s vs. Ag reference electrode in 0.1 M TBAPF <sub>6</sub> /DCM.....	50
Figure 3.2. Scan rate dependence of poly(BEDOA-6) film in 0.1 M TBAPF <sub>6</sub> /DCM solvent/electrolyte system at 100, 200, 300 and 400 mV/s.....	51
Figure 3.3. Chronoamperometry experiment for poly(BEDOA-6) on the electrode in 0.1 TBAPF <sub>6</sub> /DCM while switching between neutral and oxidized states. Each interval on the x axis stands for 5 s. ....	52
Figure 3.4. Effect of different preparation technique on biosensor response .....	53
Figure 3.5. Effect of clay dispersion in water and dichloromethane on biosensor response.....	54
Figure 3.6. Effect of nanocomposite addition on poly(BEDOA-6)/GOx biosensor (in 50 mM NaOAc buffer solution, pH 5.5, 25 °C, -0.7 V). Error bars show the standard deviation (SD) of three measurements. ....	55
Figure 3.7. The effect of the polymer film thickness on biosensor response (in 50 mM NaOAc buffer solution, pH 5.5, 25 °C, -0.7 V, 0.45 mM glucose). Error bars show the standard deviation (SD) of three measurements .....	56
Figure 3.8. The effect of enzyme amount (in 50 mM NaOAc buffer solution, pH 5.5, 25 °C, -0.7 V, 0.45 mM glucose). Error bars show the standard deviation (SD) of three measurements. ....	57
Figure 3.9. The effect of crosslinker amount (in 50 mM NaOAc buffer solution, pH 5.5, 25 °C, -0.7 V, 0.45 mM glucose). Error bars show the standard deviation (SD) of three measurements. ....	58
Figure 3.10. The effect of pH (in 50 mM NaOAc buffer solution, 25 °C, -0.7 V, 0.45 mM glucose). Error bars show the standard deviation (SD) of three measurements.....	59
Figure 3.11. The effect of clay dispersion in 5 mL water (in 50 mM NaOAc buffer solution, pH 5.5, 25 °C, -0.7 V, 0.45 mM glucose). Error bars show the standard deviation (SD) of three measurements. ....	60
Figure 3.12. C1s and N1s XPS spectra of the polymer deposited surface (A and C) and protein immobilized onto the polymer deposited surface (B and D). ....	62

Figure 3.13. SEM images of polymer (a) before and (b) after biomolecule and nanocomposite immobilization under optimized conditions. ....	63
Figure 3.14. Calibration curve for glucose (in 50 mM NaOAc buffer solution, pH 5.5, 25 °C, -0.7 V). (A typical amperometric signal of the biosensor for 0.2 mM glucose and linear range as inset.) Error bars show the standard deviation (SD) of three measurements.....	64
Figure 3.15. UV-vis spectra of Au NPs and Au NPs/MPA solutions prepared in different concentrations of MPA.....	68
Figure 3.16. UV-vis spectra of Au NPs and Au NPs/MPA solutions prepared by different modification procedures.....	69
Figure 3.17. A) UV-vis spectra of Au NPs and Au NPs/MPA; B) TEM images of (a) Au NPs and (b) Au NPs/MPA. ....	70
Figure 3.18. The effect of surface modification on performance of glucose biosensors (in 50 mM NaOAc buffer solution, pH 5.5, 25 °C, -0.7 V). Error bars show the standard deviation (SD) of three measurements.....	72
Figure 3.19. The effect of polymer film thickness on biosensor response (in pH 5.5 NaOAc, 50 mM, 25 °C, -0.7 V). Error bars show the standard deviation (SD) of three measurements.....	73
Figure 3.20. The effect of enzyme amount (in 50 mM NaOAc, 25 °C, -0.7 V). Error bars show the standard deviation (SD) of three measurements. ....	74
Figure 3.21. The effect of pH (in 50 mM NaOAc, 25 °C, -0.7 V). Error bars show the standard deviation (SD) of three measurements. ....	75
Figure 3.22. FTIR spectra of poly(BEDO A-6) and poly(BEDO A-6)/Au NPs/MPA....	77
Figure 3.23. SEM images of (A) poly(BEDO A-6), (B) poly(BEDO A-6)/GOx, (C) poly(BEDO A-6)/Au NPs/MPA and (D) poly(BEDO A-6)/Au NPs/MPA/GOx under optimized conditions.....	79
Figure 3.24. Fluorescence images of poly(BEDO A-6) (A) before and (B) after Au NPs/MPA/GOx immobilization under optimized conditions on ITO glass (with 63x magnification). ....	80

Figure 3.25. Calibration curve for glucose (in 50 mM NaOAc buffer solution, pH 5.5, 25 °C, -0.7 V). Error bars show the standard deviation (SD) of three measurements.... 81

## LIST OF ABBREVIATIONS

<b>ACN</b>	Acetonitrile
<b>Ag</b>	Silver
<b>Au NPs</b>	Gold Nanoparticles
<b>Au NPs/MPA</b>	3-mercaptopropionic acid Modified Gold Nanoparticles
<b>BEDO-6</b>	6-(4,7-bis(2,3-dihydrothieno[3,4- <i>b</i> ][1,4]dioxin-5-yl)-2 <i>H</i> -benzo[ <i>d</i> ][1,2,3]triazol-2-yl)hexan-1-amine
<b>BSA</b>	Bovine Serum Albumin
<b>CB</b>	Conduction Band
<b>CE</b>	Counter Electrode
<b>CP</b>	Conducting Polymer
<b>CV</b>	Cyclic Voltammetry
<b>Cyst</b>	Cysteamine
<b>DCM</b>	Dichloromethane
<b>DMF</b>	Dimethylformamide
<b>E<sub>g</sub></b>	Band gap
<b>EDOT</b>	3,4-Ethylenedioxythiophene
<b>EDC</b>	N-(3-dimethylaminopropyl)-N'-ethylcarbodiimide hydrochloride
<b>FAD</b>	Flavin Adenine Dinucleotide
<b>FTIR</b>	Fourier Transform Infrared Spectrophotometry
<b>GA</b>	Glutaraldehyde
<b>GOx</b>	Glucose Oxidase
<b>HRMS</b>	High Resolution Mass Spectrometer
<b>HOMO</b>	Highest Occupied Molecular Orbital
<b>ITO</b>	Indium Tin Oxide
<b>LOD</b>	Limit of Detection
<b>MPA</b>	3-Mercaptopropionic acid
<b>NHS</b>	N-Hydroxysuccinimide
<b>NMR</b>	Nuclear Magnetic Resonance Spectrometer
<b>NaOAc</b>	Sodium acetate
<b>NP</b>	Nanoparticle
<b>Pt</b>	Platinum
<b>PMMA</b>	Poly(methyl methacrylate)
<b>RSD</b>	Relative Standard Deviation
<b>SAM</b>	Self-assembled Monolayers

<b>(SN)<sub>x</sub></b>	Poly(sulfurnitride)
<b>SEM</b>	Scanning Electron Microscope
<b>XPS</b>	X-ray Photoelectron Spectroscopy
<b>SD</b>	Standard Deviation
<b>TBAPF<sub>6</sub></b>	Tetrabutylammonium hexafluorophosphate
<b>TEM</b>	Transmission Electron Microscope
<b>THF</b>	Tetrahydrofuran
<b>TLC</b>	Thin Layer Chromatography
<b>PAn</b>	Polyacetylene
<b>PANI</b>	Polyaniline
<b>PAc</b>	Polyacetylene
<b>VB</b>	Valence Band

# CHAPTER 1

## INTRODUCTION

### 1.1. Conducting Polymers

#### 1.1.1. History of Conducting Polymers

One of the oldest known conductive polymer is polyaniline (PAn), known as “aniline black”. A film on an electrode surface was produced by oxidation of aniline in the presence of sulfuric acid by Letheby in 1862, obtained a partly conductive material [1]. The first polymerization of acetylene was achieved by Natta in 1958 using coordination catalyst system to form polyacetylene (PAC), possessing semiconductor properties [2]. However, the molecule did not attract interest at that time since it was produced as an insoluble and infusible powder. Shirakawa and coworkers in 1967 carried out the synthesis of polyacetylene using tremendous amount of Ziegler-Natta catalyst unwittingly which cause to be produced a thin silvery semiconductor film. The conductivity of the polymer was changed drastically upon addition of halogens. Thus, scientists realized that an insulator polymer can be converted to a semiconductor and a metallic form changing the dopant concentration. After the discovery of poly(sulfurnitride)  $(SN)_x$  in the early 1970s, the concept of conductivity of conjugated polymer was aroused because the synthesized polymeric inorganic material,  $(SN)_x$ , revealed an increase in conductivity upon treating with bromine [3].

A new era was begun at the end of 1970s with the investigation of highly conductive poly(acetylene) in its doped state, exhibiting metallic electrical conductivity [4]. Alan MacDiarmid, Alan Heeger and Hideki Shirakawa were awarded with the Nobel Prize in Chemistry in 2000 [5]. The groundbreaking discovery was demonstrated new application areas, taking advantages of known characteristic properties of polymers. In other words, these three scientists opened up the field of “plastic electronics”. A polymer plastic has single and double bonds alternating along the polymer chain. The electrons on the polymer backbone cannot carry electric current since they remain localized. However, when the material is doped with strong electron acceptors, electrons move freely and the polymer plastics become conductive as almost a metal. In this case, conductivity of polyacetylene increased by a factor of  $10^{11}$  times.

Although polyacetylene shows high electrical conductivity, it is air sensitive. Thus, new conducting polymers (CPs) were designed and synthesized over the past decades in order to obtain better properties. In 1980s, polyheterocyclic structures were started to develop. These polymers have attracted much more interest over the past two decades due to their electron rich character, providing easy oxidation process and possible structural modifications. Moreover, polyheterocycles are stable in air. Although none demonstrate better electrical conductivity than polyacetylene, heterocyclic polymers were more processable and allow more diversity in structures. Hence, conducting polymers have attracted keen interest because of possible uses as supporting material in modern science. Figure 1.1 illustrates common conjugating polymer structures.

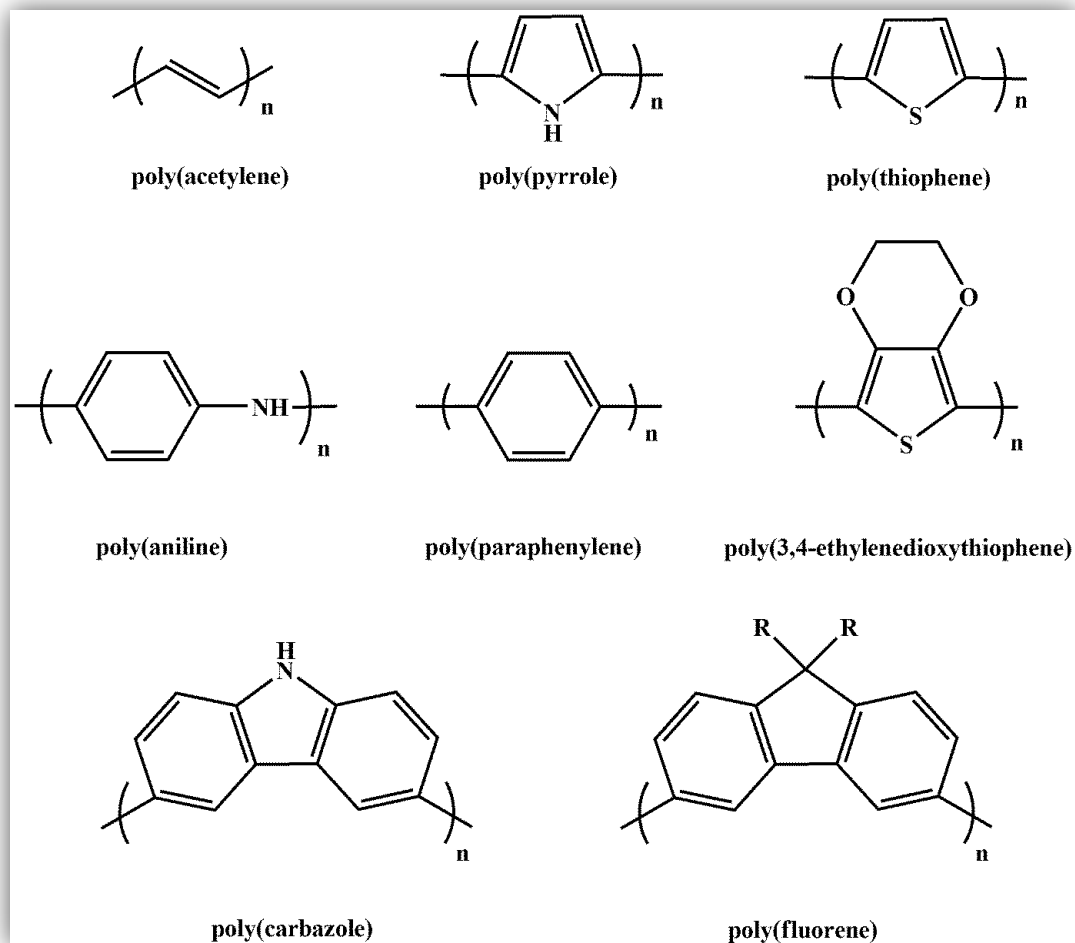


Figure 1.1. Common conjugating polymer structures

### 1.1.2. Theory of Conducting Polymers

Conductive polymers exhibit superior electrochemical properties due to the presence of conjugated  $\pi$  electrons along the polymer chain. Alternating single and double bonds result in conjugation, providing charge mobility. Each bond involves  $sp$ - or  $sp^2$ -hybridized atoms in the backbone. High degree of overlapping molecular orbitals permits delocalization of electrons, providing free movement of electrons. However, conjugation does not make the material conductive alone. The electrical conductivity

results from the presence of dopant stimulated charge carriers which allow transmitting electrical current along the conjugated polymer backbone [6].

The band theory explains the electronic structure and conduction mechanism of materials. According to this theory, orbitals are overlapped forming delocalized energy bands. The conductivity of a material is designated by the relative population of each band and energy difference between the bands. Materials are commonly classified as insulators, semiconductors and metals according to their relative separation in occupied and unoccupied energy states. Energy diagram of the classified materials are shown in Figure 1.2. The highest occupied molecular orbital (HOMO) is called the valence band (VB); the lowest unoccupied molecular orbital is called as the conduction band (CB). Energy difference between valence and conduction bands is known as the band gap ( $E_g$ ) which determines the motion of electrons. The band gap of an insulator is too large to transfer electrons between two bands which the energy difference is bigger than 3 eV. Furthermore, there is no energy gap in a metal, resulting in the flow of electrons through the material, thus high conductivity. A semiconductor material has a narrow band gap ranging from 0.5 to 3 eV with a filled valence band and an empty conduction band [7]. Conductivity of semiconductors can be increased following the doping procedure with charge carriers. It can be carried out with either holes or electrons. p-type doping is performed creating holes by taking electrons from valence band; whereas n-type doping cause adding electron to conductance band [8].

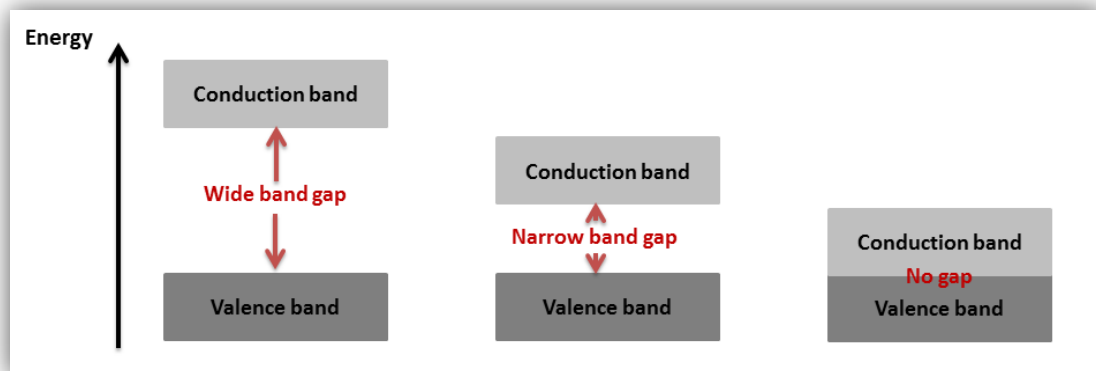


Figure 1.2. Band structure for an insulator, a semiconductor and a metal

“Doping” is the process used to enhance conductivity of a polymer. It is a redox process which involves reduction or oxidation of electrons in the polymer backbone [9]. It is possible to perform doping processes following either chemical or electrochemical treatment [5b]. During reversible doping and dedoping mechanism, no change in the chemical structure of conducting polymers is observed. Thus, band structure of conducting polymers is changed upon oxidation and reduction process (Figure 1.3).

A radical cation, known as polaron, is formed when an electron is removed from the valence band during oxidation of polymer chain (p-doping). The charge is partially delocalized over several polymer segments, resulting in the cleavage of a double bond in the backbone. If a second electron is removed upon further oxidation, a bipolaron is created. At high dopant concentration, several bipolarons lead formation of bipolaron bands. Heavily doped polymer produces partially filled bands between valence and conduction bands, yielding metallic like conductivity.

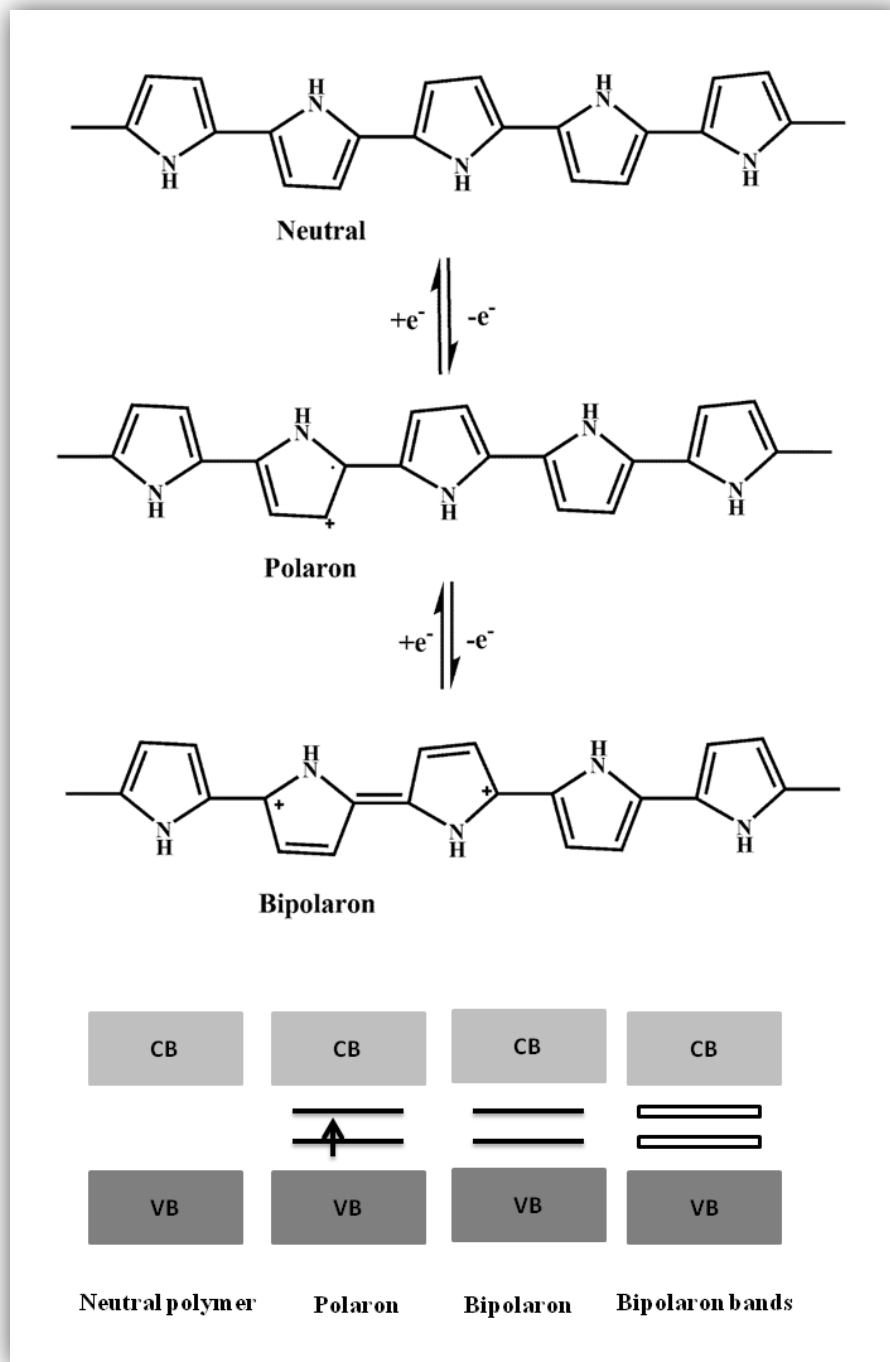


Figure 1.3. Structural representation of bipolaron formation in polypyrrole and its corresponding energy bands in the mid gap

### 1.1.3. Syntheses of Conducting Polymers

Conducting polymers can be synthesized according to two widely employed methods: chemical and electrochemical polymerization. There are several other techniques carried out like photochemical polymerization, solid state polymerization, pyrolysis [10]. Conductivity, processability, defined three dimensional structures, solubility and stability of the conducting polymers should be considered to determine the polymerization methods for a target design.

#### 1.1.3.1. Chemical Polymerization

Chemical polymerization can be performed by oxidation of monomers in the presence of oxidizing agents. For heterocyclic monomers,  $\text{FeCl}_3$  is generally preferred as oxidant chemical; although other chemicals can be used for oxidizing agent during chemical polymerization [11]. During  $\text{FeCl}_3$  catalyzed polymerization,  $\text{Fe}^{3+}$  oxidizes the monomer and the polymer growth starts while  $\text{Fe}^{3+}$  ions are reduced to  $\text{Fe}^{2+}$  ions. Reduction to its neutral state is managed upon addition of strong base like ammonium hydrazine or hydroxide (Figure 1.4). In another way, chemical polymerization can be carried out by reacting a monomer with Mg in THF, followed by self coupling with metal complex catalyst like  $\text{Ni}(\text{bipy})\text{Cl}_2$  [12].

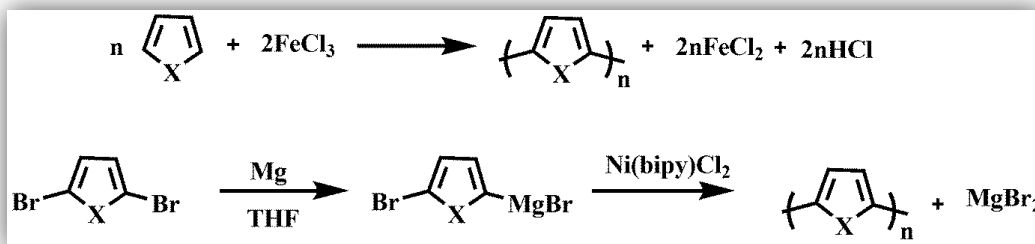


Figure 1.4. Synthetic routes of polyheterocycles for chemical polymerization

Chemical polymerization provides synthesis of conducting polymers at low cost. However, intrinsic properties of the produced polymer may not be qualified, resulted low conductivity. Moreover, strong oxidizing agents used for polymerization process may cause overoxidation and decomposition of the polymer as well as many side reactions may occur [13].

### **1.1.3.2. Electrochemical Polymerization**

Electrochemical polymerization is an effective method for synthesis of conducting polymers, offering many advantages over chemical polymerization. It is possible to deposit the polymer at the electrode surface by controlling the thickness of the coated conducting polymer in terms of charge passing through the cell. As polymer chain grows, the polymers are oxidized to their doped states. The method represents simple, reproducible and straightforward process for growth of the conducting polymers on the electrode surface which allows well defined and finely controlled deposition. The major drawback is that the synthesized polymer is insoluble, therefore, characterization of the products are difficult using traditional methods like GPC.

The electrochemical polymer synthesis is performed using various techniques like potentiostatic (constant-potential), galvanostatic (constant current) and potentiodynamic (potential scanning with cyclic voltammetry) [14]. In electrochemical polymerization method, the polymer may be produced in its insulating form, leading to a passivation of the electrode and limits accessible thickness of the deposited film [15].

Figure 1.5 illustrates the mechanism of the electropolymerization for heterocycles using pyrrole unit as an example with the steps of radical cation, radical cation coupling and resonance stabilization. The process occurs in a solution with the presence of supporting electrolyte. The process starts with the formation of radical cation upon oxidation of the monomer. The electron transfer reaction is much faster than the

diffusion of the monomer from the bulk solution. Thus, high radical concentration is retained on the electrode surface. Then, two routes can be proceeded to achieve the polymerization. Either the produced radical cation of the monomer can combine with a neutral monomer to form a dimer or two radical cation coupling form a dimer. Since the dimer is more easily oxidized than the monomer, it can be reoxidized to allow further coupling reaction, proton loss and rearomatization to progress. Hence, electrochemical polymerization is proceeded through successive electrochemical and chemical steps, known as  $E(CE)_n$  mechanism (E for electrochemical, C for chemical) until the produced oligomers during the process become insoluble in the reaction medium and precipitate onto the electrode surface [16].

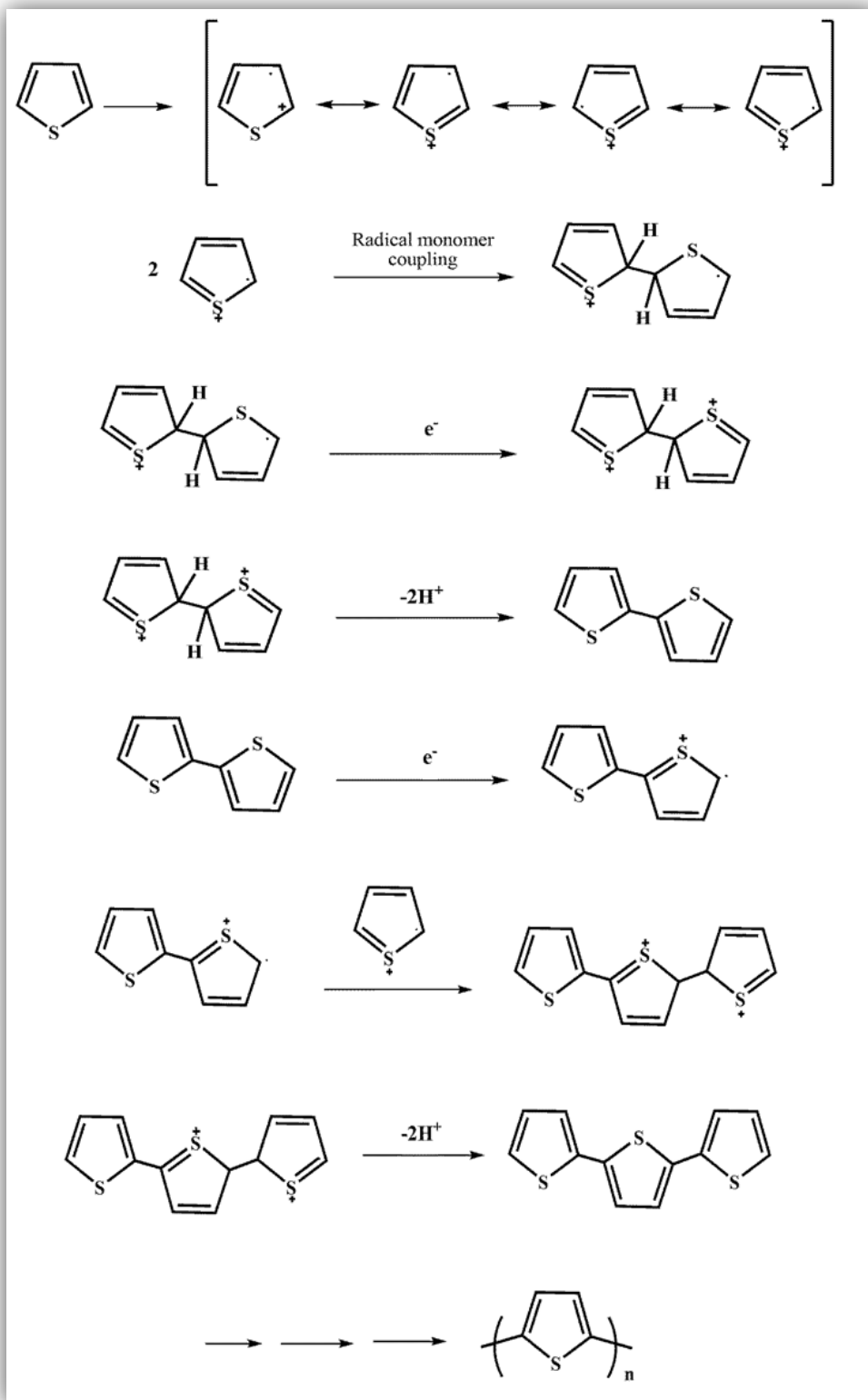


Figure 1.5. Proposed mechanism of the electropolymerization of pyrrole

#### **1.1.4. Applications of Conducting Polymers**

Conducting polymers are known as “synthetic metals”, opening new research field owing to their overwhelming characteristics. They exhibit both excellent conductivity like metal and high mechanical strengths and processability like polymers. Therefore, application areas of conducting polymers focus on usage of conducting polymers as plastic-metals which has attracted keen interest of scientific world in the last decades.

Taking the advantages of ease of processability, ability of conduct the electricity in the any desired level, low cost, straightforward preparation techniques and mechanical, optical and electrical properties make the conducting polymers fundamental materials in large areas. Chemical and biological sensors [17], light emitting diodes [18], field effect transistors [19], electrochromic devices [20], rechargeable materials [21], photovoltaic devices [22], drug delivery [23] and artificial muscles [24] are the most significant applications of conducting polymers. In this thesis, the use of conducting polymers as enzyme immobilization matrices in biological sensors is investigated.

#### **1.2. Biosensors**

A device that transforms chemical information into an analytical signal is known as the chemical sensor. Biosensors are a type of chemical sensors utilizing a biochemical mechanism. This system translates the information from the chemical domain into an output signal in order to provide the selective sensors for the analyte that can be measured [25].

In recent years, biosensors have attracted lots of attention throughout the world. The designed biosensors are specific, rapid, and simple to operate, and ease of fabrication with minimal sample pretreatment involved [26]. Besides, real time analysis can be

possible which leads rapid measurements, ability to monitor and control the process [27]. Hence, biosensors have many applications in life such as diagnosis, food technology, biotechnology, genetic engineering, environmental monitoring etc. [28]. A biosensor includes mainly two parts: a biological detection element and a transducer. The biological component in the construction system can be catalytic or non-catalytic. The catalytic groups consist of enzymes, tissues and microorganisms; whereas the non-catalytic groups have antibodies, nucleic acids and receptors. The second part, a transducer, is required to convert the biological signal into the understandable signal. Several transducer are used to fabricate the biosensor such as electrochemical (conductometric, potentiometric and amperometric), optical, colorimetric and acoustic etc [29]. According to transducer types and biological detection element types, biosensors are categorized, illustrated in Figure 1.6.

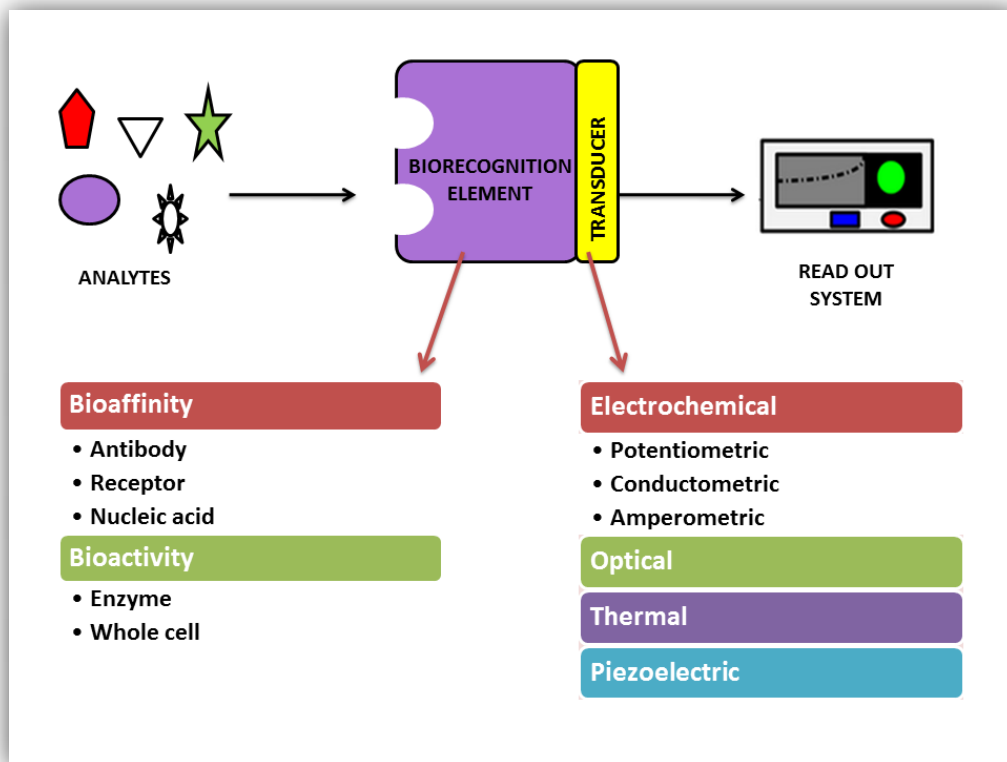


Figure 1.6. Simple representation of a biosensor

### **1.2.1. Electrochemical Biosensors**

The transducer of a sensor is used to transmit the biochemical information to an understandable signal, designating selectivity or specificity of the sensor. Suitable transducer system is adjusted according to the nature of biochemical interaction with the specific analyte [30]. There are various types of transducers: electrochemical (conductometric, potentiometric and amperometric), optical, colorimetric and acoustic etc.

In case of electrochemical transducers, electrochemical transducers are used for construction of a biosensor, which can be chosen as conducting, semiconducting, ionic conducting material to coat the electrode with the biological receptor. The working principle of electrochemical biosensors is that an electrochemical species is consumed or produced during the biological reaction, while the electrochemical signal is recorded using an electrochemical detector [31]. Combination of analytical power of electrochemical techniques and specific selectivity of biological recognition element lead to an effective electrochemical biosensor, presenting simple to handle, low cost and fast detection process for a specified biological reaction [32].

Electrochemical techniques can be classified in three main subclasses depending on the type of transducer: conductometric, potentiometric and amperometric biosensors.

#### **1.2.1.1. Conductometric Biosensors**

Conductometric biosensors detect the changes in the conductance as a consequence of the biological element, designed by a two-electrode device. They are based on either consumption or generation of charges species involved in the enzymatic reactions. The change in charges species lead difference in ionic composition of the analytes [33].

### **1.2.1.2.Potentiometric Biosensors**

The potentiometric biosensors are designed to measure the potentials at the working electrode with respect to the reference electrode under no current flow [34]. They monitor electric potential related to ion concentration in the system created by selective binding of the electrode. They are based on ion-selective electrodes (ISE) and ion-selective field effect transistors (ISFET). For instance, the electrode senses the change in electrode potential and determines several ions like  $\text{Na}^+$ ,  $\text{Ca}^{2+}$  or  $\text{NH}_4^+$  in the reaction matrix, resulting from the enzymatic reaction while the ions accumulate and bind to a suitable ion selective membrane [31].

### **1.2.1.3.Amperometric Biosensors**

Amperometric electrochemical biosensor has attracted great interest for biosensor construction compared to the others since amperometric detection is a useful technique for substrate analysis because of its selectivity, sensitivity, rapid response, ease of construction and reproducible performance [35].

Amperometric biosensors measure the differences in the current on the working electrode upon applied constant potential, created by oxidation or reduction of species in the sensing matrix during biological reaction. Therefore, the reaction generates the current change, monitoring as a function of time and the current change is related to the amount of analytes in the reaction solution.

In the amperometric detection, the electron transfer between the catalytic molecule and the electrode surface occurs where oxidation or reduction reactions are involved. Thus, the transducer surface is one of the most important factors affecting the functioning of amperometric biosensors. They are generally modified with mediators or conducting

polymers [26]. Furthermore, maintaining the applied voltage is very important to perform the process. For this purpose, a reference electrode is introduced to keep the potential stable. This leads to the improvement of repeatability of the electrochemical reaction. That is why the amperometric electrodes are preferred owing to their high sensitivity, rapidness in signal processing and better selectivity. Also, the most valuable reason for being pioneering place in biosensing applications is simple construction systems.

In 1962, Clark and Lyons developed the first amperometric type enzyme electrode [36]. They used glucose oxidase as the biomaterial. The basic setup is based on recording either production of  $\text{H}_2\text{O}_2$  or consumption of  $\text{O}_2$  during enzymatic reaction occurs. It involves a platinum cathode where oxygen is reduced and a Ag/AgCl reference electrode. Upon application of  $-0.68$  V to the cathode, a current proportional to the oxygen concentration in the reaction medium is recorded. The decisive reduction of oxygen results in the diminishing of oxygen concentration. Thus, the rate of this electrochemical reaction is strongly related to the rate of diffusion of oxygen from the bulk solution [37]. Hence, during the catalytic reaction, the reduction of the diffused oxygen concentration is detected following the current change due to the formation of new equilibrium in the reaction medium. Also, since the consumed oxygen concentration is proportional to the consumed substrate concentration, the current change determines the analyte concentration. However, the other electrochemical electrodes used equilibrium conditions to detect the changes in the reaction medium. Among them, the amperometric constructions are sensitive to changes than the other electrochemical electrodes.

Another approach to construct an amperometric biosensor is to follow the current change upon applied  $+0.68$  V potential to the cathode. The production of hydrogen peroxide is measured relative to the reference electrode, known as hydrogen peroxide electrode. However, the applied potential is much higher than the oxygen electrode. The selectivity and efficiency of the biosensor may not be good enough since electroactive

species in the reaction medium can interfere. For example, a glucose biosensor is designed to measure glucose concentration in human blood. The samples have several oxidative species like ascorbic acid, paracetamol or uric acid. By applying high potential to the reaction cell, these species may be activated and cause change in results. This limitation can be overcome by choosing the working potential as low as possible [38].

After the first enzyme based amperometric biosensor was fabricated, enzymes are widely used as a significant tool in biosensing study [39]. Such devices are used to develop efficient biosensing designs by combining the properties of the enzyme specificity to recognize a specific analyte and the direct transfer of the biocatalytic reaction rate.

There are three generations of amperometric biosensors depending on the level of integration, as shown in Figure 1.7. In the first generation, the biorecognition element is fixed onto the transducer surface via bonding or entrapment in a membrane. The product of the biological reaction during the analysis diffuses to the transducer and electrical response is recorded. Although this type of biosensor is simple and easily constructed, possible analytes in the sensing system which coexist in the real samples may interfere the analytical response, causing poor selectivity. The second generation includes “mediators” between the receptor and transducer to obtain improved signals. A redox reaction occurs during the enzymatic reaction that is reoxidized by the mediator. Then, the mediator is oxidized at the electrode. The process results in improved selectivity as using artificial mediators eliminate the interference effect, resulting in improved selectivity. In the case of third generation system, there is a direct binding between the biocatalyst and the transducer in order to facilitate direct communication without addition of promoters or mediators. The catalytic reactions cause the biosensor response. At this time, any product or mediator do not diffuse directly to the system. Although addition of mediator can improve the selectivity, easy leakage of the

mediators is possible, causing deterioration of the signals. This design promotes repeated measurements and improves the biosensor performance [28].

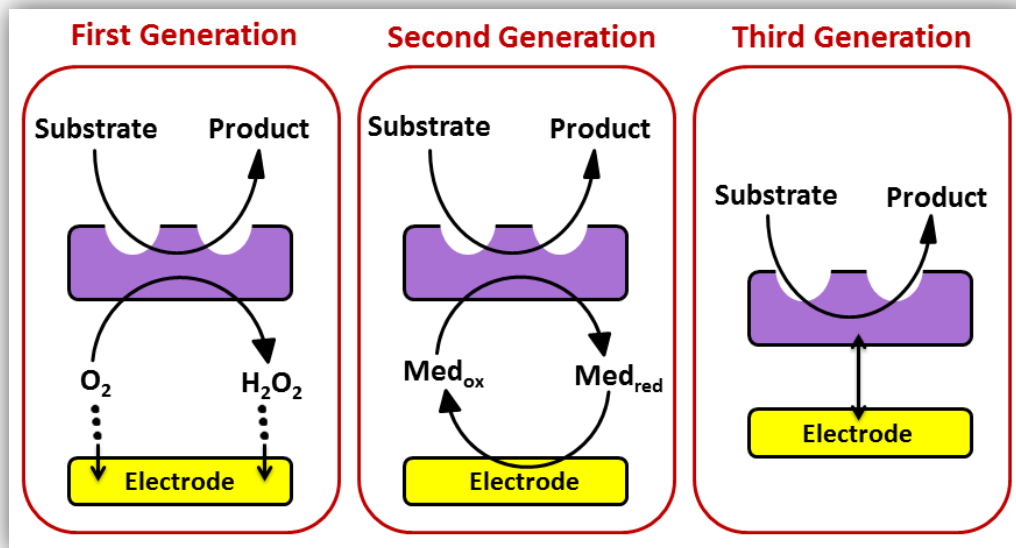


Figure 1.7. Schematic representation of three generations of amperometric biosensors

### 1.2.2. Immobilization Techniques

Immobilization means the physical localization of biomolecules with the retention of bioactivity during construction of a biosensing system. Life time of any biological materials is very short in solution phase. Thus, biomolecules should be fixed in a suitable matrix. Moreover, the incorporated biomolecule is sensitive to environment; therefore biosensing system conditions like pH, temperature, localization of the biocomponent are decisive. In biosensor fabrication, the most crucial step is the immobilization of a biomolecule onto the electrode surface to improve performance of the biosensor while sustaining their biological properties [26]. The main goal of immobilization methods is to provide an effective relation between the biological molecule and the electrode surface by improving its stability [40].

In order to maintain enzyme stability, increase shelf life of biosensor and reduce the time of enzymatic response, various immobilization methods have been developed [28]. For efficient deposition of a biomolecule, there are few pre-requisites; (1) efficient and stable way of immobilization of enzymes on the surface, (2) biomolecule must not lose its biological property, (3) it should form compatible and inert microenvironment towards host structure and (4) it should be available during immobilization procedure [41]. Hence, several techniques illustrated in Table 1.1 are developed to immobilize the biomaterial providing a suitable environment.

Table 1.1. Immobilization procedures

<b>Method</b>	<b>Advantages</b>	<b>Disadvantages</b>
<b>Physical Adsorption</b>	<p>Little or no damage to enzyme</p> <p>Simple and cheap</p> <p>No chemical changes to support or biocatalyst</p>	<p>Interactions are affected by changing the conditions in reaction matrix</p>
<b>Entrapment</b>	<p>Simple and easy.</p> <p>Only physical confinement of enzyme near transducer</p> <p>Speed of one-step procedure</p>	<p>Diffusional restrictions</p> <p>Long response time</p>
<b>Covalent bonding</b>	<p>Leaching out of the enzyme are reduced</p> <p>Long life time</p> <p>High operational stability</p>	<p>Excess attachment may cause denaturation</p>

<b>Crosslinking</b>	Compact protein structure	Not regenerable matrix
	Leaching out of the enzyme is limited	Harsh treatment of biocatalyst by toxic chemicals
	Stable	

### 1.2.2.1. Physical Adsorption

Immobilization by physical adsorption is the simplest method and involves reversible surface interactions between enzyme and various supporting material as seen in Figure 1.8. The forces are mostly electrostatic, such as Van der Waals forces, ionic and hydrogen bonding interactions, although hydrophobic bonding can be significant compared to others. These are very weak; however, most of them enable reasonable binding [42].

This process offers some advantages like little or no damage to enzyme, simple and cheap, and no chemical changes to support or enzyme cell. However, the immobilization strategy has some disadvantages like nonspecific bonding, overloading on the support and steric hindrance by the support. For example, pH can be changed by binding forces, incorporated enzyme amount is too small due to limited adsorption to the supporting material and biomaterial which can leach into the solution decreasing lifetime stability of enzyme electrode [43,44]. Hence, the interactions between the biological molecule and supporting material are affected by changing the conditions in the matrix. Furthermore, enzyme is immobilized on the outer layer of the supporting electrode; thus leaching out of the enzyme into the reaction solution is observed during the catalytic measurement. This causes decreasing in biosensor lifetime [43].

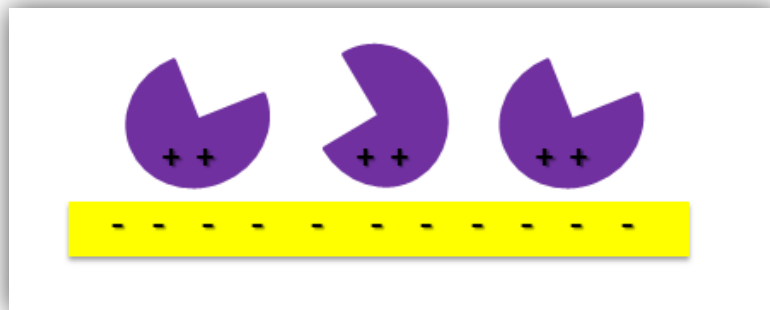


Figure 1.8. Schematic representation of physical adsorption method

#### 1.2.2.2. Entrapment

Entrapment is achieved by fixing biological materials into three-dimensional network on the surface of the electrode. The entrapment strategy was first carried out for enzyme immobilization in 1963 [45]. The immobilization technique is quite simple and easy. After the biomolecule was dissolved in a solution in the presence of some chemicals, it is caged into a network so that the desired phase is formed [46]. It differs from the other immobilization methods since the biomolecule does not bind directly to the immobilization matrix. This network can be polymer [47], dialysis membrane [48], sol-gel encapsulation [49], biological matrices [50] etc. A representative scheme for entrapment immobilization method is shown in Figure 1.9.

Biological molecules, additives or mediators can be entrapped simultaneously on the immobilization layer. Modification of biomolecule is not needed to retain the activity of the molecule. This leads high operational stability. Additionally, the major advantage of the method is that the biomolecules are immobilized via simple one-step procedure [51]. However, the major drawbacks of this immobilization method are diffusional restrictions and long response time due to the accessibility of entrapped biomolecules. The pore size of the network should be sufficient enough to facilitate the diffusion of substrates and products since the biomolecule is entrapped within a network [46,52].

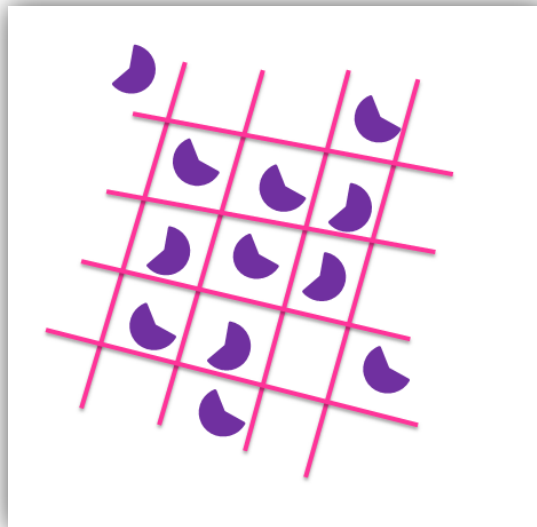


Figure 1.9. Schematic representation of entrapment method

### 1.2.2.3. Covalent Bonding

The most popular attachment strategy is covalent immobilization owing to its numerous advantages [53]. The method involves formation of covalent bonding using activated functional groups on the support materials like  $\text{NH}_2$ ,  $\text{COOH}$  with the enzyme as seen in Figure 1.10 [42].

Covalent binding between the enzyme and the support matrix is preferred to construct long life time and high operational stability of enzyme based biosensors. Several problems in the other immobilization techniques can be overcome due to the robust covalent bond formation during localization of enzyme onto the electrode. With this technique, the diffusion limitations, leaching out of the enzyme are reduced. Besides, the method facilitates high enzyme stability [28].

Following two sequential step procedure, covalent attachment is achieved. The supporting surface is first functionalized via several techniques like coating the

electrode with a functional polymer [54], incorporation of functional nanomaterials [55], formation of self-assembled monolayers (SAM) [56] or addition of sol-gel composites [57]. Then, biomolecule is introduced to the prepared support material. At this stage, biomolecule forms a covalent binding on the electrode surface using linkers. An enzyme structure contains free amino and carboxylic acid groups. These groups are free to attach to the functionalized electrode surface covalently with the help of activation agents used for the covalent attachment.

In this strategy, the major drawback is that excess attachment of the enzyme with the functional surface matrix may cause denaturation, resulting in bioactivity loss and instable biosensor construction [58]. However, optimization of the sensing system at each step is possible due that immobilization takes place only on the outer surface of the supporting material in order to obtain the most sensitive microenvironment for enzyme molecules [59].

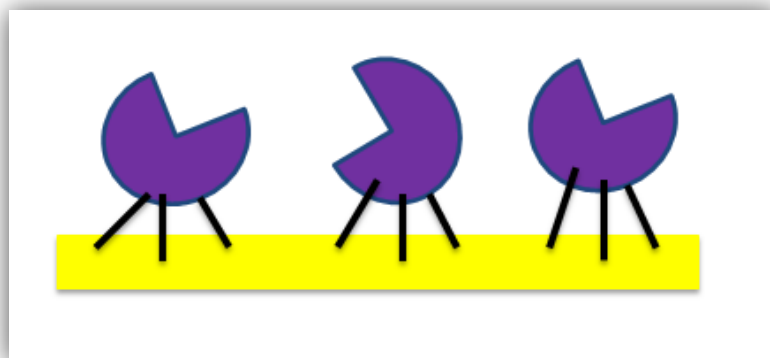


Figure 1.10. Schematic representation of (a) covalent immobilization method

#### 1.2.2.4. Intermolecular Crosslinking

Biomolecules form crosslinked or covalent bond with the support material via crosslinking as illustrated in Figure 1.11 [60]. Biomolecules can attach to the support

matrix or within itself. There are several proteins used to crosslink the biomolecules like bovine serum albumin (BSA), glutaraldehyde (GA) or carbodiimide. With this method, compact protein structure is achieved and leaching out of the enzyme is limited as well as response time is reduced. However, a high degree of crosslinking can be a problem since intermolecular crosslinking is difficult to control, resulting in the loss of activity. Although, the constructed biosensor presents a good operational and storage stability, taking these advantages of the method, it is crucial to determine the optimum amount of crosslinker for the designed biosensing system.

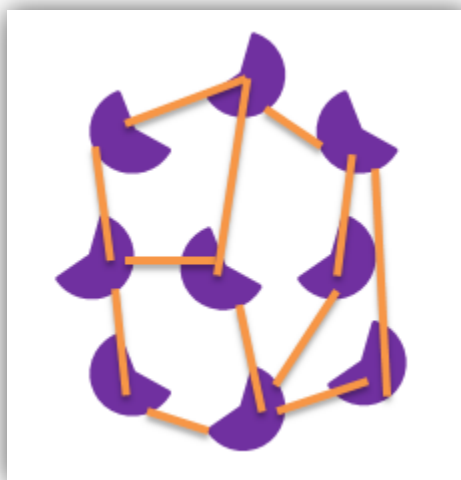


Figure 1.11. Schematic representation of intermolecular crosslinking immobilization method

### 1.2.3. Applications of Biosensors

The biosensor technology has attracted great interest due to its many important applications. The new developed techniques also have advantages over conventional laboratory based assays. The conventional methods are time consuming, expensive, required well trained personnel and not used for real time measurements. Nevertheless, biosensors are inexpensive, portable with minimized design, easy to handle, selective

and sensitive. A wide variety of application field of modern biosensors is listed in Table 1.2.

Table 1.2. Applications of biosensors

<b>Field</b>	<b>Applications</b>
Health care	Drug screening Analysis of glucose, alcohol, cholesterol etc. and hormone Diagnosis of genetic diseases Markers of diseases Detection of species in growing cells
Environmental monitoring	Water and soil analysis Detection of pesticides and other toxic substances Waste water analysis Bacterial and viral analysis
Food and drink analysis	Food freshness Detection of glucose content in beverages Analysis of cholesterol in butter Food components of sugars Pathogenic organisms test

Defense and military  
applications

Detection of biological warfare agents  
Quantification of organophosphorous nerve agents

---

#### 1.2.4. Glucose Biosensors

Diabetes has become one of the world wide health concerns, causing death and disability. The number of people suffering from diabetes was 200 million nowadays. It is expected to rise to 366 million in 2030 [61]. Diabetes is abnormality in the level of insulin in human body. Insulin is a hormone which converts the sugar existing in human body into energy. When glucose level is above a certain value in human blood, urgent consideration must be required. Hence, monitoring glucose level and maintaining blood glucose levels to normal values is very crucial for diabetic diagnosis.

In the last decades, effective glucose monitoring biosensors has been developing [62]. Glucose oxidase (GOx,  *$\beta$ -D-glucose:oxygen 1-oxidoreductase; EC 1.1.3.4*) is widely employed in construction of glucose biosensors. GOx is flavoprotein, containing *two tightly bounded flavine adenine dinucleotide redox centers*. The redox centers lead electron transfer during the enzymatic reaction. GOx from *Aspergillus niger* catalyzes the oxidation of  *$\beta$ -glucose* to *D-glucono- $\delta$ -lactone* in the presence of molecular oxygen which subsequently is hydrolyzed into *gluconic acid* non-enzymatically and hydrogen peroxide, spontaneously [63] (Figure 1.12).

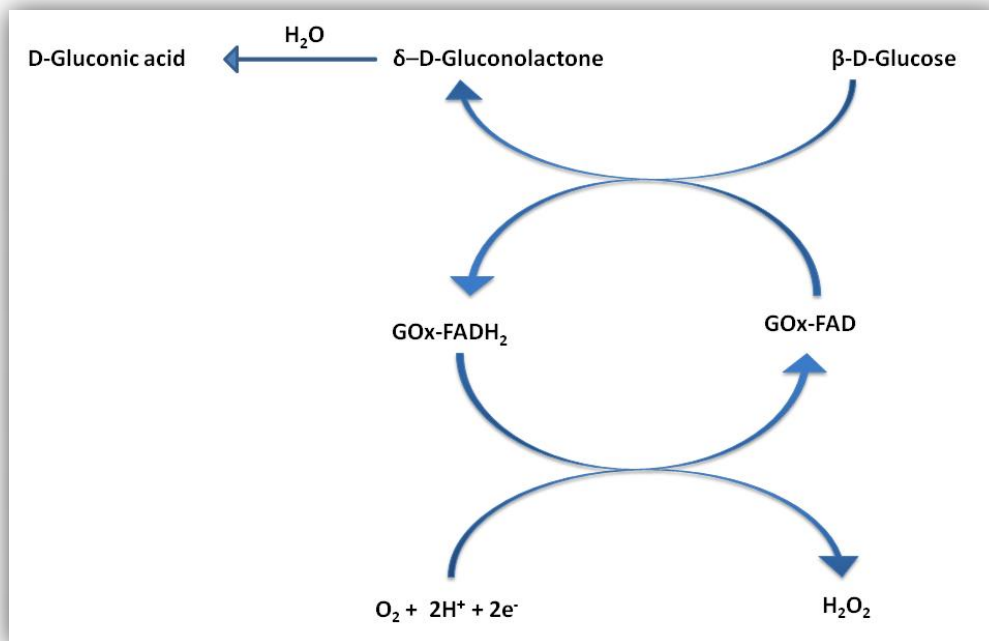


Figure 1.12. Representation of Reaction mechanism of glucose oxidase

### 1.2.5. Conducting Polymers in Biosensing Design

Conducting polymers have attracted great interest throughout the world owing to their physical and chemical properties. They can be preferred to enhance sensitivity, speed and stability in biosensor design as a suitable matrix of biologic molecules for different purposes like medical diagnostics, environmental monitoring etc. [64]. Conjugated polymers are promising materials for biosensor construction due to several advantages:

- ❖ CPs provide simplicity and high reproducibility in fabrication of biosensor [26].
- ❖ CPs are able to transfer electrical charge produced by the enzymatic reaction. Since electrons can move freely on the conjugated  $\pi$  electron backbones [28], accelerated electron transfer is achieved. By this way, using CP in biosensor construction enhances the electrocatalytic properties of biomolecules; thus,

promotes rapid electron transfer and direct communication between the transducer and the biomolecule. [59,65].

- ❖ CPs as immobilization platforms offer extensive stability of enzymes on the electrode surface [66]. In an enzymatic biosensor, it is crucial to immobilize enzyme molecules onto the substrate stable and for long-term without activity lost. For this reason, conducting polymers are excellent materials with their structure, electronic character and compatibility.
- ❖ CPs are deposited on the electrode surface during electrochemical synthesis. Whatever surface properties are, the electrodes can be coated with the conducting polymers by arranging thickness of the film upon demand [67]. Besides, it is possible to produce CPs at room temperature electrochemically which is very crucial for biomolecules [51].
- ❖ CPs have organized structures on electrode surfaces, created a three dimensional matrix onto the electrode surface for efficient deposition of the enzymes. This leads retaining the enzyme activity for a long time [68,69].
- ❖ CPs allow the structural and electronic modifications of various surfaces to be used as immobilization matrices for biomolecules [70]. They can be functionalized upon interest and used for various kinds of purposes. The polymer structure can be tuned by according to the properties of resultant materials and widely applied in the construction of biomedical devices. They can be functionalized and used in covalent immobilization technique to achieve a stronger biosensor construction. Besides, electronic and mechanical properties can be also altered chemical modeling or synthesis. For instance, a polymer which has characteristics of hydrophobicity can be modified by introducing hydrophilic groups. As a result, the hydrophilic groups bring the highest interaction with biological materials whereas the former one has not.

- ❖ CPs are used to produce sensitive and reproducible microenvironment for biological reactions to mimic the naturally occurring environment of biological molecules.

### **1.2.6. Nanostructures in Biosensing Design**

In recent years, the design of electrochemical biosensors with nanostructures has received great attention to provide better analytical properties in terms of sensitivity, selectivity and reliability [71]. Nanomaterials exhibit remarkable properties and due to the constantly growing demand for high and long-term efficiency in every kind of research, nanomaterials are always preferred due to their distinct properties [72-74].

The introduction of nanomaterials into conducting polymers attracted attention in material science since both production of nanostructures and conducting polymer is simple and easy to fabricate [75,76]. The effect due to the combination of these two valuable materials brings many advantages such as enhanced conductivity [77]. Furthermore, introduction of nanomaterials can also provide substantial electronic interaction with the polymer which improves the charge transfer. Besides, the charge can be travel along the conducting polymer chain and transferred to the desired positions via nanostructures bringing on an improved electronic activity of the material [78].

Nanostructures are extensively used in the fabrication of electrochemical biosensors to get a combination of suitable immobilization method and support material. There are various types of nanomaterials; however, in this context, the use of clay nanocomposite and gold nanoparticles incorporated in conducting polymer as an immobilization platform for the construction of different glucose biosensors is mentioned.

Modification of the electrode surfaces with clay is one of the convenient ways to improve the analytical characteristics and long-term stability of biosensors due to their ion exchange capability, well defined layered structure and large surface area [79-81]. Additionally, clay modified matrices have been used in biosensor fabrication to assure the retention of activity and functionality of enzymes after immobilization. There are several types of clay minerals and their related layered structures: laponite, montmorillonite, nontronite and layered double hydroxides [82]. Specially, laponite, cationic clay, is used as a matrix for biomolecules deposition improving performance of the biosensors to immobilize several redox biomolecules. Laponite is manufactured from abundant inorganic mineral sources and has a chemical composition analogous to that of naturally occurring smectite clay minerals. It is also used as a film forming agent to produce electrically conductive, antistatic and barrier coatings. Its porous structure provides high hydrophilic property [83]. However, hydrophilicity of the clay makes the clay less compatible with the organic polymers. Thus, various polymer/clay nanomaterials are prepared to make the organic clays compatible with the polymers. Hence, the preparation of polymer/clay nanocomposite (Figure 1.13) material ends up with enhanced compatibility with the organic polymers, namely conducting polymers. These composites have used in many applications owing to their unique structures. They exhibit better properties than virgin polymers or clay materials [84]. Taking the advantage of clay nanocomposite for its high chemical stability, well adsorption capacity, high surface area and intercalation property [85], clay-modified biosensors exhibit good stability and efficiency [83,86-88].

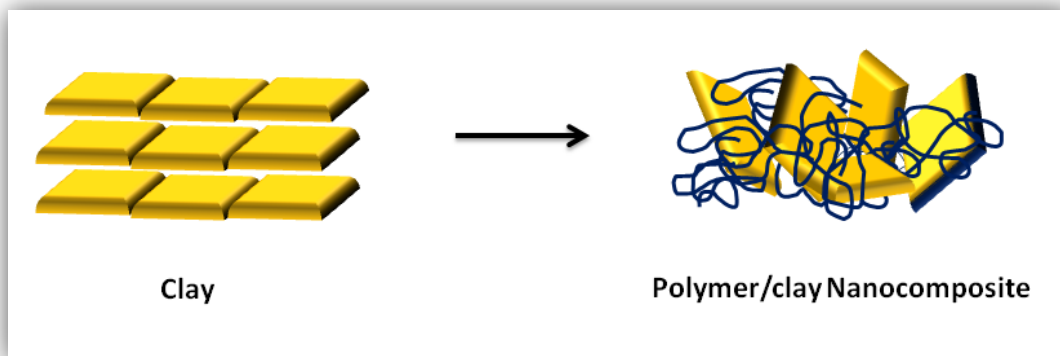


Figure 1.13. Representation of clay and polymer/clay nanocomposite

Nanomaterials exhibit remarkable properties and due to the constantly growing demand for high and long-term efficiency in every kind of research, nanomaterials are always preferred due to their distinct properties [74,89]. Nanoparticles, particularly gold nanoparticles with contributions of their localized surface plasmon resonance, improved light absorption, electron transport, excellent conducting properties as well as self-assemble structures [90] become convenient candidates for wide range of applications. Gold nanoparticles (Au NPs) can play an important role in the construction of biosensors due to their large specific area, excellent biocompatibility, good conductivity capability, desirable catalytic properties and small size [91]. Deposition of biomolecules incorporated with gold nanoparticles leads to provide stable immobilization retaining activity of the biomolecules. Additionally, Au NPs allow direct electron transfer between active site of the enzyme and the electrode. By this way, there is no need additional material like mediators for electron transfer in electrochemical biosensor construction. They are used to promote the electron transfer from redox enzymes; thus, Au NPs let good communication with redox enzyme molecules [92]. In biosensor fabrication, Au NPs are recently used and one of the most effective methods is binding gold nanoparticles via functionalization as a self-assembled monolayer (SAM). This modification takes advantages of increased surface area of three dimensional electrode surfaces [92,93]. Sulfur containing compounds like alkanethiol have high affinity to metals. In recent studies, Au NPs are self-assembled with short-chain molecules such as

cysteamine (Cyst) and 3-mercaptopropionic acid (MPA) [94]. Biosensors fabricated with SAM technique can possess high sensitivity and short response time. MPA is a bifunctional molecule containing both thiol and carboxylic acid functional groups. The thiol groups serve as binding sites for covalent attachment of MPA to Au NPs (Figure 1.14). Moreover, the carboxylic acid groups can further react covalently with amino groups of a functional material and also with the enzyme molecules in order to achieve effective immobilization and increase lifetime stability [28].

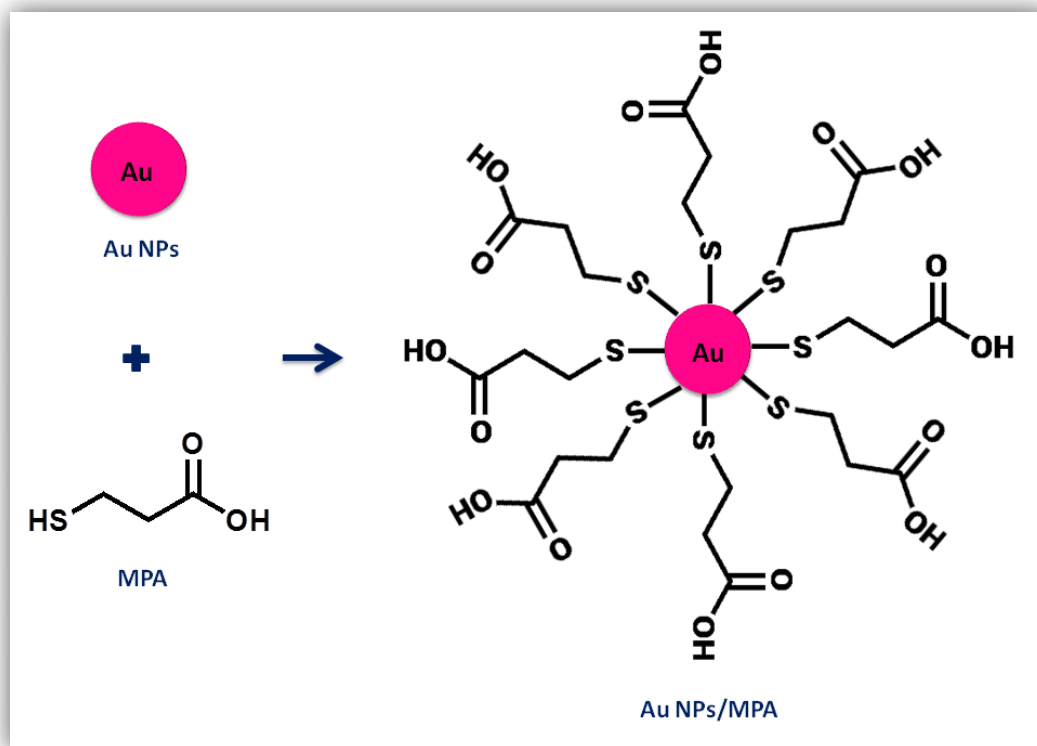


Figure 1.14. Representation of self-assembled gold nanoparticles functionalized with MPA



## CHAPTER 2

### EXPERIMENTAL

#### 2.1. Materials

Glucose oxidase (GOx,  $\beta$ -D-glucose: Oxygen 1-oxidoreductase, EC 1.1.3.4, 47200 units/g) from *Aspergillus niger*, D-glucose, 3-mercaptopropionic acid (MPA) and glutaraldehyde (GA) (50 wt. % solution in water) were purchased from Sigma (St. Louis, USA; [www.sigmaaldrich.com](http://www.sigmaaldrich.com)). N-Hydroxysuccinimide (NHS) and N-(3-dimethylaminopropyl)-N'-ethylcarbodiimide hydrochloride (EDC) were purchased from Fluka (Buchs, Switzerland) and Sigma, respectively. Dichloromethane (DCM), acetonitrile (ACN), sodium hydroxide was obtained from Merck (Darmstadt, Germany; [www.merck.com](http://www.merck.com)). Tetrabutylammonium hexafluorophosphate (TBAPF<sub>6</sub>) was supplied by Aldrich. All chemicals for the synthesis of monomer were purchased from Aldrich except tetrahydrofuran (THF) which was obtained from Acros (Geel, Belgium, [www.acros.com](http://www.acros.com)). All other chemicals were analytical grade.

Spectrophotometric enzyme assay kit for glucose measurements HUMAN 10260, Glucose Liquicolor (Wiesbaden, Germany) was used to determine reliability of the biosensor. Column chromatography of all products was performed using Merck Silica Gel 60 (particle size: 0.040–0.063 mm, 230–400 mesh ASTM). All reactions were carried out under argon atmosphere unless otherwise mentioned.

## **2.2.Instrumentations**

### **2.2.1. Electrochemical measurements**

For the amperometric studies and cyclic voltammetry measurements *Ivium CompactStat* potentiostat (*Ivium Technologies, The Netherlands*) and *Palm Instrument (PalmSens, Houten, The Netherlands)* were used. All electrochemical measurements were performed in a three-electrode cell consisting of a graphite electrode (*Ringsdorff Werke GmbH, Bonn, Germany, type RW001, 3.05 mm diameter and 13 % porosity*) as the working electrode, a platinum (Pt) wire as the counter electrode and a silver (Ag) wire as the reference electrode.

### **2.2.2. Characterization studies**

#### **2.2.2.1.Nuclear Magnetic Resonance Spectrometer (NMR)**

$^1\text{H}$  NMR and  $^{13}\text{C}$  NMR spectra were recorded in  $\text{CDCl}_3$  on *Bruker Spectrospin Avance DPX-400* spectrometer and chemical shifts (d) were given relative to tetramethyl silane.

#### **2.2.2.2.High Resolution Mass Spectrometer (HRMS)**

A *Waters Synapt MS System HRMS* confirm the structures by measuring on the exact molecular weight of the target molecules.

### **2.2.2.3.Scanning electron microscope (SEM)**

*JEOL JSM-6400* model scanning electron microscope was used for surface imaging and characterization studies of the electrode surfaces after successive modification procedures.

### **2.2.2.4.Fluorescence microscope**

*Epifluorescence microscope (Olympus, Tokyo, Japan)* was used for surface imaging for both conducting polymer coated graphite electrode and biomolecules/nanocomposite immobilized enzyme electrode, taking advantage of fluorescent character of conducting polymer and enzyme.

### **2.2.2.5.Transmission electron microscope (TEM)**

*FEI Tecnai G2 Spirit BioTwin Transmission electron microscope* was used to depict changes in the morphology of gold nanoparticles and functionalized gold nanoparticles.

### **2.2.2.6.X-ray photoelectron spectroscope (XPS)**

XPS was performed on a *PHI 5000 Versa Probe (FULVAC-PHI, Inc., Japan/USA)* model X-ray photoelectron spectrometer instrument with *monochromatized Al K $\alpha$*  radiation (1486.6 eV) as an X-ray anode at 24.9 W.

### 2.2.2.7.UV-vis-NIR spectrophotometer

*Varian Cary 5000 UV-vis-NIR spectrophotometer* was used to perform the characterization studies of the nanoparticles.

### 2.2.2.8.Fourier Transform Infrared Spectrophotometry (FTIR)

FTIR spectra were recorded on a *Varian 1000 FTIR spectrometer* to investigate functional groups after successive layer formation onto the graphite electrode surface.

## 2.3.Synthesis of the Monomer

Synthesis and characterization of the monomer, BEDOA-6, were carried out according to a previously described method [95]. Figure 2.1 represents synthetic route to BEDOA-6.

1*H*-benzo[*d*][1,2,3]triazole, potassium tert-butoxide and 1,6-dibromohexane were reacted to obtain 2-(6-bromohexyl)-2*H*-benzo[*d*][1,2,3] triazole as a colorless oil. The product, 2-(6-bromohexyl)-2*H*-benzo[*d*][1,2,3] triazole, an aqueous HBr solution and bromine was used to obtain 4,7-dibromo-2-(6-bromohexyl)-2*H*- benzo[*d*][1,2,3] triazole was obtained as light yellow oil. For stannylation of 2,3-dihydrothieno[3,4-*b*][1,4]dioxine, at -78 °C, under argon atmosphere, to a solution of 3,4-Ethylenedioxythiophene (EDOT) and THF, n-butyl lithium was added slowly. Then, tributyltin chloride was added very slowly. 4,7-Dibromo-2-(6-bromohexyl)-2*H*-benzo[*d*][1,2,3] triazole and tributyl(2,3-dihydrothieno[3,4-*b*][1,4]dioxin-5-yl)stannane were dissolved in anhydrous THF) and dichlorobis(triphenylphosphine)-palladium(II)

was added at room temperature to synthesize 2-(6-bromohexyl)-4,7-bis(2,3-dihydrothieno[3,4-*b*][1,4]dioxin-5-yl)-2H-benzo[*d*][1,2,3]triazole. A mixture of 2-(6-bromohexyl)-4,7-bis(2,3-dihydrothieno[3,4-*b*][1,4]dioxin-5-yl)-2H-benzo[*d*][1,2,3]triazole and potassium phthalimide in DMF was allowed to get 2-(6-(4,7-bis(2,3-dihydrothieno[3,4-*b*][1,4]dioxin-5-yl)-2H-benzo[*d*][1,2,3]triazol-2-yl)hexyl)isoindoline-1,3-dione as a yellow solid. To a solution of 2-(6-(4,7-bis(2,3-dihydrothieno[3,4-*b*][1,4]dioxin-5-yl)-2H-benzo[*d*][1,2,3]triazol-2-yl)hexyl)isoindoline-1,3-dione in ethanol, hydrazine monohydrate was used to obtain the target compound 6-(4,7-bis(2,3-dihydrothieno[3,4-*b*][1,4]dioxin-5-yl)-2H-benzo[*d*][1,2,3]triazol-2-yl)hexan-1-amine (BEDOA-6).

<sup>1</sup>H NMR (400 MHz, CDCl<sub>3</sub>): δ (ppm) 8.05 (s, 2H), 6.41 (s, 2H), 4.72 (t, J=7.1 Hz, 2H), 4.23 (m, 4H), 4.20 (m, 4H), 2.58 (t, J=6.5, 2H), 2.51 (b, 2H), 1.42-1.28 (m, 8H).

<sup>13</sup>C NMR (100 MHz, CDCl<sub>3</sub>): δ (ppm) 140.3, 138.0, 122.2, 119.7, 116.5, 112.6, 99.2, 63.5, 63.0, 55.1, 40.6, 32.1, 28.5, 25.0, 24.8. HRMS: Calculated [M]<sup>+</sup> 499.1474, Measured [M]<sup>+</sup> 499.1459

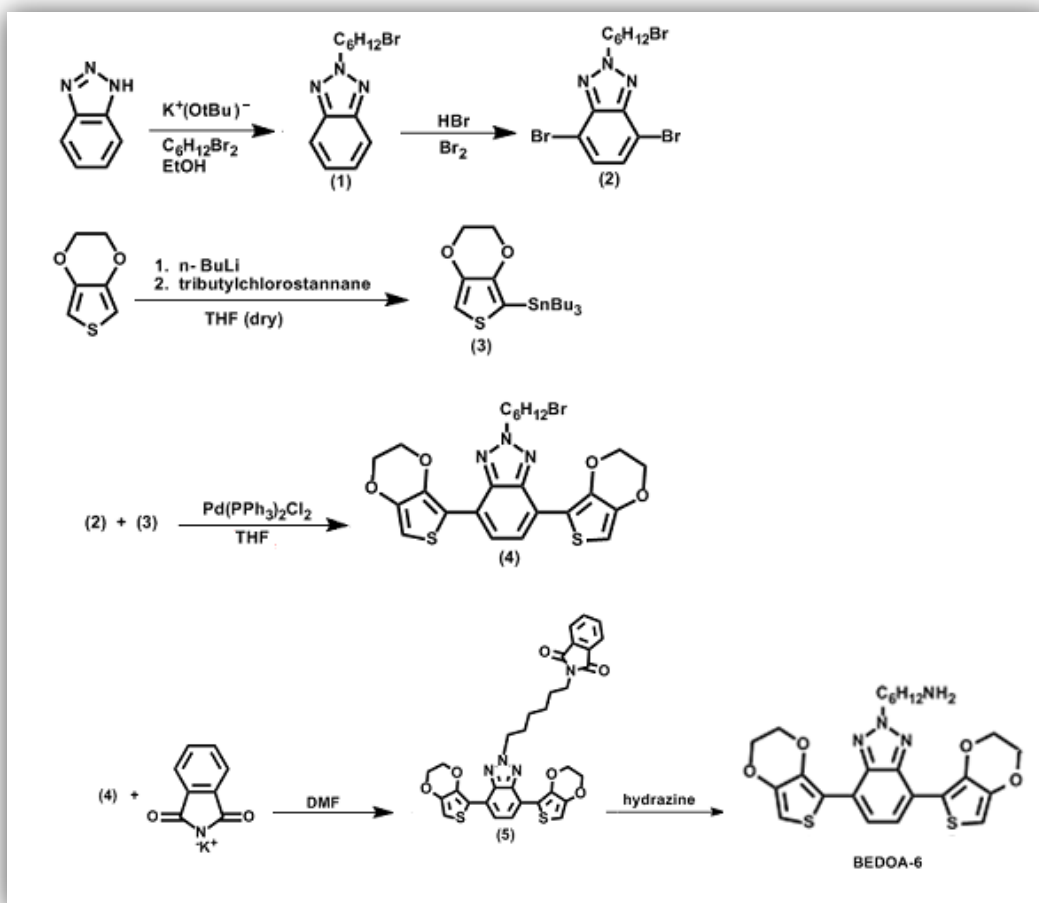


Figure 2.1. Synthetic route to BEDOA-6

#### 2.4. Electrochemical Polymerization of the Monomer

Spectroscopic grade graphite rods were polished on an emery paper and washed thoroughly with distilled water. In order to achieve electrochemical polymerization and film deposition, the monomer was subjected to cyclic voltammetry (CV) in DCM solution containing 0.1 M TBAPF<sub>6</sub> as the supporting electrolyte. Repeated potential-scan electropolymerization of 0.01 M monomer in 0.1 M TBAPF<sub>6</sub>/DCM solvent-electrolyte couple on the graphite electrode was performed at a scan rate of 100 mV/s.

## **2.5.Construction of Biosensors**

### **2.5.1. PMMA/laponite nanocomposite/ poly(BEDOA-6)/GOx Biosensor**

For the immobilization of enzyme, the nanocomposite (laponite and poly(methyl methacrylate) (PMMA)) solution was used. 4 mg clay-laponite was stirred in 5 mL distilled water for 2.5 days at 1000 rpm. Then, a proper amount of GOx solution (2.5 mg GOx in 5  $\mu$ L 50 mM sodium phosphate buffer, pH 7.0) was mixed with clay dispersion solution (3  $\mu$ L clay-water dispersion). This solutions were spread over the polymer coated electrodes and glutaraldehyde solution (5  $\mu$ L 1% GA, in 50 mM sodium phosphate buffer, pH 7.0) was then added as cross-linker and the electrodes were allowed to stand at ambient conditions to dry for 120 min. After the immobilization, the electrode surface was washed with water and the prepared electrode was stored at + 4 ° C overnight. Figure 2.2 illustrates the preparation for the proposed sensing system.

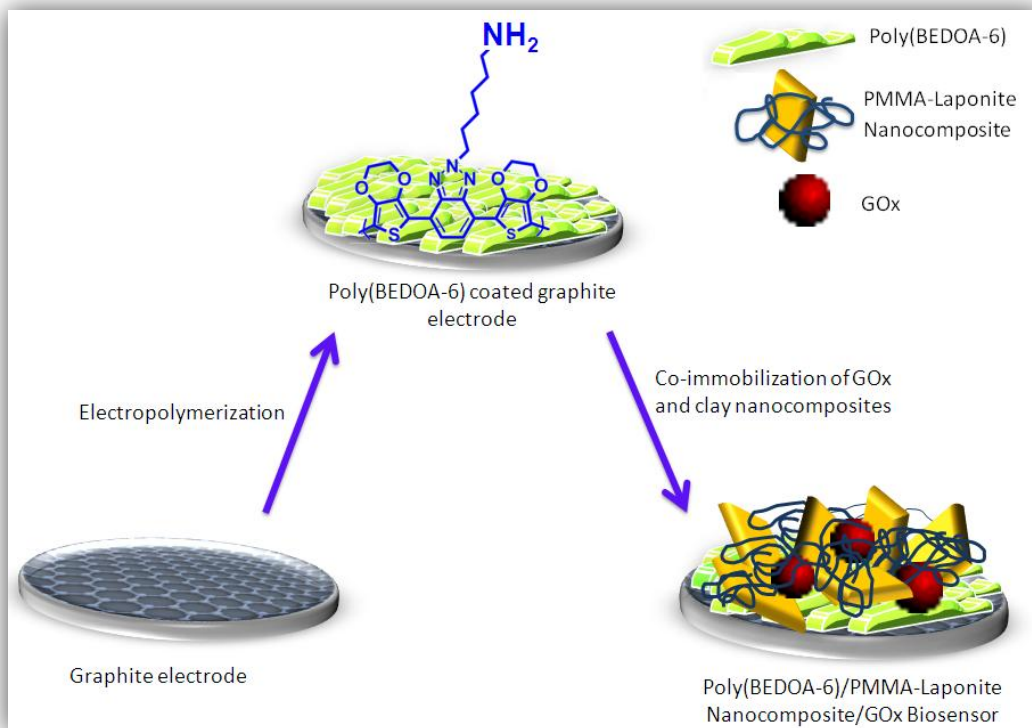


Figure 2.2. Schematic representation of PMMA/laponite nanocomposite/poly(BEDO-6)/GOx Biosensor

### 2.5.2. Au NPs/MPA/ poly(BEDO-6)/GOx Biosensor

A self-assembled monolayer of mercaptopropionic acid (MPA) was formed by adding 20  $\mu\text{L}$  of MPA into 1.0 mL of the Au NPs solution via 30 s stirring. Then, this mixture was kept at 4  $^{\circ}\text{C}$  overnight. MPA modified Au NPs (Au NPs/MPA) solution was prepared before each immobilization, freshly.

After deposition of BEDOA-6 on the electrode surface by electropolymerization using cyclic voltammety, for the immobilization of enzyme, suitable amount of GOx solution (1.5 mg (60 U) in 5.0 mL, 50 mM sodium phosphate buffer (pH 7.0)) was prepared in a vial. Moreover, 0.4 M EDC, 0.1 M NHS and modified Au NPs/MPA solution (4.0  $\mu\text{L}$ )

were mixed in a separate vial and kept at room temperature for 20 min where crosslinking agents activated the carboxylic acid moieties of the reagents. Enzyme and nanoparticle solutions were mixed homogeneously and spread over the polymer coated electrode surface and the electrodes were allowed to stand at ambient conditions to dry for 3 h. The enzyme electrodes were then rinsed with distilled water to remove unbound enzyme. The electrodes were kept at 4 °C overnight. The solutions were prepared freshly prior to preparation of the biosensors. Figure 2.3 displays the procedure for the construction of the proposed amperometric glucose biosensor.

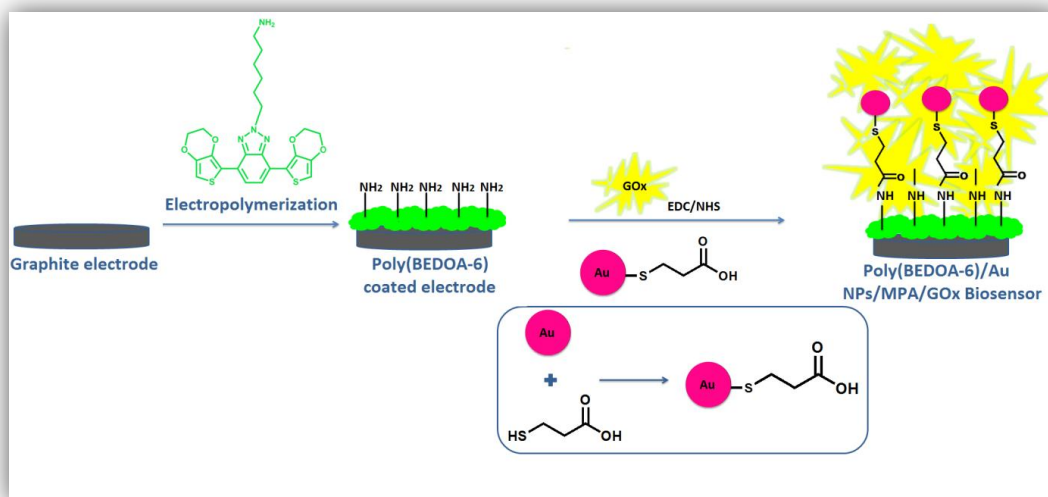


Figure 2.3. Schematic representation of Au NPs/MPA/ poly(BEDO-6)/GOx biosensor

## 2.6. Amperometric Measurements

All amperometric studies were performed in 10 mL buffer solution. In this method, under constant potential, the current change due to the enzymatic reactions was measured. After the three electrodes system was constructed, applied potential was chosen as - 0.7 V since at that potential oxygen is reduced to hydrogen peroxide; as a result, oxygen consumption can be monitored [96]. When the signal baseline reaches a

steady state, certain amount of glucose was injected to the reaction cell. At this point, the biosensor response with respect to the current change ( $\mu\text{A}$ ) was detected when equilibrium was established (Figure 2.4). Buffer solution was refreshed and enzyme electrodes were washed with distilled water, kept in buffer solutions for 5 min after each measurement.

In all amperometric studies, each measurement was carried out three times repetitively, results were recorded and standard deviations were calculated. In the figures, error bars show the standard deviation (SD) of the measurements.

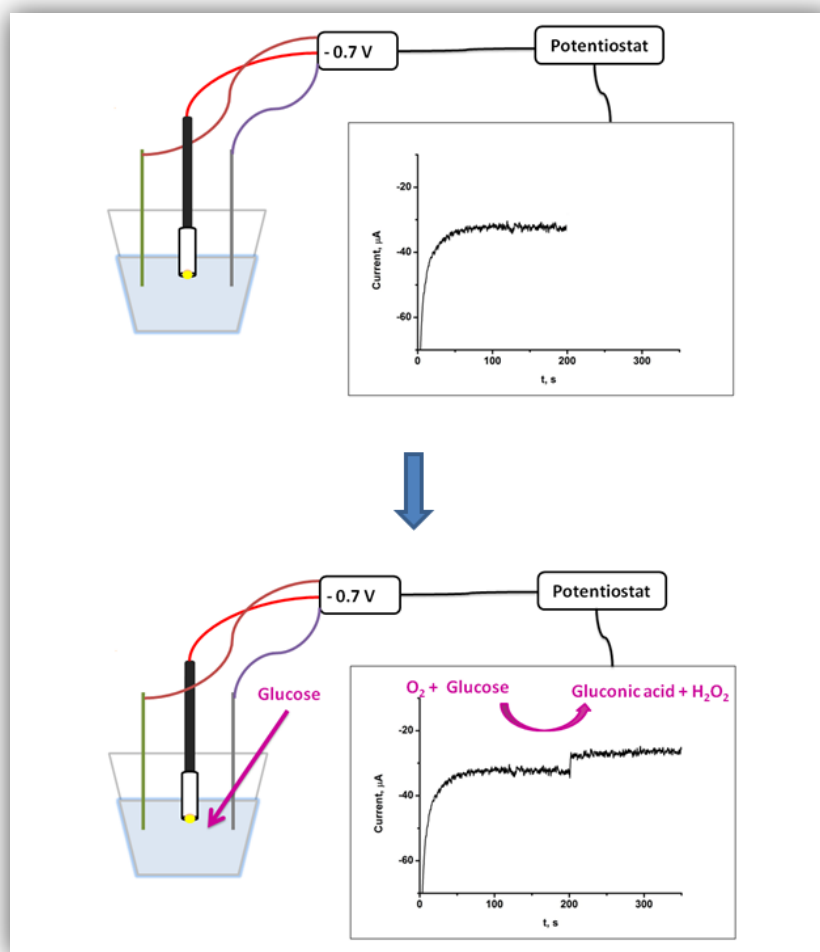


Figure 2.4. Representation of amperometric measurement procedure

## **2.7.Effect of nanostructure addition on biosensor responses**

### **2.7.1. PMMA/laponite nanocomposite/ poly(BEDO-6)/GOx Biosensor**

To prove the contribution of PMMA/laponite nanocomposite on poly(BEDO-6)/GOx biosensor response, two different electrodes were prepared with and without nanocomposite while keeping the other ingredients in constant amount. Amperometric measurements were carried out in a 10 mL 50 mM NaOAc buffer solution (pH 5.5) by applying a constant potential of - 0.7 V. Changes in current were recorded upon glucose addition as a substrate and calibration curves were drawn for these two different electrodes.

### **2.7.2. Au NPs/MPA/ poly(BEDO-6)/GOx Biosensor**

In order to investigate the effect of Au NPs and modified Au NPs on the performance of glucose biosensor, different biosensors were prepared with Au NPs and modified Au NPs (Au NPs/MPA). This was also repeated in the absence of Au NPs just by keeping the enzyme amount and polymer thickness constant.

## **2.8.Optimization of Biosensor Performance**

### **2.8.1. Optimization of Conducting Polymer Thickness**

Quality of the polymer film is affected by the duration of electropolymerization; consequently, the properties like stability of the biosensor depend on film thickness. The polymer layer thickness is directly related to scan number during the electropolymerization. The thickness can be measured in terms of the charge passing through the cell [97]. In order to detect the optimum thickness, polymers with different

thicknesses were deposited on the graphite working electrode with different number of scans. After polymerization in different scan numbers, using same amount of reagents, different biosensors were prepared and the amperometric responses to same amount of glucose were recorded. The biosensor with optimum polymer layer thickness gives the highest amperometric response. For further experimental steps, this optimum thickness was selected.

### **2.8.2. Optimization of Enzyme Amount**

In order to examine the relationship between enzyme amount and biosensor response, different amounts of enzyme were used to construct different biosensors. Amperometric responses were detected and compared. By keeping other parameters like polymer thickness, pH and crosslinker amount constant, the optimum enzyme amount was determined.

### **2.8.3. Effect of pH**

Glucose oxidase is acidic (pI=4.2) and active over a wide range of pH values (pH 3.0–8.0) [97]. Regarding the influence of the pH of working buffer on the amperometric response of biosensors, pH dependence of the responses was investigated over a pH range. Buffer solutions in different pH affect the enzyme activity. Thus, after optimization of pH of working buffer solutions, the measurements were performed in that working condition for further studies.

### **2.8.4. Optimization of Nanostructures Amounts**

The amounts of nanostructures and the adsorbed glucose oxidase might influence the biosensor response, and have an effect on the performance of the developed biosensor. The effect of the composition of nanostructures on the biosensor response was

investigated. Amperometric responses of electrodes prepared with same amount of GOx and different amounts of nanostructures were recorded to obtain the most effective combination.

## 2.9. Analytical characterization of Biosensors

The analytical characteristics of the sensor were examined under optimized conditions using glucose as the substrate. All the experiments were performed at ambient conditions. Calibration curve was plotted with respect to substrate concentration (mM) versus current ( $\mu\text{A}$ ). Several analytical parameters like linearity equations, linear dynamic ranges with limits of detection (LOD) were investigated under the optimized conditions.

Also, kinetic parameters were investigated. Since amperometric detection technique measures current with respect to time, apparent Michealis-Menten constant,  $K_M^{app}$ , and  $I_{max}$  were obtained from Lineweaver-Burk plots [99].

The repeatability of the analytical responses corresponding to exact glucose solutions was analyzed for ten times. The standard deviation (SD) and the relative standard deviation (RSD) were calculated. In order to test shelf life stability, the optimized biosensor was used in the detection of glucose concentration every other day until activity loss was observed. Biosensor systems were stored at  $+4^\circ\text{C}$  when not in use.

Furthermore, possible interferents were analyzed with the proposed biosensors. Ascorbic acid, cholesterol and urea (between 0.01 and 0.1 M) were examined by injecting into the reaction cell instead of glucose during amperometric measurements under optimized working conditions by applying  $-0.7\text{ V}$ .

## **2.10. Sample Application**

### **2.10.1. PMMA/laponite nanocomposite/ poly(BEDO-6)/GOx Biosensor**

The GOx biosensor was tested to analyze the glucose amount in real human blood serum. The real human serum samples were obtained from Middle East Technical University (METU) Medical Center from patients who volunteered for that matter and all experiments were carried out in compliance with relevant and ethical laws. The serum samples were added to the reaction cell instead of the substrate. The reaction medium consists of 10 mL 50 mM NaOAc (pH 5.5) buffer solution. By adding different volume of serum samples without any pre-treatment, the concentration in the reaction cell was arranged in order to be in the linear range of the glucose biosensor. Then, signals were recorded and concentrations were calculated from the calibration curve. Values obtained were compared with glucose amounts analyzed by the local hospital. The measured results by the proposed biosensing system were compared.

### **2.10.2. Au NPs/MPA/ poly(BEDO-6)/GOx Biosensor**

Glucose contents in various beverages were detected using the biosensor. Beverage samples can be used without any pretreatments for the analyses. In those measurements, instead of glucose, beverage samples were injected as the substrate directly into the measurement cell. The reliability of the biosensor was determined with a reference method using a commercial enzyme assay kit for glucose measurements. This enzyme assay kit is based on GOx-PAP method including glucose oxidase, peroxidase, phenol and 4-aminophenazone. Colorimetric test depends on enzymatic oxidation of glucose by the help of glucose oxidase. Hydrogen peroxide, the product, reacts with phenol and 4-aminophenazone in the presence of peroxidase which gives a red-violet color via

quinoneimine dye indicator [100]. Real samples with no dilution were analyzed both with the proposed sensing system and a spectrophotometric technique.



## CHAPTER 3

### RESULTS AND DISCUSSION

#### 3.1. Electrochemical Studies

##### 3.1.1. Electrochemical Polymerization of the Monomer

Electrochemical polymerization and film deposition were achieved via cyclic voltammetry. Repeated potential-scan electropolymerization on the graphite electrode up to 10 cycles is shown in Figure 3.1. As seen from the figure, during the first cycle, monomer oxidation occurs followed by a reduction. While the polymerization proceeds during scanning, the increase in the current density shows the successful deposition of the polymer on the working electrode. The deposited charge increases with the increasing cycles. After the polymerization, the surface of the electrode was rinsed with distilled water to remove the impurities.

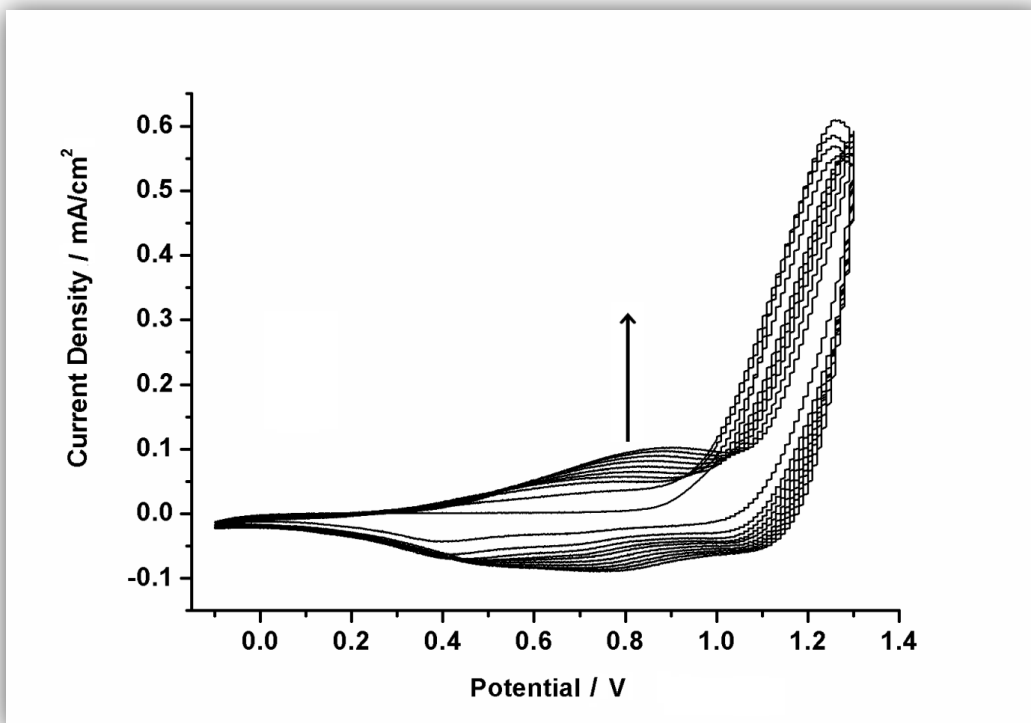


Figure 3.1. Repeated potential scan electropolymerization of monomer at 100 mV/s vs. Ag reference electrode in 0.1 M TBAPF<sub>6</sub>/DCM

### 3.1.2. Electrochemical Behavior of the Conducting Polymer

In order to investigate the diffusion property of thin polymer film (30 cycles), the corresponding polymer was subjected to scan rate experiments. In scan rate studies, a monomer free system was used and CVs were recorded between 0 and 1.0 V vs. Ag wire reference electrode (Figure 3.2). The polymer redox processes are quasi-reversible and since the polymer is immobilized at the electrode surface, the redox processes (doping-dedoping) are not diffusion controlled. Thus, the investigation of the peak current intensity with respect to the scan rate will indicate the nature of electrochemical process as being diffusion controlled or whether the polymer is well-adhered to the electrode surface or not. The process is non-diffusion controlled as the current density scan rate graph is linear for both oxidation and reduction. It proves that the thin film is

well-adhered to the electrode surface and enables the electron transfer efficiently while improving the electrochemical performance of the corresponding biosensors.

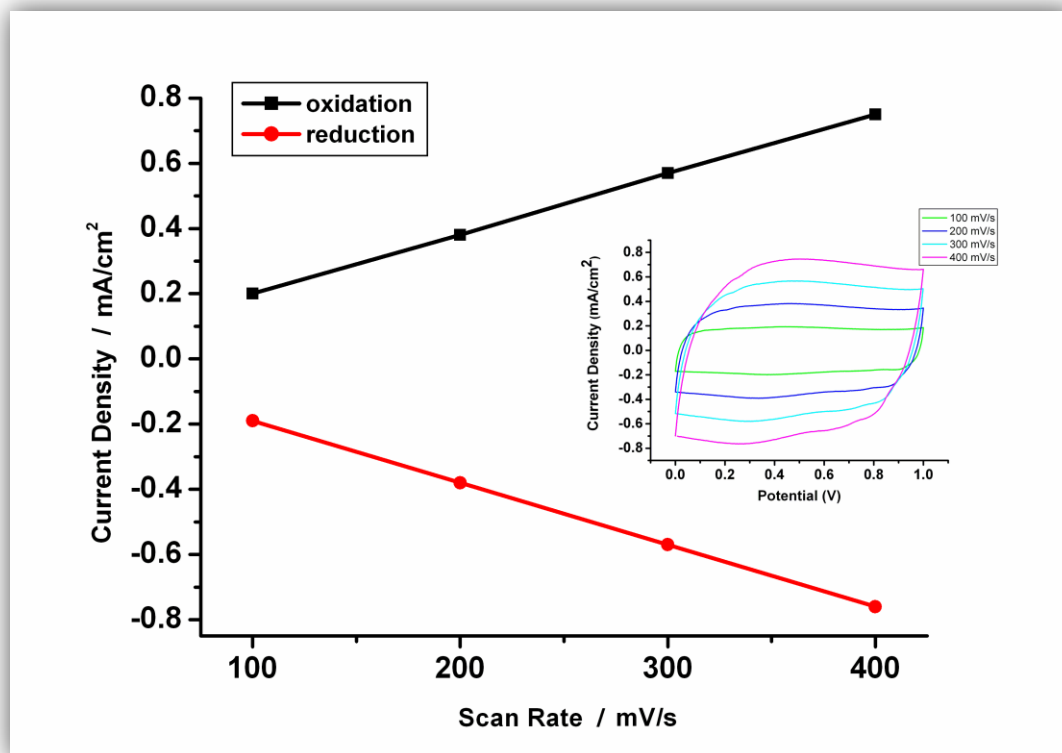


Figure 3.2. Scan rate dependence of poly(BEDO A-6) film in 0.1 M TBAPF<sub>6</sub>/DCM solvent/electrolyte system at 100, 200, 300 and 400 mV/s

To examine the stability of the polymer film between doped and neutral states, poly(BEDO A-6) film was deposited on the electrode and switched between its redox states in TBAPF<sub>6</sub>/DCM electrolyte/solvent couple for 100 times. Poly(BEDO A-6) film showed high stability since 96 % of the electroactivity remains even after 100 cycles (Figure 3.3). The stability data of the poly(BEDO A-6) film confirm that the polymer has a potential use in electrochemical applications such as biosensors. This brings the successful repeatable use of the biosensor.

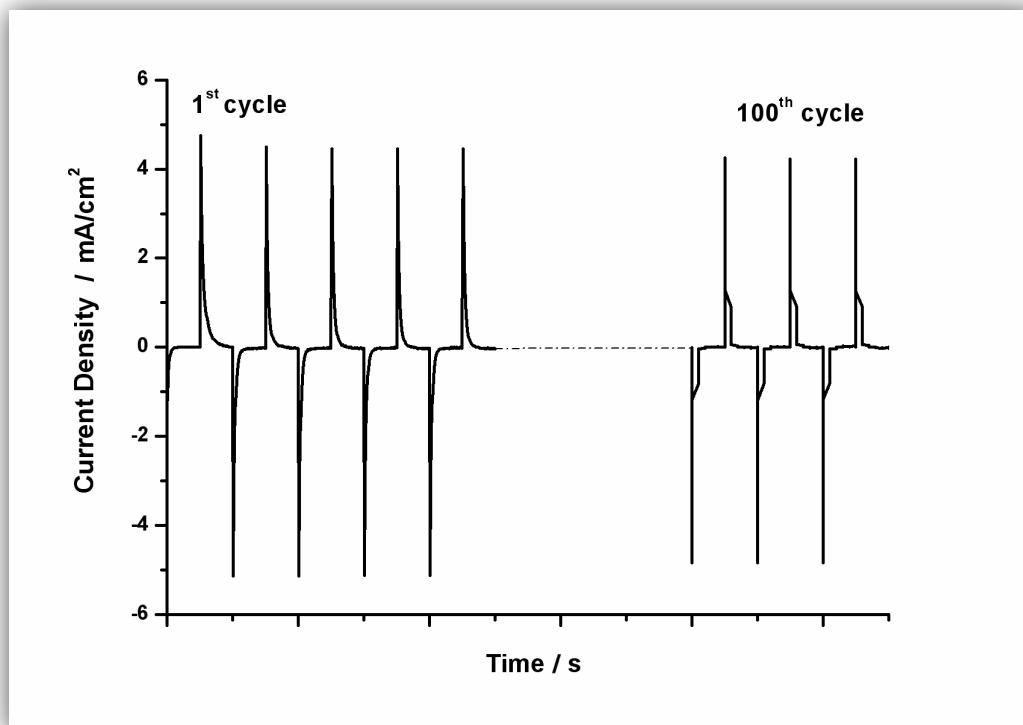


Figure 3.3. Chronoamperometry experiment for poly(BEDO-6) on the electrode in 0.1 TBAPF<sub>6</sub>/DCM while switching between neutral and oxidized states. Each interval on the x axis stands for 5 s

### 3.2. PMMA/laponite nanocomposite/ poly(BEDO-6)/GOx Biosensor

#### 3.2.1. Investigation of biosensor construction method

Different preparation techniques were tried to detect the most proper way of construction of the proposed biosensor. For the first one, after electropolymerization, clay dispersion was added on the electrode and then a certain amount of glucose oxidase was spread over the electrode following glutaraldehyde solution. The second preparation technique was based on that after electropolymerization, glucose oxidase and clay dispersion solution were mixed and added on the polymer coated electrode

surface and then GA solution were used. As seen in Figure 3.4, second technique is the most efficient one, hence it was used for further experiments.

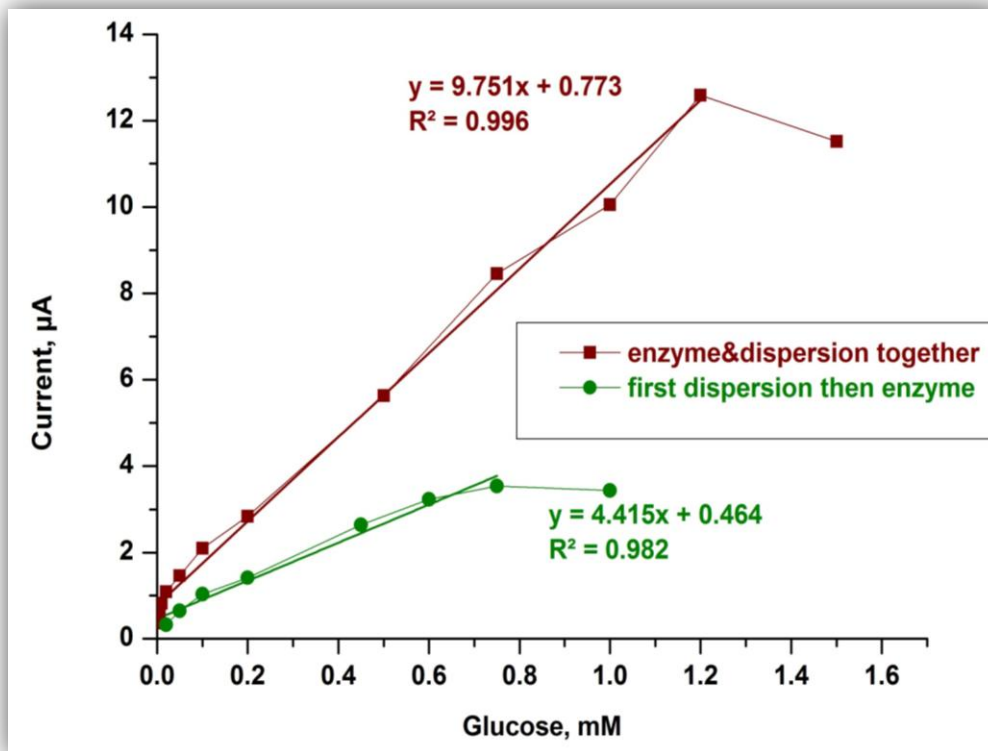


Figure 3.4. Effect of different preparation technique on biosensor response

### 3.2.2. Effect of PMMA/Laponite Nanocomposite dispersion for biosensor construction

Since clay mixture was not soluble in water, there could be a dispersion problem during the biosensor preparation. Nevertheless, this mixture was fully dissolved in DCM. Therefore, efficiency of nanocomposite dispersion on the detection signal was investigated. As seen in Figure 3.5, although clay mixture was not dissolved in water, it had a better effect on biosensor responses.

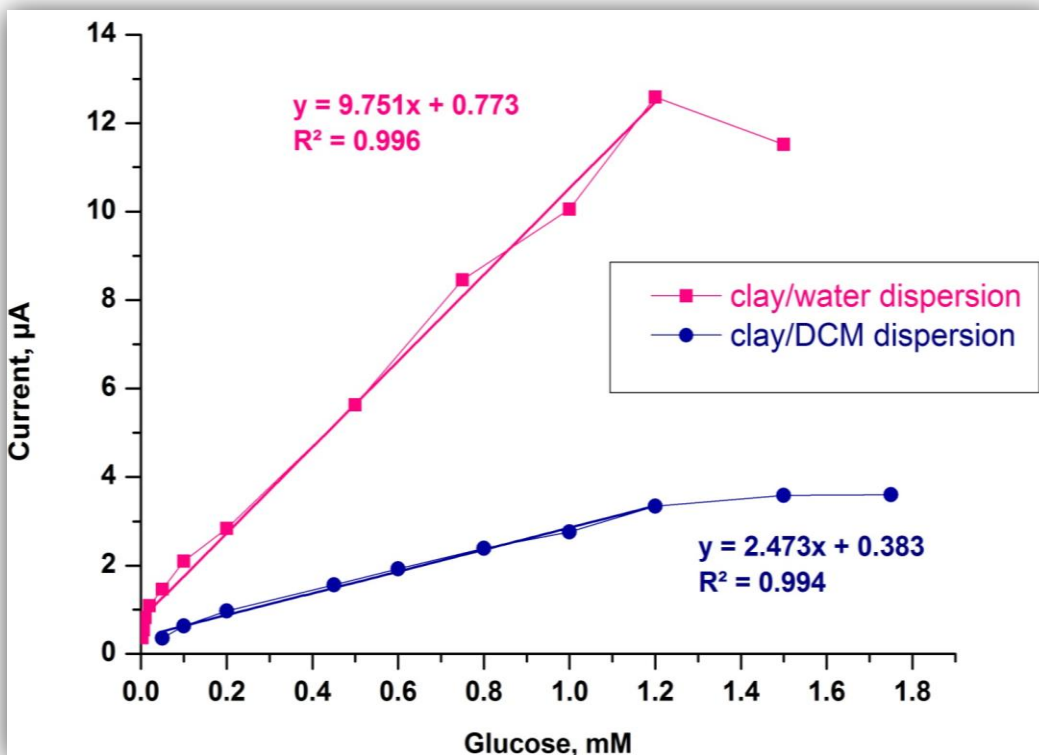


Figure 3.5. Effect of clay dispersion in water and dichloromethane on biosensor response

### 3.2.3. Effect of PMMA/Laponite Nanocomposite Introduction

Taking the advantage of the clay nanocomposite for its high chemical stability, well adsorption capacity, high surface area and intercalation property [85], an efficient glucose biosensor design was achieved. The biosensor performance after addition of nanocomposite to the biosensing system justified the contribution of PMMA/laponite nanocomposite on poly(BEDO A-6)/GOx on biosensor response. Figure 3.6 illustrates amperometric responses of two different prepared electrodes. Moreover, possible electrostatic interactions between positively charged conducting polymer [101] and negatively charged enzyme [102] and laponite molecules [103] may also improve the biosensor responses due to the enhanced stabilization of the enzyme molecules on the

electrode surface. These stronger interactions contribute stability of the enzyme molecules and generation of appropriate microenvironment promoting the reactions on the active site of the enzyme molecules.

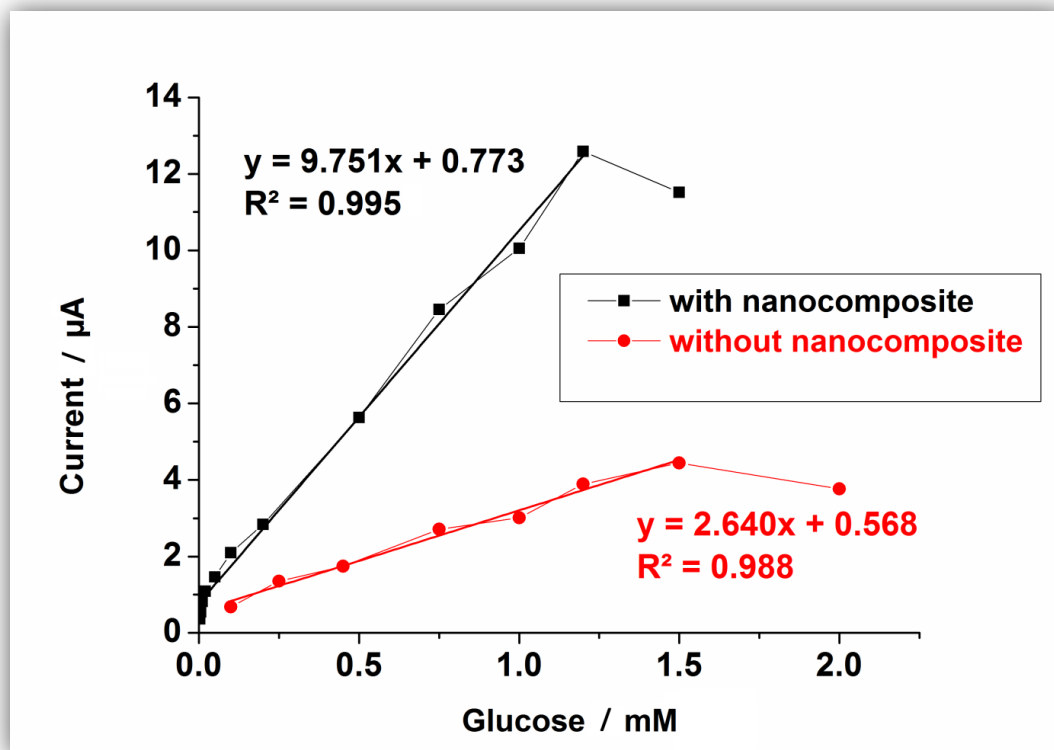


Figure 3.6. Effect of nanocomposite addition on poly(BEDOA-6)/GOx biosensor (in 50 mM NaOAc buffer solution, pH 5.5, 25 °C, -0.7 V). Error bars show the standard deviation (SD) of three measurements

### 3.2.4. Optimization of Biosensor Performance

#### 3.2.4.1. Optimization of Conducting Polymer Thickness

The effect of film thickness on the biosensor responses was shown in Figure 3.7. Polymers with different thicknesses were deposited on graphite working electrodes with 20, 30, 40, 50 scans to find the optimum thickness. The highest response was recorded with 30-cycle deposition. The charges and film thicknesses for 20, 30, 40 and 50-cycle

polymer films were calculated as 0.56 mC (12 nm), 0.72 mC (16 nm), 0.90 mC (20 nm) and 1.63 mC (36 nm), respectively. Due to the possible diffusion problems which may arise from high polymer layer thickness, lower responses were recorded for the higher scan numbers. On the other hand, not only to achieve a strong covalent binding between enzyme molecules and polymer matrix, but also to stabilize the huge protein molecules and nanocomposite structures on the electrode surface, a sufficient amount of polymer layer has to be generated. Moreover, in blank experiments, to observe the nourishing impact of conducting polymer on the biosensor responses, a biosensor containing the same amount of nanocomposite without a poly(BEDO-6) layer was prepared. At optimized conditions, the biolayer was directly adsorbed on graphite working electrode; nevertheless, lower response signals were recorded with a linearity between 0.02 and 0.6 mM for glucose and an equation of  $y = 4.846x + 0.400$ ,  $R^2 = 0.991$ .

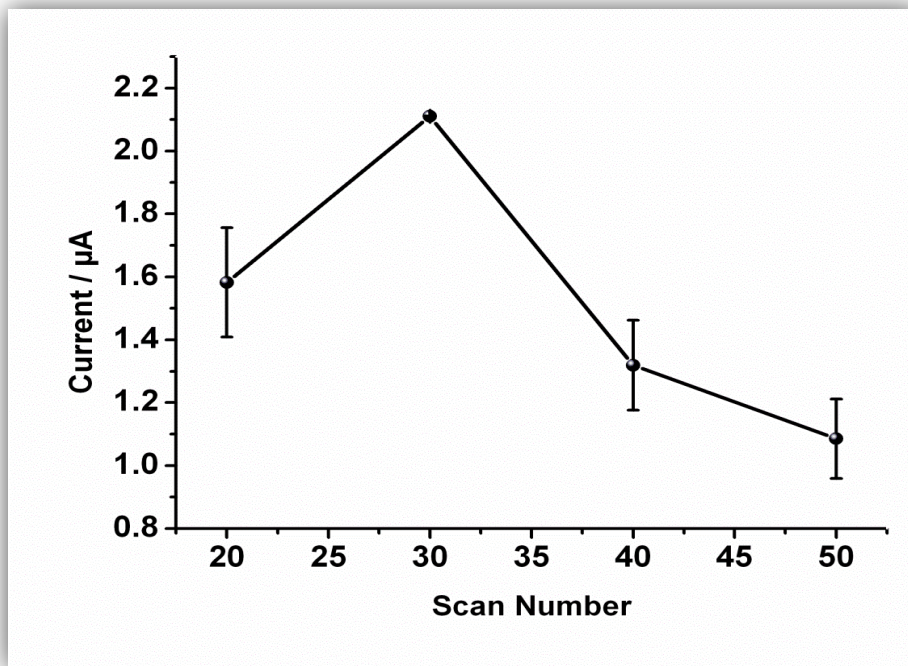


Figure 3.7. The effect of the polymer film thickness on biosensor response (in 50 mM NaOAc buffer solution, pH 5.5, 25 °C, -0.7 V, 0.45 mM glucose). Error bars show the standard deviation (SD) of three measurements

### 3.2.4.2. Optimization of enzyme amount

To optimize the enzyme amount, three different enzyme electrodes were prepared with different GOx amounts (1.50 mg (69 U), 2.50 mg (115 U) and 3.50 mg (162 U)). To stabilize the enzyme on the polymer surface, GA (1%) was used as the crosslinker [102]. The highest signals were obtained with 2.50 mg GOx for the proposed biosensor (Figure 3.8).

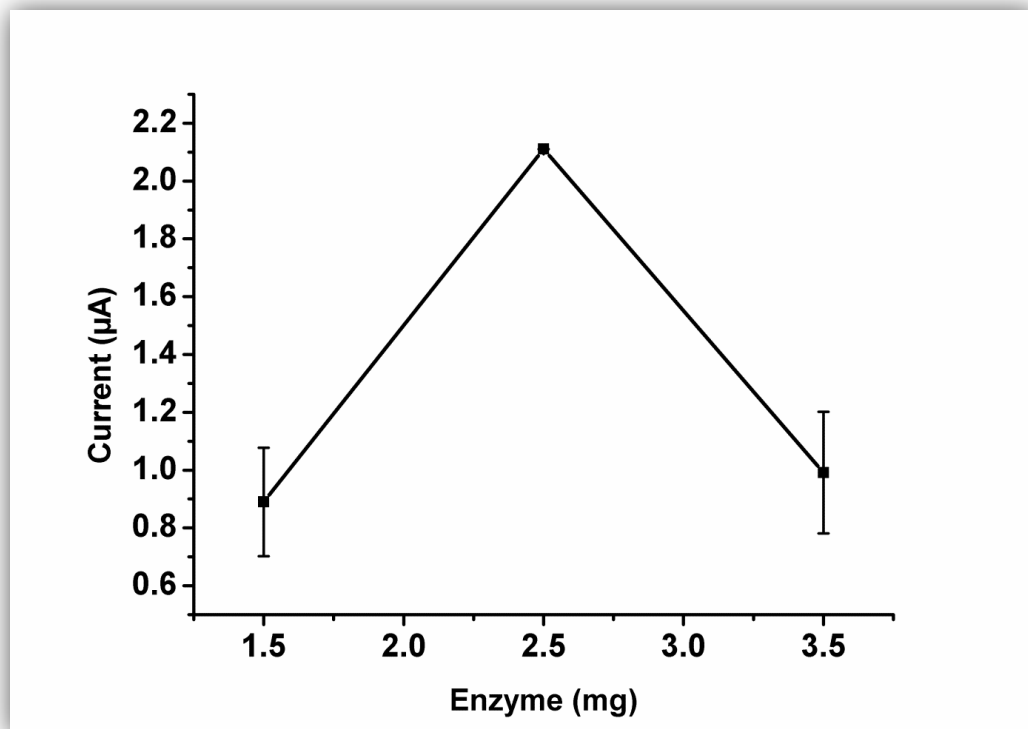


Figure 3.8. The effect of enzyme amount (in 50 mM NaOAc buffer solution, pH 5.5, 25 °C, -0.7 V, 0.45 mM glucose). Error bars show the standard deviation (SD) of three measurements

### 3.2.4.3. Optimization of crosslinker (glutaraldehyde) amount

Glutaraldehyde is an important crosslinking agent to obtain successful immobilization leading to effective covalent binding between functional group of the polymer and the biomolecule. To obtain the ideal crosslinking between the amino groups in the protein structure and amino groups of the polymer, glutaraldehyde amount was optimized. Three different GA solutions were prepared (0.5 %, 1 % and 2.5 %) and they were used in preparation of the GOx biosensors. The highest response was recorded the one using 1 % GA solution (Figure 3.9).

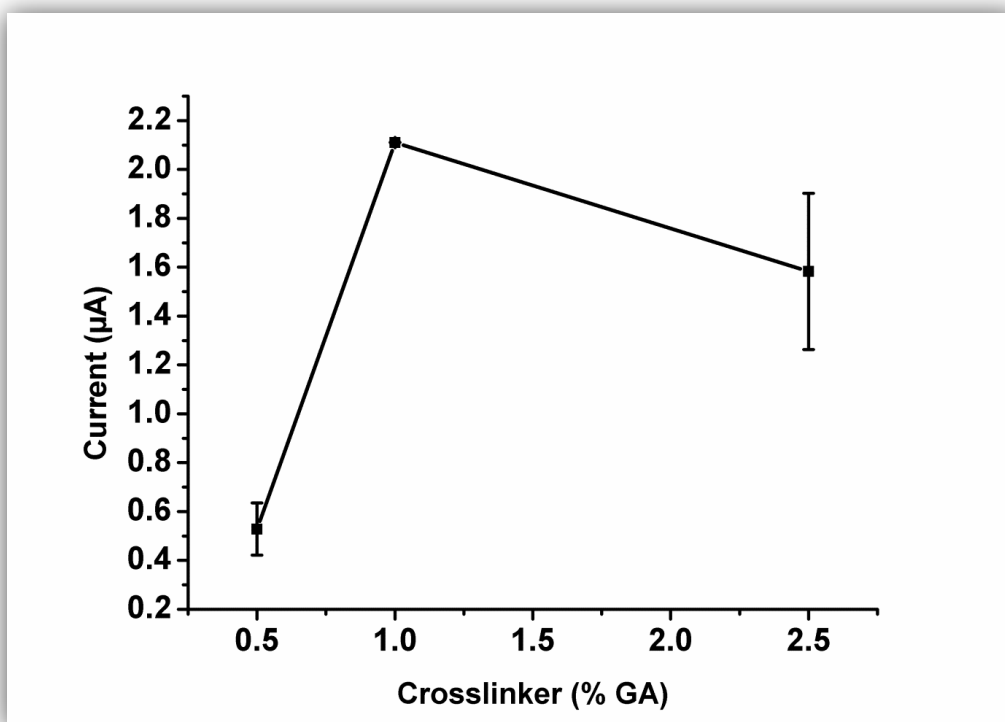


Figure 3.9. The effect of crosslinker amount (in 50 mM NaOAc buffer solution, pH 5.5, 25 °C, -0.7 V, 0.45 mM glucose). Error bars show the standard deviation (SD) of three measurements

#### 3.2.4.4. Optimization of pH

pH dependence of the responses was investigated over a pH range between 3.5 and 8.0 with sodium citrate buffer (50 mM) at pH 3.5, sodium acetate buffer (50 mM) at pH 4.0 – 6.0 and phosphate buffer (50 mM) at pH 6.5 – 8.0 in the presence of 0.45 mM glucose. The biosensor revealed the best result at pH 5.5 as given in Figure 3.10. pH 5.5 buffer was used as the working solution.

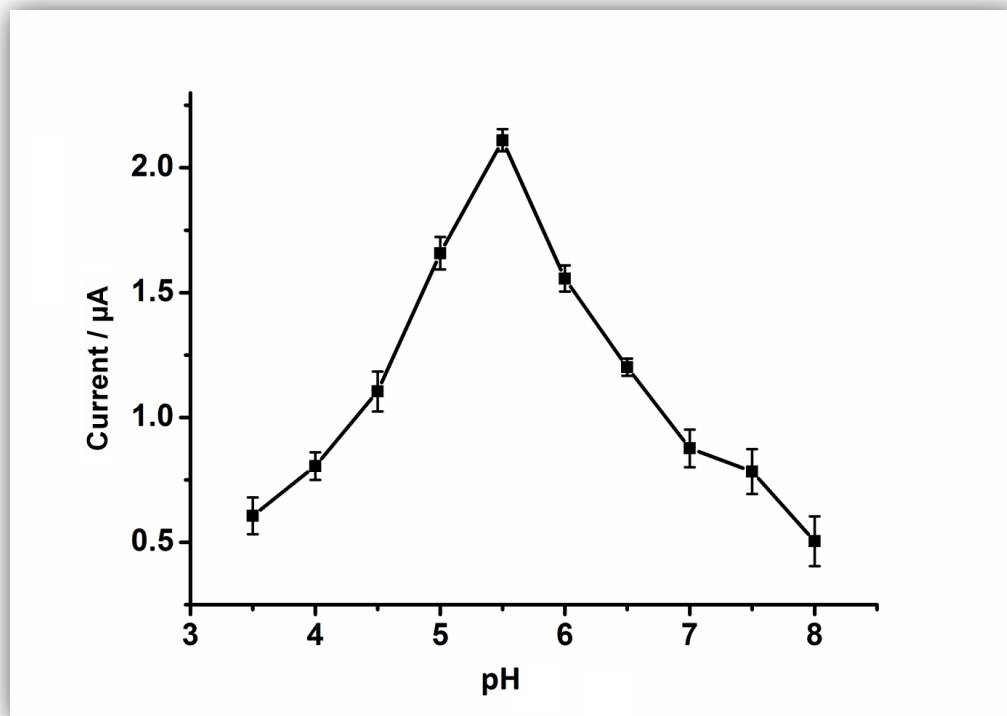


Figure 3.10. The effect of pH (in 50 mM NaOAc buffer solution, 25 °C, -0.7 V, 0.45 mM glucose). Error bars show the standard deviation (SD) of three measurements

### 3.2.4.5. Optimization of nanocomposite amounts

The effect of the composition of PMMA/ laponite clay nanocomposite suspension on the biosensor response was investigated. Amperometric responses of electrodes prepared with same amount of GOx and different amounts of nanocomposite (clay suspensions with 2, 4 and 6 mg nanocomposite by dispersing in 5 mL water) were recorded to obtain the most effective dispersion. The highest response to glucose was observed in the 4 mg/5 mL water nanocomposite dispersion containing biosensor (Figure 3.11).

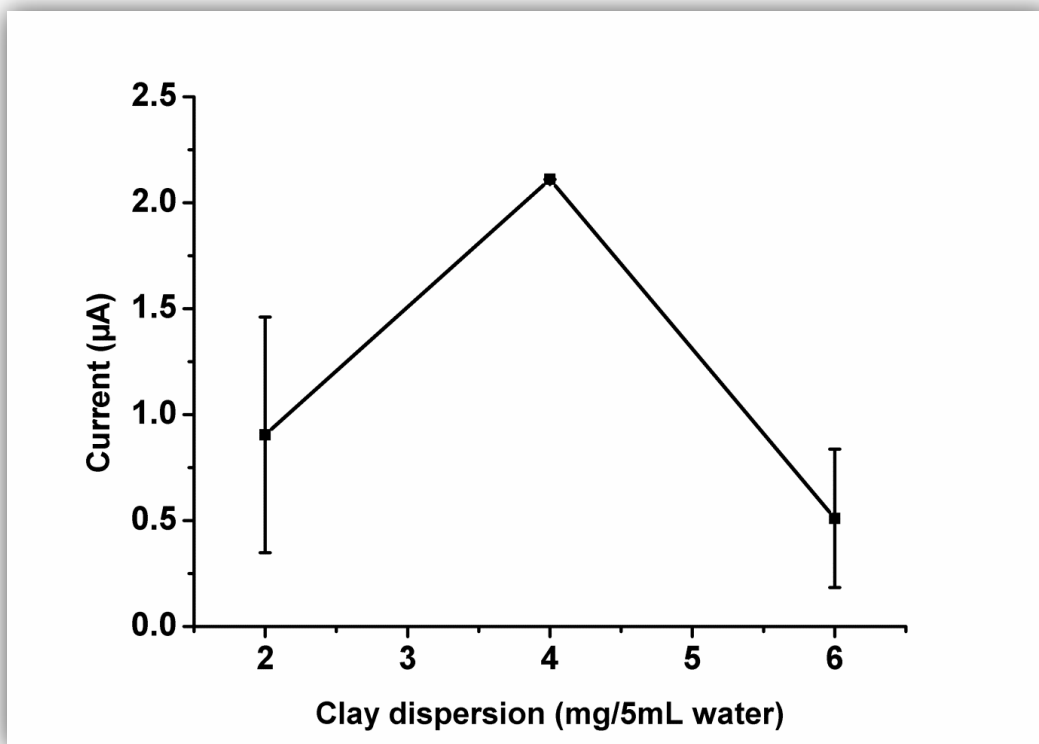


Figure 3.11. The effect of clay dispersion in 5 mL water (in 50 mM NaOAc buffer solution, pH 5.5, 25 °C, -0.7 V, 0.45 mM glucose). Error bars show the standard deviation (SD) of three measurements

### **3.2.5. Surface Characterization of the biosensor design**

In order to investigate and characterize the modifications on the graphite electrode surface, X-ray photoelectron spectroscopy (XPS) and Scanning electron microscope (SEM) experiments were carried out.

#### **3.2.5.1. X-ray photoelectron spectroscopy (XPS)**

Through XPS, the interactions and linking between free amino groups on the polymer chain and the functional amino groups on the enzyme molecules can be detected. The carbon and nitrogen signals were resolved using a fitting program as depicted in Figure 3.12. The successful immobilization of the enzyme molecules via crosslinking and the presence of PMMA nanocomposite material were confirmed with the XPS analyses. Polymer coating exhibits signals corresponding to aromatic bonds (aromatic and alkyl carbons and C-S in EDOTs at 283.9 eV and 284.6 eV, respectively), C=N and C-O groups (286.8 eV), C=N and characteristic amino groups (285.7 eV) (Figure 3.12A) [104,105]. Beyond these signals, after immobilization, characteristic PMMA signals (C-C at 285.3 eV, C-O at 287.8 eV, O-C=O at 288.7 eV) [106] and two signals at 287.8 eV and 286.7 eV (for C=O, C=N and O=C-N, respectively) indicating the presence of covalent binding attributed to the linkages with the help of glutaraldehyde were observed (Figure 3.12B) [104]. Additionally, a shake-up peak for PMMA carbons was also observed at 291.8 eV [107]. The perfect attachment of GOx to the polymer coating can also be detected from the N1s spectra. The differentiation in the nitrogen envelope after immobilization can be clearly seen in Figures 3.12C and 3.12D. The peaks centered at 399.1 eV are assigned to amine (-NH-) and C=N groups, 401.3 eV corresponds to protonated amine and nitrogens of triazole ring in the polymer backbone (Figure 3.12C) [108]. However, the decrease in the protonated nitrogens and the appearance of the new groups at 401.6 eV is attributed to the nitrogen of immobilized protein (Figure 3.12D) [104].

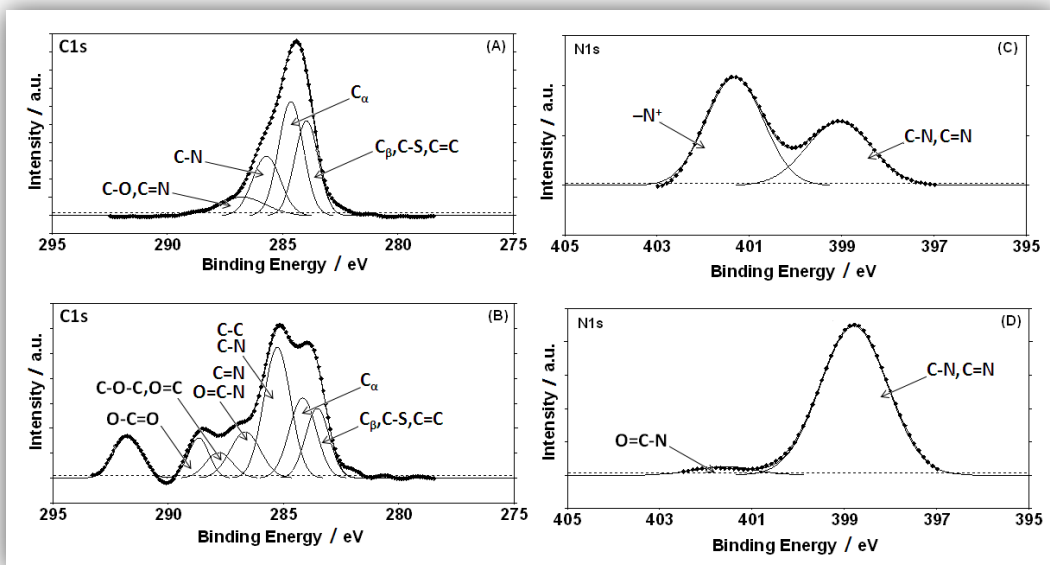


Figure 3.12. C1s and N1s XPS spectra of the polymer deposited surface (A and C) and protein immobilized onto the polymer deposited surface (B and D)

### 3.2.5.2. Scanning electron microscope (SEM)

Figure 3.13 depicts SEM images of the conducting polymer coated on graphite electrode and the polymer/ PMMA-clay nanocomposite/GOx modified electrode surfaces. The typical homogeneous, cauliflower-like structure of the conducting polymer can be observed in the first image (Figure 3.13a). After the protein-nanocomposite mixture immobilization, the change in the morphology of the polymeric composition can be clearly seen in Figure 3.13b. Compare to the polymer, the nonuniform and irregular coating on the surface was observed. The morphology in figure (b) represents the irregular and network-like structure due to the porous nature of PMMA/laponite nanocomposites. Moreover, besides the crosslinking between the polymer and the enzyme molecules, the entrapment of enzyme molecules within this porous network also enhances the high enzyme loading and stability of the biosensor keeping the biomolecules on the electrode surface firmly.

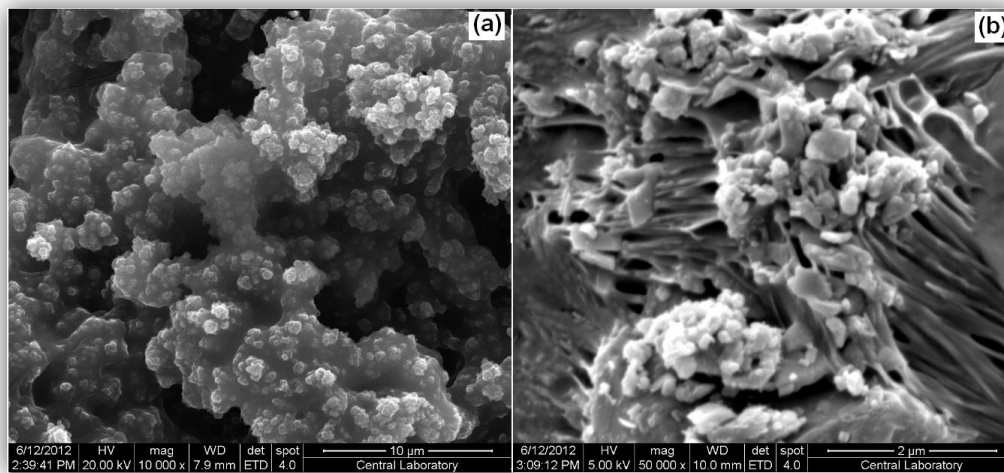


Figure 3.13. SEM images of polymer (a) before and (b) after biomolecule and nanocomposite immobilization under optimized conditions

### 3.2.6. Analytical characterization of the proposed biosensor

Calibration curve was plotted with respect to substrate concentration under optimized conditions as given in Figure 3.14. A linear relationship was observed between 2.8 mM and 1.2 mM glucose concentration satisfying the equation  $y=9.651x+0.773$  and  $R^2=0.995$  (given as inset in Figure 14). Furthermore, to calculate the limit of detection (LOD), the intercept of the linear range of the calibration curve was set as zero using  $S/N$  (signal-to-noise ratio) =3 criterion found as 1.99 mM for the biosensor. Also, kinetic parameters were investigated. Since amperometric detection technique measures current with respect to time, thus, apparent Michealis-Menten constant,  $K_M^{app}$ , and  $I_{max}$  were obtained from Lineweaver-Burk plots [99].  $K_M^{app}$  value was estimated to be 1.31 mM and  $I_{max}$  value was found as 12.59 mA for poly(BEDO A-6)/PMMA-laponite nanocomposite/ GOx biosensor.

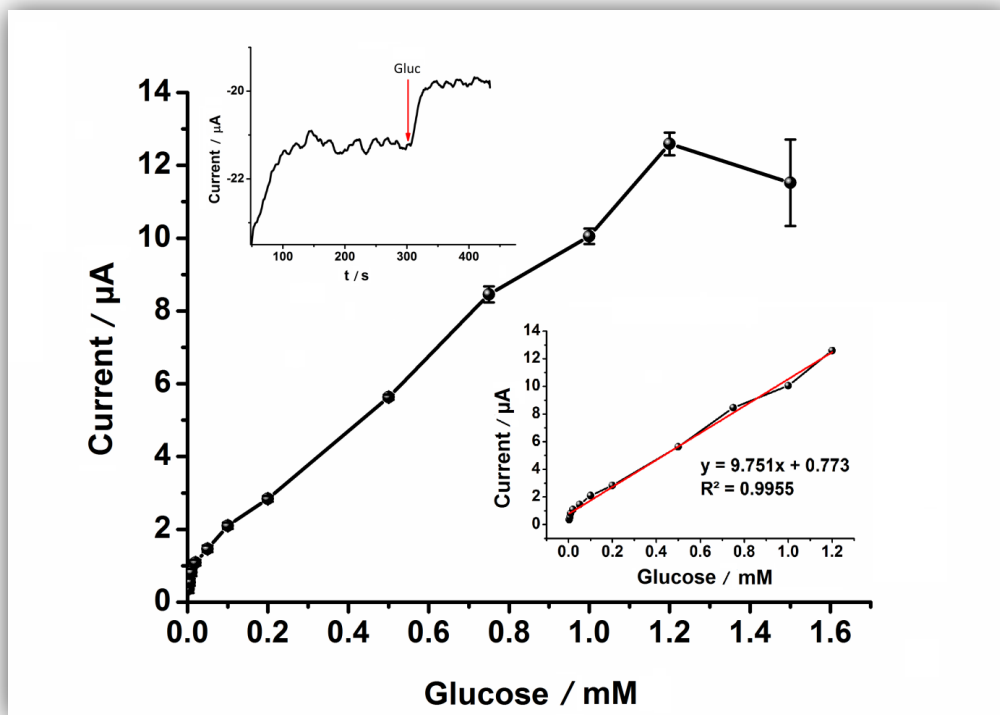


Figure 3.14. Calibration curve for glucose (in 50 mM NaOAc buffer solution, pH 5.5, 25 °C, -0.7 V). (A typical amperometric signal of the biosensor for 0.2 mM glucose and linear range as inset.) Error bars show the standard deviation (SD) of three measurements

Additionally, in order to discover the role of modifications, poly-(BEDOA-6)/GOx and PMMA-laponite nanocomposite/ GOx biosensors were also analytically characterized and illustrated in Table 3.1. As seen in Table 3.1,  $K_M^{app}$  values are close for three modifications. Thus, it shows the excellent accessibility of the enzyme molecules to the substrate in each modification. Moreover, in comparison to the others, results for poly(BEDOA-6)/PMMA-laponite nanocomposite containing surface modification illustrates well-permeability of the superior matrix. Also, PMMA-laponite nanocomposite provides a better microenvironment for GOx. Exquisite contribution of the conducting polymer taking the advantage of covalent binding of biomolecules can also be seen compared to LOD and sensitivity values which remained inferior to those

recorded for poly(BEDOA-6)/PMMA-laponite nanocomposite/GOx biosensor. Sensitivity calculations were done using the surface area of the electrode.

Table 3.1. Analytical characteristics of the biosensors

<b>Biosensor</b>	$K_M^{app}(\text{mM})/$ $I_{max}(\mu\text{A})$	<b>Sensitivity</b> $(\text{mA M}^{-1}\text{cm}^{-2})$	<b>Linear</b> <b>Range (mM)</b>	<b>LOD</b> <b>(<math>\mu\text{M}</math>)</b>
Poly(BEDOA-6)/GOx	0.96 / 6.34	11.10	0.1 - 1.5	98.10
PMMA-Laponite nanocomposite/GOx	0.43 / 5.25	20.14	0.02 - 0.6	54.0
Poly(BEDOA-6)/ PMMA-Laponite nanocomposite/GOx	1.31 / 12.59	37.16	0.0028 - 1.2	1.99

A typical amperometric response of the biosensor is shown as an inset in Figure 3.14. This rapid signal is an indication of the fast mass transfer of the substrate through the matrix. The catalytic properties of the immobilized GOx molecules are also promoted by poly(BEDOA-6)/PMMA-laponite nanocomposite matrix due to a good preservation of the accessibility of the enzyme molecules.

The repeatability of the analytical responses corresponding to 0.45 mM glucose solutions was analyzed for ten times. The standard deviation (SD) and the relative standard deviation (RSD) were calculated as  $\pm 0.2$  and 3.8 %, respectively. In order to test shelf life stability, the optimized biosensor was used in the detection of glucose concentration every other day during 6 weeks by using 0.45 mM glucose and the biosensor was stored at  $+4^\circ\text{C}$  when not in use. For a period of 6 weeks no activity loss was observed. These results proved that the covalent binding between the biomolecules and the polymer matrix and the electrostatic interactions between enzyme molecules and clay matrix improved the analytical properties and the long-term stability.

Furthermore, possible interferences were analyzed with the proposed biosensor. Ascorbic acid, cholesterol and urea (between 0.01 and 0.1 M) were examined by injecting into the reaction cell instead of glucose during amperometric measurements; however, no responses were observed for those substances revealing the interference free quality of the measurements.

### 3.2.7. Sample Application

The glucose amounts in real human blood serum samples were analyzed with the proposed sensing system. The measured results by our biosensing system were in good agreement with values obtained from the local hospital (as seen in Table 3.2), showing the reliability of the biosensor for real time analysis. Moreover, traditional methods are often slower, high cost and for single use which makes them unfavorable for the routine analysis whereas this proposed biosensor has the advantages such as simple measurement procedure, short response time, easy to fabricate and sufficient sensitivity and selectivity. Thus, this enzyme based amperometric biosensor has become an important tool for detection of glucose samples.

Table 3.2 Glucose analyses in the serum samples

Sample	Hospital Data (mM)	Biosensor Response (mM)	Relative Error (%)
1	0.120	0.110	6.2%
2	0.172	0.168	2.3%
3	0.145	0.148	2.1%

### **3.3.Au NPs/MPA/ poly(BEDOA-6)/GOx Biosensor**

#### **3.3.1. Characterization of Modified Gold Nanoparticles**

In order to modify colloidal Au NPs with 3-mercaptopropionic acid (MPA), different MPA concentrations were applied [109-111] and various procedures described in literature were performed [109,112,113]. First of all, for efficient self-assembling of MPA to Au NPs (Au NPs/MPA), MPA concentration in modification process was optimized. UV-vis spectra of corresponding solutions were given in Figure 3.15. As seen the characteristic absorbance of spherical Au NPs appears at 530 nm. Upon modification, a decrease in intensity of this peak and formation of a new absorbance band around 800 nm suggest a change in surface characteristics of NPs and thus successful modification of Au NPs through Au-S bond. Fig. 3.15 also shows the change in the intensity of newly formed absorbance band with the use of different MPA concentrations. This suggests that the optimum MPA concentration for modification is 0.225 M (Figure 3.15).

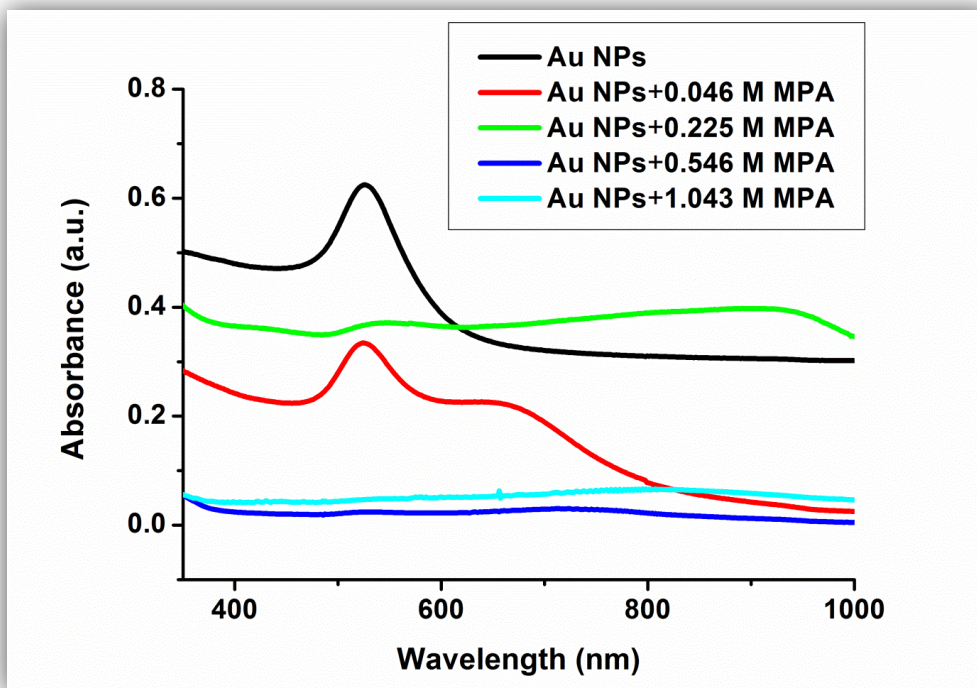


Figure 3.15. UV-vis spectra of Au NPs and Au NPs/MPA solutions prepared in different concentrations of MPA

Afterwards, different modification procedures were applied by keeping the MPA concentration at optimum value (0.225 M). Figure 3.16 demonstrates the UV-vis analysis results of different methods employed for modification. By considering the depletion in the characteristic absorbance of Au NPs and appearance of a new absorption band corresponding Au NPs/MPA in UV-vis spectra, the most adequate preparation method for modification was determined to be 30 s stirring time and overnight storing at 4 °C (Figure 3.16).

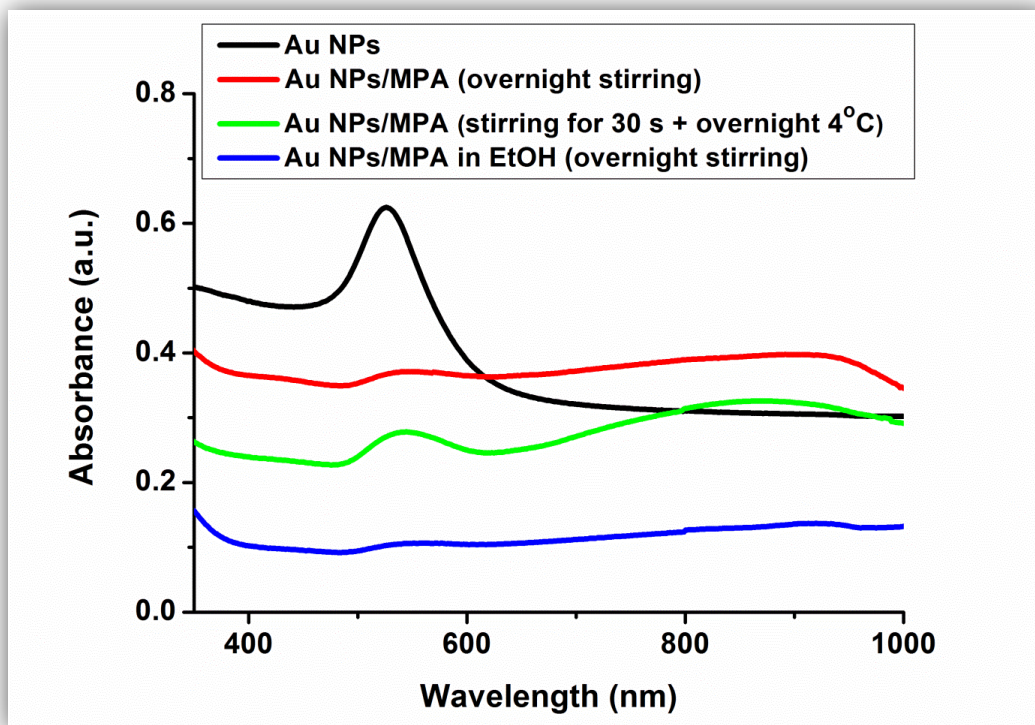


Figure 3.16. UV-vis spectra of Au NPs and Au NPs/MPA solutions prepared by different modification procedures

UV-vis spectra of Au NPs and Au NPs/MPA prepared under optimum conditions were given in Fig. 3.17A. The figure also shows that the surface modification can be tracked by the change in the color of the NP solution (inset of Fig. 3.17A). TEM analysis was performed to investigate any possible change in NP morphology after modification. Fig 3.17B (a) and (b) show that uniformly dispersed spherical Au NPs with ca. 15 nm diameter were synthesized and their morphology were remained after surface modification with MPA.

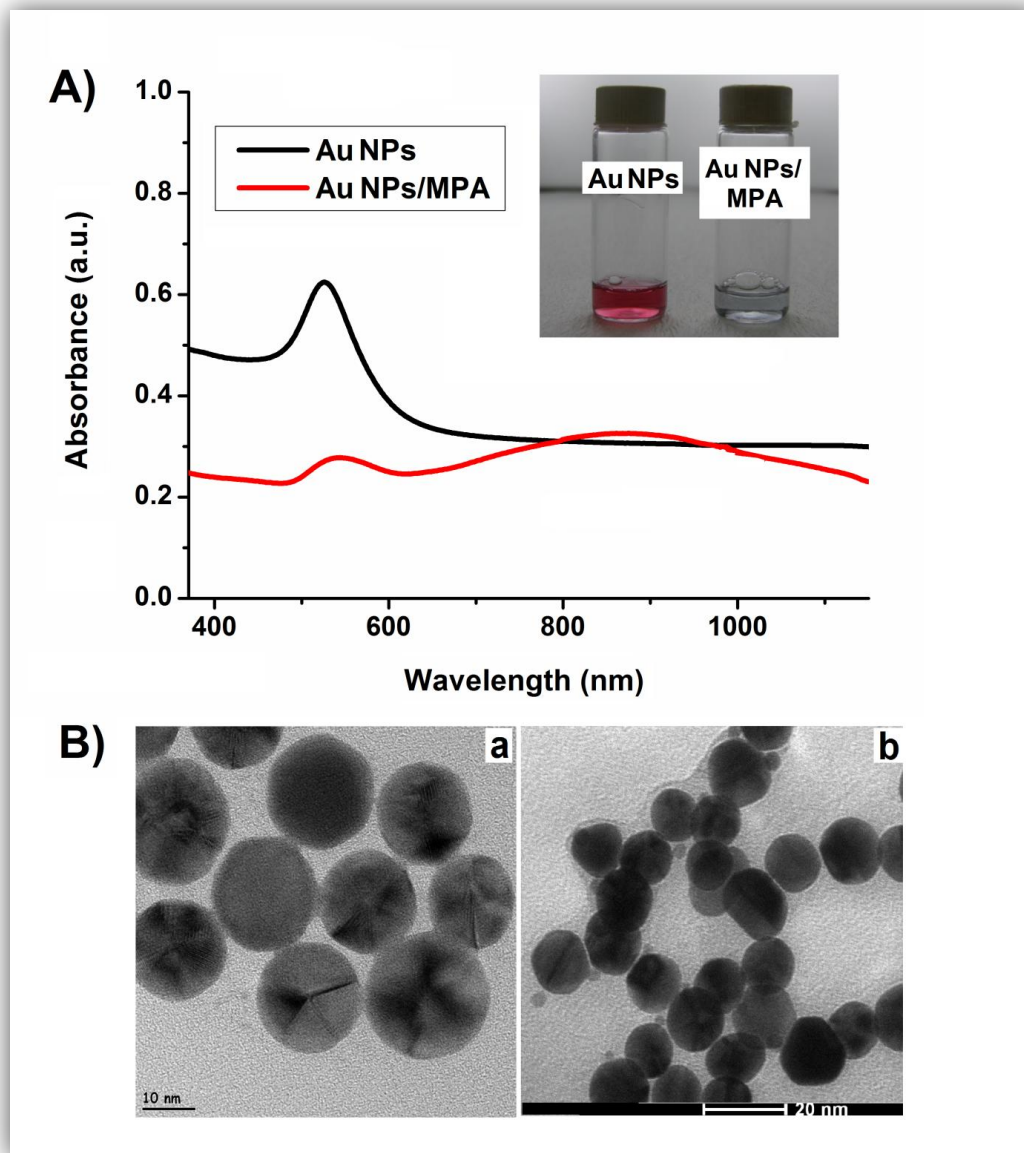


Figure 3.17. A) UV-vis spectra of Au NPs and Au NPs/MPA; B) TEM images of (a) Au NPs and (b) Au NPs/MPA

### 3.3.2. Effect of Au NPs/MPA in Biosensor Fabrication

Figure 3.18 illustrates that the addition of modified Au NPs improved biosensor performance. Since MPA self-assembled Au NPs led to an increase in the surface area of three-dimensional electrodes [93a], the one with Au NPs/MPA gave the highest

response for glucose. Moreover, the effect of conducting polymer (poly(BEDO-6)) on biosensor performance was also investigated. It can be easily seen that presence of conducting polymer on the electrode surface resulted in achieving an excellent glucose biosensor. Hence, this additional interface enhanced the stability of the enzyme molecules on the electrode surface supplying higher enzyme activity. Due to the presence of functional groups on the polymer backbone the polymer, modified Au NPs and enzyme molecules may be linked together revealing a better interface and electronically more active structure. The functional conducting polymer provides a robust and efficient conjugation between enzyme molecules and Au NPs/MPA by incorporating them and behaves as an excellent transducer in the biosensor construction [114]. Therefore, from the amplified signals, it is obvious that Au NPs/MPA lie between the conducting polymer and enzyme molecules on the electrode surface. The presence of these nanostructures brings the wiring effect on electron transfer between active site of the enzymes and polymer coated transducer which accelerates and facilitates the electron transfer and diminishes the diffusion problems [115,116]. Modified architecture of Au NPs/MPA induces the effectiveness of the NPs together with the immobilization stability.

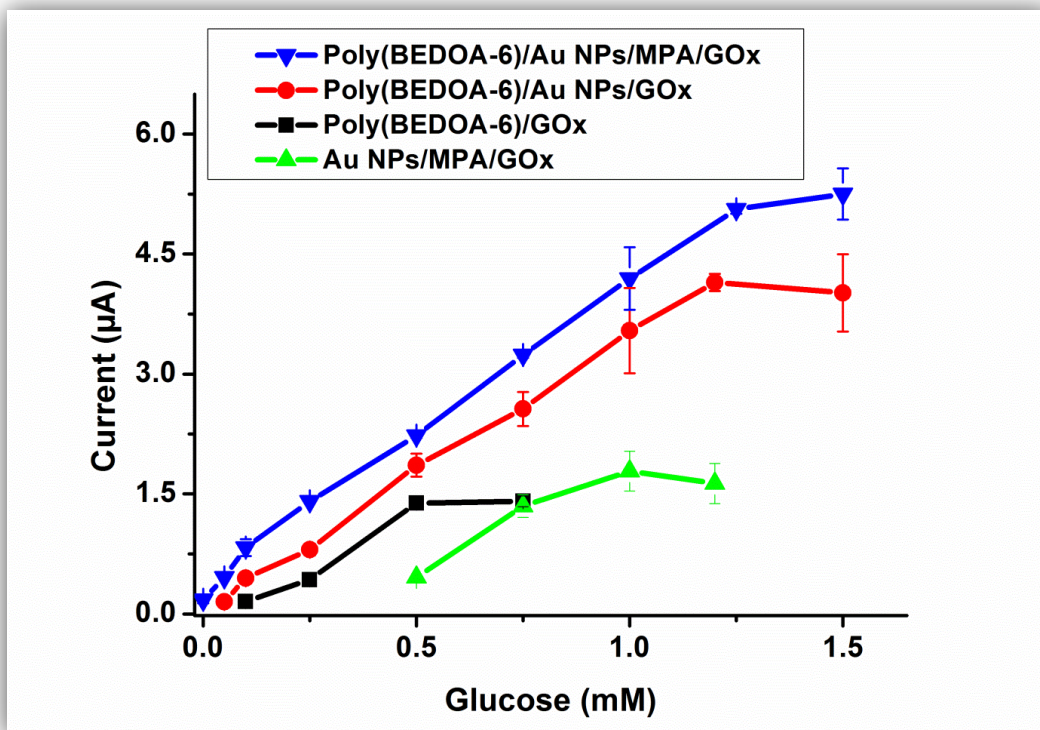


Figure 3.18. The effect of surface modification on performance of glucose biosensors (in 50 mM NaOAc buffer solution, pH 5.5, 25 °C, -0.7 V). Error bars show the standard deviation (SD) of three measurements

### 3.3.3. Optimization Studies

#### 3.3.3.1. Optimization of Conducting polymer thickness

Polymer was coated onto the graphite electrode with 30, 40, 50, 60 scans by keeping all the other parameters constant. Since quality of the polymer layer is crucial in fabrication of the biosensor; stability of conducting polymer directly depends on film thickness. The coated polymer layer should be sufficient enough to stabilize enzyme molecule on the electrode surface. On the other hand, if the layer is too thick electron transfer between the working electrode and enzyme molecules may be hindered causing

a lower charge transfer rate. Also applying enzyme molecules on a more than 50 cycle coated-electrode may result in an alteration of the 3D structure causing a sort of denaturation. As seen in Figure 3.19, 50 cycle deposition was determined as the optimum thickness for the biosensor application which corresponds to 5.70 nm in thickness.

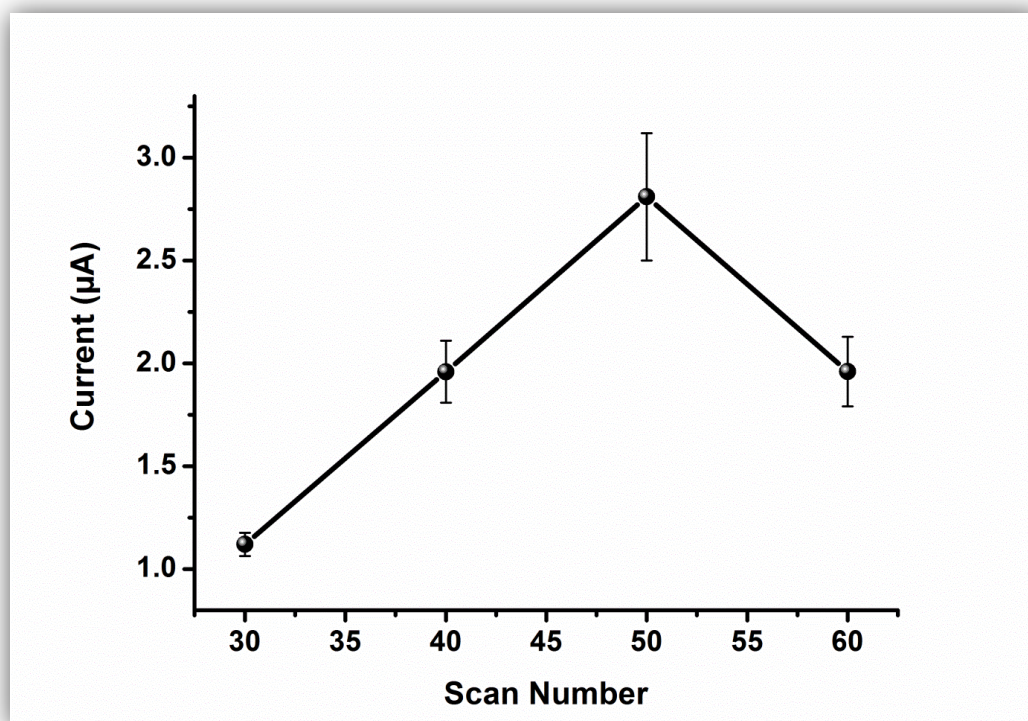


Figure 3.19. The effect of polymer film thickness on biosensor response (in pH 5.5 NaOAc, 50 mM, 25 °C, -0.7 V). Error bars show the standard deviation (SD) of three measurements

### 3.3.3.2. Optimization of enzyme amount

To optimize enzyme amount, three electrodes were prepared with different amount of GOx as 0.5 mg (20 U), 1.5 mg (60 U), 2.5 mg (100 U) (Figure 3.20). The highest signals were obtained with the biosensor having 1.5 mg (60 U) GOx. In lower amounts

of GOx, sufficient responses as regards to sensitivity could not be recorded. Besides, for higher amounts of enzyme, suitable binding between enzyme molecules and polymer was not possible; hence, leaching of enzyme molecules from the electrode surface was observed. Moreover, due to the diffusion problems, the signals decreased and response times extended. Thus, 60 U enzyme was used for further experimental steps as the biorecognition element in biosensor construction.

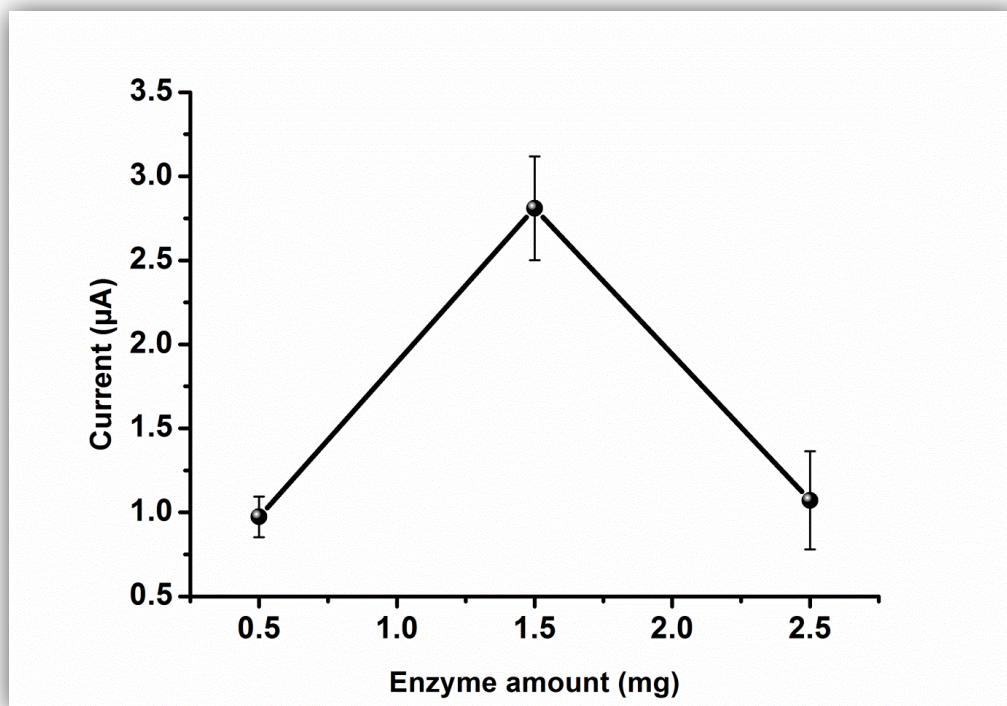


Figure 3.20. The effect of enzyme amount (in 50 mM NaOAc, 25 °C, -0.7 V). Error bars show the standard deviation (SD) of three measurements

The pH dependence of the glucose biosensor responses to 0.5 mM glucose was investigated between pH 4.5 and 7.0 (sodium acetate buffer at pH 4.5; 5.0; 5.5 and sodium phosphate buffer at pH 6.0; 6.5; 7.0, 25 °C.) The best result was achieved at pH 5.5 sodium acetate buffer solution as given in Figure 3.21. pH 5.5 sodium acetate buffer was used as the working buffer solution.

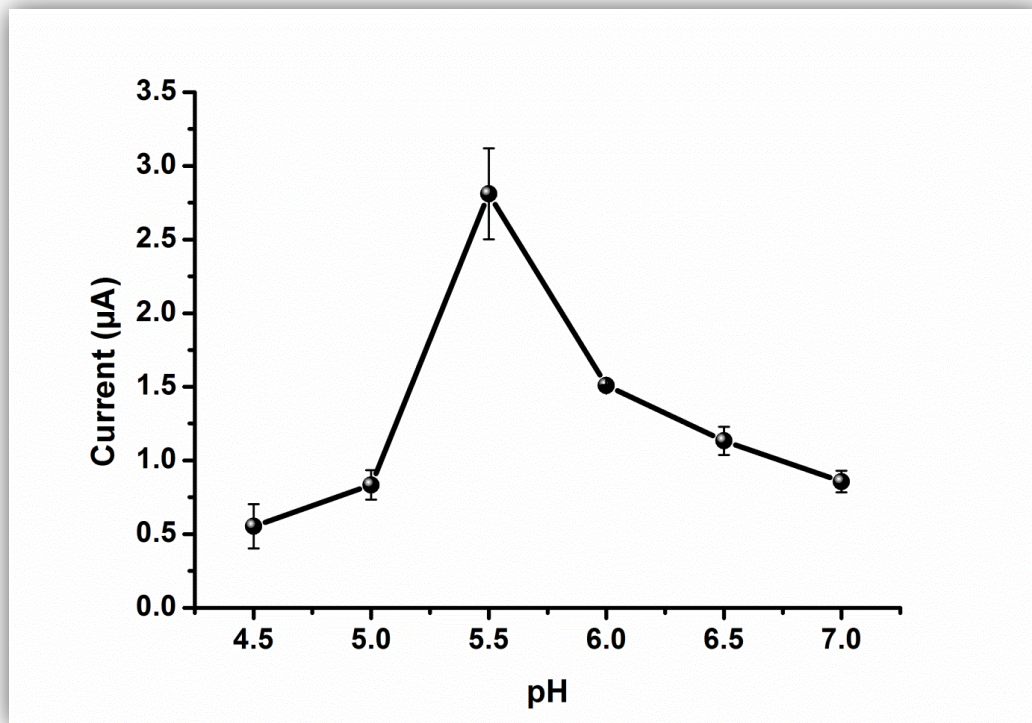


Figure 3.21. The effect of pH (in 50 mM NaOAc, 25 °C, -0.7 V). Error bars show the standard deviation (SD) of three measurements

### 3.3.3.3. Optimization of Au NPs/MPA amount

During the biosensor preparation different amounts of Au NPs/MPA solutions (2.0-6.0 µL) were introduced to surface of the biosensor where 4.0 µL Au NPs/MPA solution was found as the optimum. The decrease in the response for higher amounts of Au NPs/MPA may originate due to the excess covalent attachments between carboxylic acid modified Au NPs/MPA, enzymes and polymer. Both orientation and 3D structure of enzyme molecules may be destroyed. This may bring denaturation. Moreover, due to the excess crosslinking, diffusion problems may arise [117]. In lower amounts, Au NPs/MPA may not show their wiring affects enough which reveals lower signals.

### 3.3.4. Characterizations of the proposed biosensor

#### 3.3.4.1. Fourier Transform Infrared Spectrophotometry (FTIR)

FTIR spectroscopy was used to examine the alternation of functional groups upon modification. The FTIR spectra of poly(BEDOA-6) and poly(BEDOA-6)/Au NPs/MPA were shown in Figure 3.22. Five characteristic bands corresponding to poly(BEDOA-6) were observed. The peaks at  $3435\text{ cm}^{-1}$  and  $3136\text{ cm}^{-1}$  were assigned to the stretching vibration of free primary  $\text{NH}_2$  groups as two spikes. The adsorption bands observed at  $840\text{ cm}^{-1}$ ,  $1440\text{ cm}^{-1}$ ,  $1628\text{ cm}^{-1}$  were due to C-H (aromatic), C-H ( $\text{CH}_2$ ) stretching and N-H bending frequencies, respectively. These results confirmed the presence of functional groups of the polymer. Moreover, FTIR spectrum of poly(BEDOA-6)/Au NPs/MPA in Fig. 3.23 demonstrates the presence of MPA and covalent linkage between MPA and polymer via amide bond. There are two characteristic peaks that differed from the spectrum of poly(BEDOA-6) due to the modification of polymer. While the corresponding primary amine peaks of the polymer disappeared, the  $3435\text{ cm}^{-1}$  peak remains proving the secondary amine ( $-\text{N}-\text{H}$ ) stretching arising from an amide bond. That is generated by covalent binding of free amine groups of the polymer with the carboxylic acid end groups of MPA. Second peak at  $1707\text{ cm}^{-1}$  was attributed to  $\text{C}=\text{O}$  stretching frequency which proved the existence of carbonyl groups caused of MPA and by the formation of an amide linkage. The results demonstrate successful modifications via covalent linkage that would be used in target biosensor construction.

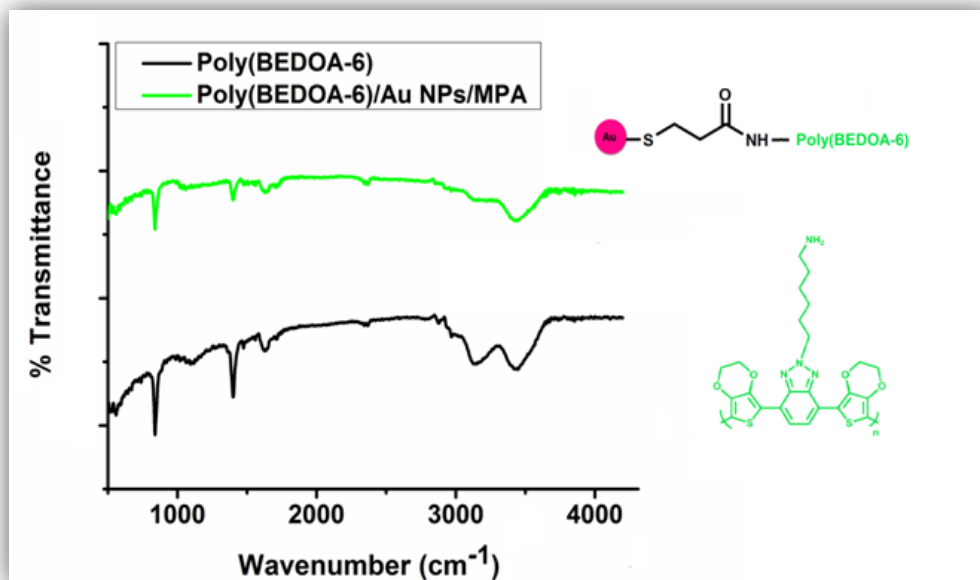


Figure 3.22. FTIR spectra of poly(BEDO-6) and poly(BEDO-6)/Au NPs/MPA

### 3.3.4.2. Scanning electron microscope (SEM)

The scanning electron microscopy (SEM) was used to characterize the surface morphologies of modified electrodes during stepwise modification. Figure 3.23A-D shows SEM images of the conducting polymer coated graphite electrode (poly(BEDO-6)), poly(BEDO-6)/GO<sub>x</sub>, poly(BEDO-6)/Au NPs/MPA and poly(BEDO-6)/Au NPs/MPA/GO<sub>x</sub> modified electrode surfaces, respectively. After each alternation of graphite electrode, the images showed that the change in the morphology can be easily detected. The typical cauliflower-like structure of the conducting polymer can be observed in the first image (Figure 3.23A). After immobilization of GO<sub>x</sub> onto the polymer coated electrode, the morphology looks like a 2D structure (Figure 3.23B). On the other hand, when modified gold nanoparticles (Au NPs/MPA) were immobilized onto polymer coated electrode (Figure 3.23C), MPA acts like spacer arms and they were regularly dispersed around spherical gold nanoparticles nearby the surface. Such surfaces increase the effective surface area for the

immobilization of enzymes. It is easily seen that the gold nanoparticle loading homogeneously covers the entire polymer surface. Functional  $\pi$ -conjugated conductive support stimulates the self-assembly of modified nanoparticles resulting in a three dimensional wiring system and stabilization of nanoparticle assemblies on the polymer surface. When GOx was immobilized onto the poly(BEDOA-6)/Au NPs/MPA modified surface (Figure 3.23D), the immobilization resulted in a bundle-like structure in three dimension. This 3D structure stabilizes the immobilized enzyme; thus, the performance of glucose biosensor increases considerably. The introduction of Au NPs/MPA increases the stability while locking the structures into an ordered orientation. Polymer coating also supports the orientation. Au NPs/MPA act as the electrical wiring of the network via tiny bridges which enhances the electron transfer between redox center of the enzyme molecules and transducer surface [114,118].

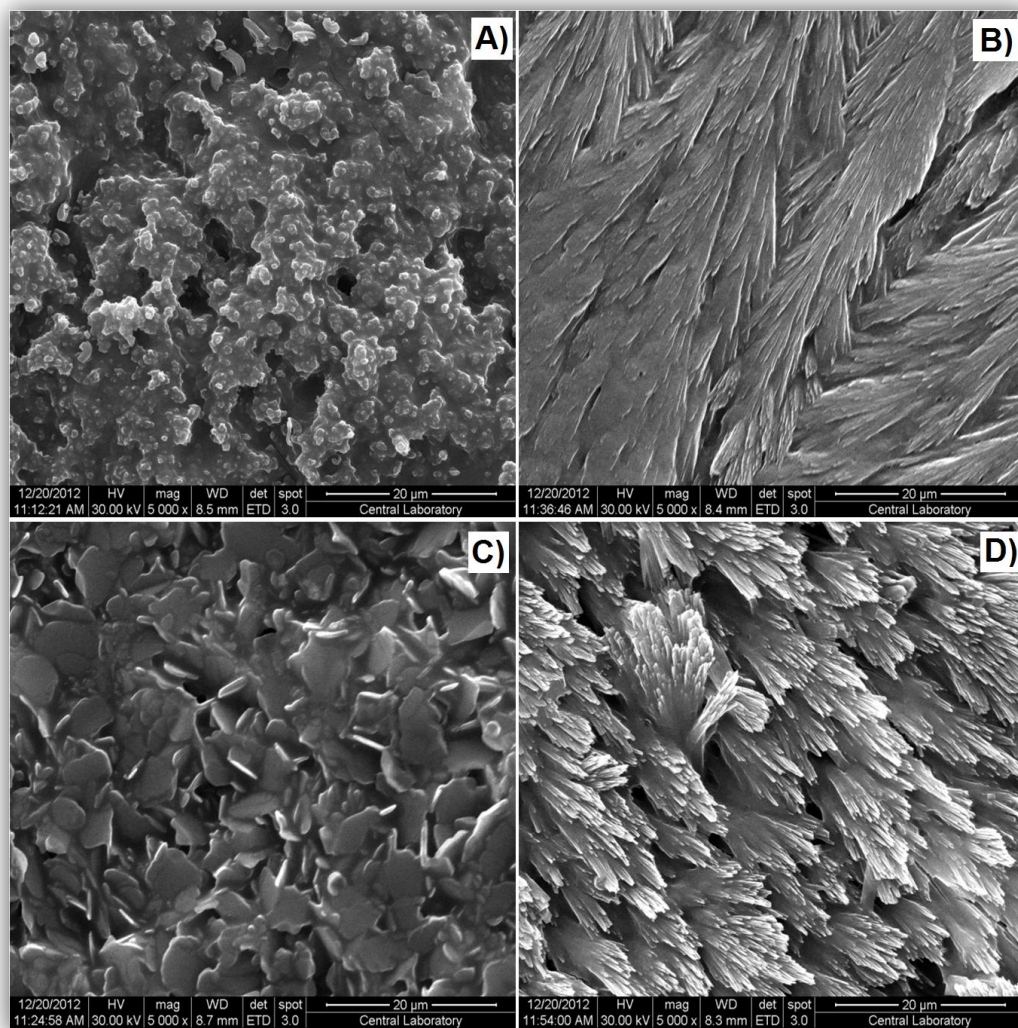


Figure 3.23. SEM images of (A) poly(BEDO-6), (B) poly(BEDO-6)/GO<sub>x</sub>, (C) poly(BEDO-6)/Au NPs/MPA and (D) poly(BEDO-6)/Au NPs/MPA/GO<sub>x</sub> under optimized conditions

### 3.3.4.3. Fluorescence microscopy

To inquire surface characteristics of the modified immobilization matrices, wide field fluorescence microscopy technique was used where the substrate is an indium tin oxide (ITO) glass. The conducting polymer exhibits a characteristic fluorescence property due

to its highly conjugated structure. This property can be used to examine the surface characteristics of stepwise modifications. By the virtue of fluorescent flavin adenine dinucleotide (FAD) redox centers of GOx molecules, the enzyme molecules can be differentiated under fluorescence microscope. As seen in Figure 3.24A, the fluorescent polymer appears as green fluorescent while retaining the cauliflower-like structure as also revealed by SEM images. On the other hand, due to the fluorescent structure of enzyme molecules, the successful immobilization can be followed by the fluorescence image of Au NPs/MPA/GOx modified polymer coated electrode. Moreover, the homogeneous distribution of the enzyme molecules on the electrode surface and their globular structure can also be verified from Figure 3.24B.

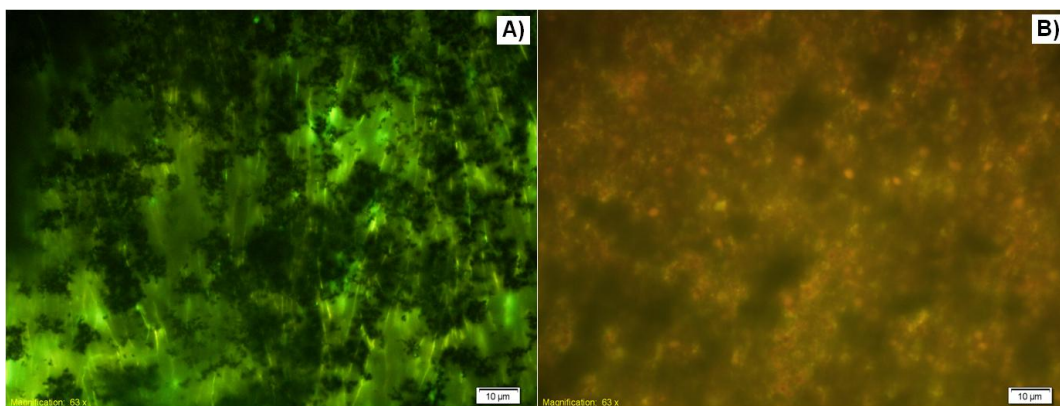


Figure 3.24. Fluorescence images of poly(BEDO A-6) (A) before and (B) after Au NPs/MPA/GOx immobilization under optimized conditions on ITO glass (with 63x magnification)

### 3.3.5. Analytical characterization of Biosensors

A calibration curve for glucose was plotted with respect to substrate concentration as given in Figure 3.25. A perfect linearity was obtained between 0.025 mM and 1.25 mM glucose in 50 mM sodium acetate pH 5.5 buffer solution as given with an equation;  $y=3.900x+0.316$  and  $R^2=0.994$ .

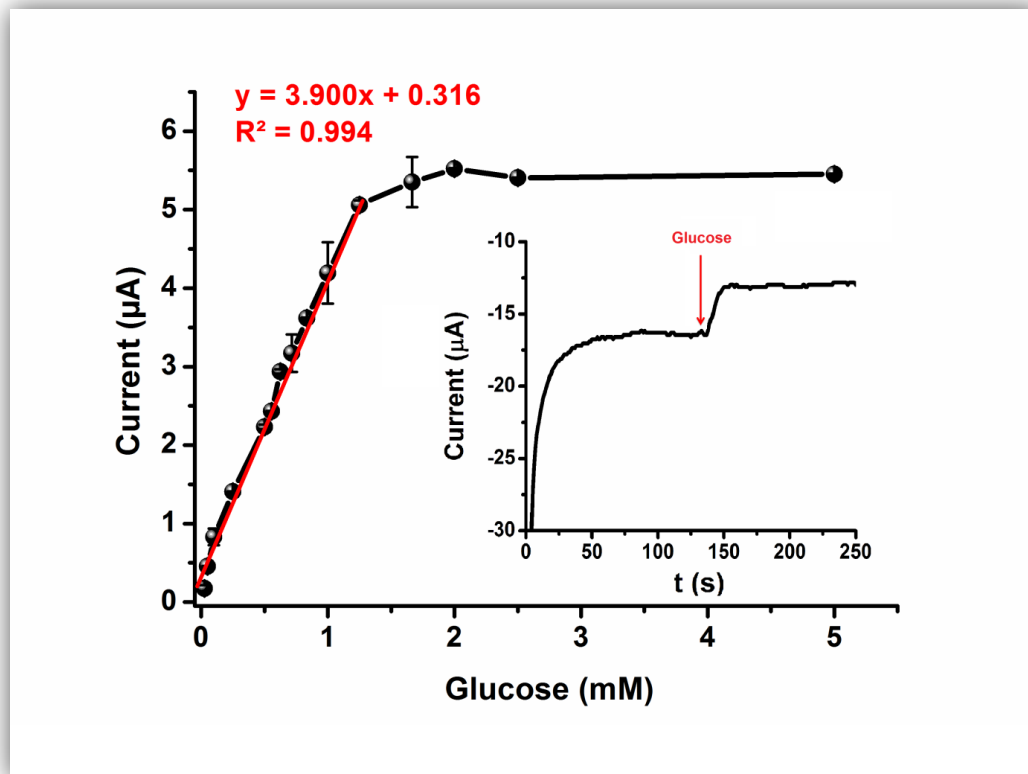


Figure 3.25. Calibration curve for glucose (in 50 mM NaOAc buffer solution, pH 5.5, 25 °C, -0.7 V). Error bars show the standard deviation (SD) of three measurements

Moreover, the biosensor signals corresponding to 0.1 mM glucose solution were measured for ten times in order to prove repeatability of the biosensor response. The standard deviation (SD) and the relative standard deviation (RSD) were calculated as 0.124 and 5.87 % respectively. Limit of detection (LOD) was also calculated as 25  $\mu\text{M}$  according to  $S/N=3$ . Also, a typical amperometric response of the biosensor was given as an inset in Figure 3.25.

Furthermore, kinetic characterizations were carried out using Lineweaver-Burk plot [99]. In amperometric detection technique, current was measured with respect to time; apparent Michealis-Menten constant,  $K_M^{\text{app}}$ , and  $I_{\text{max}}$  were calculated as 0.81 mM and

7.10  $\mu\text{A}$  respectively. A low  $K_M^{\text{app}}$  value was observed. Hence, with the help of the modified polymer matrix, immobilized enzyme molecules exhibit higher affinity toward glucose. With the help of wiring effect of Au NPs/MPA, such a low  $K_M^{\text{app}}$  value and LOD was achieved.

Shelf life of the proposed biosensor was also examined. The optimized biosensor was used in glucose detection everyday and no activity loss was observed for 3 weeks. It was stored at +4 °C when not in use. Covalent linkage between enzyme molecules and immobilization matrix brings considerable shelf life stability. Moreover, it is reported that Au NPs assembling around GOx brings an environment congruent with the native system where the redox proteins can be oriented freely [118,119]. The results also verified this situation with long-term stability and amplified signals.

In addition, interference studies were carried out with the proposed biosensor. Possible interferents like ascorbic acid, cholesterol and urea (between 0.01 and 0.1 M) were used as the substrate. Amperometric measurements were done under optimized working conditions by applying -0.7 V and no current change were detected. Hence this proposed biosensor can be used for sample applications even in the presence of such interferents in the analyte.

### **3.3.6. Sample Application**

To investigate the performance and reliability of the constructed biosensor, it was used to analyze the glucose content in various beverages. Real samples with no dilution were analyzed both with poly(BEDO A-6)/Au NPs/MPA/GOx biosensor and a spectrophotometric technique (Table 3.3). Results prove that there exists no significant difference between the two methods showing the reliability and accuracy of the biosensor.

Table 3.3. Results of glucose analyses in beverages

<b>Glucose (mol/L)</b>		
<b>Sample</b>	<b>Spectrophotometric</b>	<b>Poly(BEDOA-6)/Au NPs/ MPA/ GOx</b>
E <sup>®</sup> Lemonade	0.183	0.189
C <sup>®</sup> Soda	0.076	0.074
T <sup>®</sup> Ice Tea	0.031	0.035
L <sup>®</sup> Ice Tea	0.035	0.041
C <sup>®</sup> Orange Juice	0.107	0.106



## CHAPTER 4

### CONCLUSION

In this thesis, two different biosensors with different matrices were constructed for detection of glucose concentration in a test solution. Glucose oxidase was used as a model enzyme for fabrication of these two biosensing systems. A functional conducting polymer poly(BEDO A-6) was used as an immobilization platform for both sensors. The pendant amino groups on the polymer backbone serve as binding sites to form covalent linkage to enzyme molecule with the help of crosslinking agents. The covalent attachment improved the stability of the biosensors.

Taking the several advantages of usage of nanostructures, the analytical characteristics and long-term efficiency of designed sensing systems were improved. Electrode surfaces were modified with clay nanocomposite and functional gold nanoparticles, respectively. Then, effect of presence of each layer used in construction was investigated and best results were revealed detecting the most effective biosensing designs.

To prove applicability of both biosensing systems, the biosensors were used to analyze glucose content in real human blood samples and various beverages. Both biosensors were in good agreement with corresponding reference methods.

In the first glucose biosensors prepared by poly(BEDO A-6) and PMMA/Clay nanocomposite, the conducting polymer coated graphite electrode was modified with PMMA/laponite nanocomposites in order to improve the interaction of enzyme with the immobilization matrix, enhancing stability of the biosensor. After the effect of

introduction of clay nanocomposite to the sensing design was proved, surface morphology of the biosensor was studied via SEM and XPS techniques. The optimized biosensor showed good kinetic and analytical parameters, summarized as follows:

- ✚ The optimum biosensor was prepared using 30 cycle conducting polymer deposition, 2.50 mg GOx, 1% GA solution, 4 mg/5 mL water nanocomposite dispersion. Amperometric measurements were performed in 50 mM NaOAc buffer solution at pH 5.5.
- ✚  $K_M^{app}$  and  $I_{max}$  were found as 1.31 mM and 12.59  $\mu A$ , respectively.
- ✚ The biosensor showed a wide linear range between 2.8 mM and 1.2 mM to glucose with a low detection limit of 1.99 mM. Selectivity of the designed system was 37.16  $mAM^{-1}cm^{-2}$ .
- ✚ For a period of 6 weeks no activity loss was observed.

*This study was published in Electroanalysis in 2013 [95].*

Second glucose biosensor was constructed with pristine and functional gold nanoparticles. After effective modification technique was achieved, the effect of nanoparticles on biosensor response was investigated. Deposition of conducting polymer was achieved electrochemically and functional gold nanoparticles and enzyme was immobilized onto the coated graphite electrode. Surface morphology of the functional nanoparticles and the biosensor was carried out via TEM, SEM, Fluorescence Microscope techniques. Also, the covalent bond formation between both the polymer and modified particles and the polymer and enzyme was confirmed by FTIR. The results of optimized biosensor were summarized as follows:

- ✚ The biosensor response was maximized using 50 cycle deposition, 1.5 mg GOx, 4.0  $\mu\text{L}$  Au NPs/MPA solution during construction. Amperometric measurements were performed at pH 5.5 NaOAc buffer solution.
- ✚  $K_M^{\text{app}}$  and  $I_{\text{max}}$  were calculated as 0.81 mM and 7.10 mA respectively.
- ✚ The biosensor showed a wide linear range between 0.025 mM and 1.25 mM glucose concentration with a low detection limit of 0.025 mM. Selectivity was found as  $14.97 \text{ mAM}^{-1} \text{ cm}^{-2}$ .
- ✚ No activity loss was observed for 3 weeks.

*This study was published in Polymer in 2013 [120].*



## REFERENCES

- [1] H. Letheby, *J. Chem. Soc.*, 1862, 15, 161.
- [2] G. Natta, G. Mazzanti, P. Corradini, *Atti Accad. Lincei Cl. Sci. Fis. Mat. Nat. Rend.*, 1958, 25, 3.
- [3] (a) A. G. MacDiarmid, *J. Am. Chem. Soc.*, 1976, 98, 388; (b) F. B. Burt, *Journal of Chemical Society*, 1910, 68, 105.
- [4] H. Shirakawa, F. J. Louis, A. G. MacDiarmid, C. K. Chiang, A.J. Heeger, *J. Chem. Soc., Chem. Commun.*, 1977, 578, 578.
- [5] (a) H. Shirakawa, *Angew. Chem. Int. Ed.*, 2001, 40, 2574; (b) A. G. MacDiarmid, *Angew. Chem. Int. Ed.*, 2001, 40, 2581; (c) A.J. Heeger, *Angew. Chem. Int. Ed.*, 2001, 40, 2591; (d) H. Shirakawa, *Synth. Met.*, 2002, 125, 3; (e) A. G. MacDiarmid, *Synth. Met.*, 2002, 125, 11; (f) A. J. Heeger, *Synth. Met.*, 2002, 125, 23.
- [6] A. Heeger, A. G. MacDiarmid, H. Shirakawa, "The Nobel Prize in Chemistry 2000 - Advanced Information". Nobelprize.org. Nobel Media AB 2013. Web. 12 Jan 2014.  
[http://www.nobelprize.org/nobel\\_prizes/chemistry/laureates/2000/advanced.html](http://www.nobelprize.org/nobel_prizes/chemistry/laureates/2000/advanced.html).
- [7] G. Blasse, B.C. Grabmaier, *Luminescent Materials*, 1994, Springer-Verlag.
- [8] M. E. G. Lyons, *Electroactive Polymer Electrochemistry*, 1994, New York, p48.
- [9] A. G. MacDiarmid, A. J. Heeger, *Synth. Met.*, 1979, 1, 101.
- [10] J. A. Rogers, Z. Bao, V. R. Raju, *Appl. Phys. Lett.*, 72 (1998) 2716.
- [11] (a) N. Toshima, O. Ihata, *Synth. Met.*, 1996, 79, 165; (b) Z.C. Sun, Y. H. Geng, J. Li, X. H. Wang, X. B. Jing, F. S. Wang, *J. Appl. Polym. Sci.*, 1999,

- 72, 1077; (c) K.Yoshino, R. Hayashi, R. Sugimoto, *Jpn. J. Appl. Phys.*, 1984, 23, L899.
- [12] A. Malinauskas, *Polymer*, 2001, 42, 3957.
- [13] R. H. Baughman, J. L. Bredas, R.R. Chance, R. L. Elsenbaumer, L. W. Shacklette, *Chem. Rev.*, 1982, 82, 209.
- [14] (a) L. Toppare, *Encyclopedia of Engineering Materials Part A, Polymer Science and Technology*, New York: Marcel Dekker, 1988, Vol. 1, Chapter 8; (b) K. Doblhofer, Rajeshwar in *Handbook of Conducting Polymers*, 2nd Edn., ed.; T.A. SSKotheim, R.L.Elsenbaumer, (c) J.R. Reynolds, Marcel Dekker, New York, 1998, 531.
- [15] R. J. Mortimer, A. L. Dyer, J. R. Reynolds, *Displays*, 2006, 27, 2.
- [16] (a) A. F. Diaz, A. Martinez, K. K. Kanazawa, M. M. Salmon, *J.Electroanal. Chem.*, 1981, 130, 181; (b) J. Roncali, *Chem. Rev.*, 1992, 92, 711.
- [17] (a) S. Kıralp, L. Toppare, Y. Yagcı, *Int. J. Biol. Macromol.*, 2003, 33, 37; (b) Ö. Türkarslan, A.E. Büyükbayram, L. Toppare, *Synth. Met.*, 2010, 160, 808; (c) A. Mulchandani, N.V. Myung, *Curr. Opin. Biotech.*, 2011, 22, 502; (d) V. Mazeiko, A. Kausaite-Minkstimiene, A. Ramanaviciene, Z. Balevicius, A. Ramanavicius, *Sensor Actuat. B-Chem.*, 2013, 189, 187; (e) S. Soylemez, F. Ekiz Kanik, A.G. Nurioglu, H.Akpınar, L. Toppare, *Sensor Actuat. B-Chem.*, 2013, 182, 322.
- [18] (a) E. J. W. List, L. Holzer, S. Tasch, G. Leising, U. Scherf, K. Mullen, M. Catellani, S. Luzzati, *Solid State Commun.*, 1999, 109, 455, (b) H. Kang, G. Kim, I. Hwang, Y. Kim, K. Cheol Lee, S.H. Park, K. Lee, *Sol. Energ. Mat. Sol. C.*, 2012, 107, 148; (c) F. Xu, W.Q. Zhu, L.Yan, H. Xu, L.H. Xiong, J.H. Li, *Org. Electron.*, 2012, 13, 302; (d) P. Zacharias, M. C. Gather, A. Köhnen, N. Rehmman, K. Meerholz, *Angew. Chem. Int. Ed.*, 2009, 48, 4038.
- [19] (a) D. S. H. Charrier, T. Vries, S. G. J. Mathijssen, E. J. Geluk, E. C. P. Smits, M. Kemerink, R. A. J. Janssen, *Org. Electron.*, 2009, 10, 994; (b) P. Jha, S.P. Koiry, Vibha Saxena, P. Veerender, Abhay Gusain, A.K. Chauhan, A.K. Debnath, D.K. Aswal, S.K. Gupta, *Org. Electron.*, 2013, 14, 2635; (c) J. Lee, W.

- Kim, H. Lim, *Microelectron. Eng.*, 2012, 98, 382; (d) F. Garnier, G. Horowitz, X. Peng, D. Fichou, *Adv. Mater.*, 1990, 2, 592.
- [20] (a) U. Bulut, A. Cirpan, *Synth. Met.*, 2005, 148, 68; (b) A. Balan, G. Gunbas, A. Durmus, L. Toppare, *Chem. Mater.*, 2008, 20, 7510; (c) A. Kumar, S. Jang, J. Padilla, T. F. Otero, G. A. Sotzing, *Polymer*, 2008, 49, 3686; (d) H. Li, K. Xie, Y. Pan, H. Wang, H. Wang, *Synth. Met.*, 2012, 162, 22.
- [21] (a) F. Li, W.J. Albery, *J. Electroanal. Chem. Interfacial Electrochem.*, 1991, 302, 279. (b) P. Novak, K. Muller, K. Santhanam, O. Haas, *Chem. Rev.*, 1997, 97, 207; (c) A. Guerfi, J. Trottier, I. Boyano, I. De Meazza, J.A. Blazquez, S. Brewer, K.S. Ryder, A. Vijh, K. Zaghib, *J. Power Sources*, 2014, 248, 1099; (d) K. Gurunathan, D.P. Amalnerkar, D.C. Trivedi, *Mater. Lett.*, 2003, 57, 1642.
- [22] (a) C. J. Brabec, N. S. Sariciftci, J. C. Hummelen., *Adv. Funct. Mater.*, 2001, 11, 15, (b) E. Kaya, A. Balan, D. Baran, A. Cirpan, L. Toppare, *Org. Electron.*, 2011, 12, 202. (c) C.O. Too, G.G. Wallace, A.K. Burrell, G.E. Collis, D.L. Officer, E.W. Boge, S.G. Brodie, E.J. Evans, *Synth. Met.*, 2001, 123, 53; (d) J. Wang, Y. Wang, D. He, Z. Liu, H. Wu, H. Wang, P. Zhou, M. Fu, *Sol. Energ. Mat. Sol. C.*, 2012, 96, 58.
- [23] (a) G. Valdés-Ramírez, J. R. Windmiller, J.C. Claussen, A.G. Martinez, F.Kuralay, M. Zhou, N. Zhou, R. Polsky, P.R. Miller, R. Narayan, J. Wang, *Sensor Actuat. B-Chem.*, 2012, 161, 1018; (b) M. Sharma, G.I.N. Waterhouse, S.W.C. Loader, S. Garg, D. Svirskis, *Int. J. Pharm.*, 2013, 443, 163.
- [24] (a) A. Katchalsky, H. Eisenberg, *Nature* 1950, 166, 267; (b) R. Kiefer, S.Y. Chu, P.A. Kilmartin, G.A. Bowmaker, R.P. Cooney, J. Travas-Sejdic, *Electrochim. Acta*, 2007, 52, 2386; (c) Y. A. Ismail, J. G. Martínez, A. S. Al Harrasi, S.J. Kim, Toribio F. Otero, *Sensor Actuat. B-Chem.*, 2011, 160, 1180.
- [25] D. Thevenot, K. Toth, R.A. Durst, G.S. Wilson, *Biosens. Bioelectron.*, 2001, 16, 121.
- [26] M.Gerard, A. Chaubey, B.D. Malhotra, *Biosens. Bioelectron.* 2002, 17, 345.
- [27] I. Karube, K. Nakanishi, *IEEE Eng. Med. Biol.*, 1994, 13, 364.

- [28] T. Ahuja, I.A. Mir, D. Kumar, Rajesh, *Biomaterials*, 2007, 28, 791.
- [29] S. K. Sharma, N. Sehgal, A.Kumar, *Curr. Appl. Phys.*, 2003, 3, 307.
- [30] J. Svorc, S. Miertu, J. Katrlík, M. Stredanský, *Anal. Chem.*, 1997, 69, 2086.
- [31] A. Chaubey, B.D. Malhotra, *Biosens. Bioelectron.* 2002, 17, 441.
- [32] S. Cosnier, *Biosens. Bioelectron.*, 1999, 14, 443.
- [33] A. J. Lawrence, G.R. Moores, *Eur. J. Biochem.*, 1972, 24, 538.
- [34] M. Pohanka, P. Skládal, *J. Appl. Biomed.*, 2008, 6, 57.
- [35] P. Yang, L. Wang, Q. Wu, Z. Chen, X. Lin, *Sensor Actuat B-Chem.*, 2014, 194, 71.
- [36] L. Clark, C. Lyons, *Ann. N.Y. (1962). Acad. Sci.* 102. 29.
- [37] S. F. Petcu, D. Emerson, R. M. Worden, *Biosens. Bioelectron.*, 1996, 11, 1059.
- [38] L. Gorton, A. Lindgren, T. Larsson, F.D. Munteanu, T. Ruzgas, I. Gazaryan, *Anal. Chim. Acta*, 1999, 400, 91.
- [39] (a) R. Devi, B. Batra, S. Lata, S. Yadav, C.S. Pundir, *Process Biochem.*, 2013, 48, 242; (b) C. He, J. Liu, Q. Zhang, C. Wu, *Sensor Actuat. B-Chem.*, 2012, 166-167, 802; (c) D. Odaci, A. Telefoncu, S.Timur, *Sensor Actuat. B-Chem.*, 2008, 132, 159.
- [40] S.Tuncagil, S.K. Kayahan, G. Bayramoglu, M.Y. Arica, L. Toppare, *J.Mol. Catal. B-Enzym.*, 2009, 58, 187-193.
- [41] S. Cosnier, *Anal. Bioanal. Chem.*, 2003, 377, 507.
- [42] Bickerstaff, *Immobilization of Enzymes and Cells*, 1997, New Jersey: Humana Press.
- [43] Rajesh, V. Bisht, W. Takashima, K. Kaneto, *Biomaterials*, 2005, 26, 3683.
- [44] J.M. Dicks, M.F. Cardosi, A.P.F. Turner, *Electroanalysis*, 1993, 5, 1.
- [45] P. Bernfeld, J. Wan., *Science*, 1963, 142, 678.
- [46] O.R. Zaborsky, *Immobilized Enzymes*, 1973, CRC Press, Cleveland.

- [47] Ö. Yılmaz, D.Odacı Demirkol, S. Gülcemal, A. Kılınç, S. Timur, B. Çetinkaya, *Colloid Surface B.*, 2012, 100, 62.
- [48] E. Başkurt, F. Ekiz, D. Odacı Demirkol, S. Timur, L. Toppare, *Colloid Surface B.*, 2012, 97, 13.
- [49] S. Singh, D.V.S. Jain, M.L. Singla, *Sensor Actuat. B-Chem.*, 2013, 182, 161.
- [50] C.Situ, A.R.G. Wylie, A. Douglas, C.T. Elliott, *Talanta*, 2008, 76, 832.
- [51] S. Cosnier, M. Holzinger., *Chem. Soc. Rev.*, 2011, 40, 2146.
- [52] S. Borgmann, G. Hartwich, A. Schulte, W. Schuhmann, *Perspectives in Bioanalysis*, 2005.
- [53] W.H. Scouten, J.H.T. Luong, R.S. Brown, *Trends in Biotechnology*, 1995, 13, 178.
- [54] N.C. Kekec, F. Ekiz Kanik, Y. Arslan Udum, C. Gundogdu Hizliates, Y. Ergun, L.Toppare, *Sensor Actuat. B-Chem.*, 2014, 193, 306.
- [55] S. Demirci, F.B. Emre, F. Ekiz, F. Oğuzkaya, S. Timur, C. Tanyeli, L. Toppare, *Analyst*, 2012, 137, 4254.
- [56] H. Wang, H. Ohnuki, H. Endo, M. Izumi, *Sensor Actuat. B-Chem.*, 2012, 168, 249.
- [57] F. Li, Wei Chen, Shusheng Zhang, *Biosens. Bioelectron.*, 2008, 24, 781.
- [58] M. Aizawa, S. Yabuki. In: *Proceedings of the 51st annual meeting Japan chemical society*. 1985, p. 6.
- [59] J.C. Vidal, E.G. Ruiz, J.R. Castillo, *Microchim. Acta*, 2003, 143, 93.
- [60] R.E. Gyurcsanyi, Z. Vagföldi, G. Nagy, *Electroanalysis*, 1999, 11, 712.
- [61] S. Wild, G. Roglic, A. Green, R. Sicree, H. King, *Diabetes Care*, 2004, 27, 1047.
- [62] (a) H.B. Yildiz, S. Kiralp, L. Toppare, Y.Yağci, *Int. J. Biol. Macromol.*, 2005, 37, 174; (b) O. Lioubashevski, V.I. Chegel, F. Patolsky, E. Katz, I. Willner, *J. Am. Chem. Soc.* 2004, 126, 7133; (c) A. Guerrieri, G.E. De Benedetto, F. Palmisanot, P.G. Zambonint, *Biosens. Bioelectron.*, 1998, 13, 103.

- [63] D.G. Hatzinikolaou, B.J. Macris, *Enzyme Microb. Technol.*, 1995, 17, 530.
- [64] (a) T. F. Otero, J. G. Martinez, J. Arias-Pardilla, *Electrochim. Acta* 2012, 84,112. (b) V. Serafin, L. Agui, P. Yanez-Sedeno, J. M. Pingarron, *J. Electroanal. Chem.* 2011, 656, 152, (c) Parham, H., Rahbar, N., 2010. *J. Hazard. Mater.* 177, 1077–1084.
- [65] S. Tuncagil, D. Odaci, E. Yildiz, S. Timur, L. Toppare, *Sensors Actuat. B-Chem*, 2009, 137, 42.
- [66] W. Schuhmann, *Microchim. Acta*, 1995, 21, 1.
- [67] S. Cosnier, *Appl. Biochem. Biotech.*, 2000, 89, 127.
- [68] K.V. Santhanam, *Pure Appl. Chem.*, 1998, 70, 1259.
- [69] Y. Xian, Y. Hu, F. Liu, Y. Xian, H. Wang, L. Jin, *Biosens. Bioelectron*, 2006, 21, 1996.
- [70] B.D. Malhotra, A. Chaubey, S.P.Singh, *Anal. Chim. Acta*, 2006, 578, 59.
- [71] J.M. Pingarron, P. Yanez-Sedeno, A. Gonzalez-Cortes, *Electrochim. Acta*, 2008, 53, 5848.
- [72] H. Li, W.Hong, F. Cai, Q. Tang, Y.Yan, X. Hu, B. Zhao, D.Zhang, Z.Xu, *J. Mater. Chem.*, 2012, 22, 24734.
- [73] K. Kamps, R. Leek, L. Luebke, R. Price, M. Nelson, S. Simonet, D. J. Eggert, T. Aygan Atesin, E. M. Bratsolias Brown, *Integr. Biol.*, 2013, 5, 133.
- [74] J. Yuan, A.H.E. Müller, *Polymer*, 2010, 51, 4015.
- [75] Y. Yoon, H. Sohn, J. Lee, *Polymer*, 2009, 50, 1395.
- [76] J. Kim, C. Hwang, S. Jo, W. Jung, *Appl. Phys. Lett.*, 2011, 99, 233304.
- [77] J. Choi, K. Park, H. Lee, Y. Kim, J. Lee, Y. Sung, *Electrochim. Acta*, 2003, 48, 2781.
- [78] V. Armel, O. Winther-Jensen, R. Kerr, D.R. MacFarlane, B. Winther-Jensen, *J. Mater. Chem.*, 2012, 22, 19767.
- [79] P. K. Ghosh, J. A. Bard, *J. Am. Chem. Soc.*, 1983, 105, 5691.

- [80] J. V. De Melo, S. Cosnier, C. Mousty, C. Martelet, N. Jaffrezic- Renault, *Anal. Chem.* 2002, 74, 4037.
- [81] W. Schuhmann, *Rev. Mol. Biotechnol.* 2002, 82, 425.
- [82] C. Mousty, *Anal. Bioanal. Chem.*, 2010, 396, 315.
- [83] C. Mousty, *Appl. Clay Sci.*, 2004, 27, 159.
- [84] Y. Mansoori, S.V. Atghia, M.R. Zamanloo, Gh. Imanzadeh, M. Sirousazar, *Eur. Polym. J.*, 2010, 46, 1844.
- [85] Y. Liu, H. Y. Liu, N. F. Hu, *Biophys. Chem.*, 2005, 117, 27.
- [86] E. Han, D. Shan, H. Xue, S. Cosnier, *Biomacromolecules*, 2007, 8, 971.
- [87] C. Mousty, *Appl. Clay Sci.*, 2004, 27, 159.
- [88] S. Cosnier, C. Gondran, A. Senillou, M. Gratzel, N. Vlachopoulos, *Electroanalysis*, 1997, 9, 1387.
- [89] J. Zhang, X. Xu, X. Yang, *Analyst*, 2012, 137, 3437.
- [90] (a) C. C. D. Wang, W. C. H. Choy, C. Duan, D. D. S. Fung, W. E. I. Sha, F. X. Xie, F. Huang and Y. Cao, *J. Mater. Chem.*, 2012, 22, 1206; (b) Y. Leroux, E. Eang, C. Fave, G. Trippe and J. C. Lacroix, *Electrochem. Commun.*, 2007, 9, 1258.
- [91] (a) S. Guo, E. Wang, *Anal. Chim. Acta*, 2007, 598, 181; (b) R. Ladj, A. Bitar, M. Eissa, Y. Mugnier, R. Le Dantec, H. Fessia, A. Elaissaria, *J. Mater. Chem. B*, 2013, 1, 1381.
- [92] (a) P. Yanez-Sedeno, J.M. Pingarron, *Anal. Bioanal. Chem.* 382, 2005, 884; (b) S. Liu, D. Leech, H. Ju, *Anal. Lett.*, 36, 2003, 1.
- [93] (a) S. Zhang, N. Wang, Y. Niu, C. Sun. *Sens. Actuators B-Chem.*, 2005, 109, 367, (b) M. Adamovski, A. Zaja, P. Gründler, G. Flechsig, *Electrochem. Commun.*, 2006, 8, 932; (c) X. Zhong, R. Yuan, Y. Chai, Y. Liu, J. Dai, D. Tang, *Sens. Actuators B-Chem.*, 2005, 104, 191.
- [94] Y. Zhang, W. Jiang, *Electrochim. Acta*, 2012, 71, 239.
- [95] M. Kesik, O. Kocer, F. Ekiz Kanik, N. Akbasoglu Unlu, E. Rende, E. Aslan-Gurel, R. M. Rossi, Y. Arslan Udum, L. Toppare, *Electroanalysis*, 2013, 25, 1995.

- [96] L. Gorton, *Electroanalysis*, 1995, 7, 23.
- [97] S. Tuncagil, D. Odaci, S. Varis, S. Timur, L. Toppare, *Bioelectrochemistry*, 2009, 76, 169.
- [98] H. J. Brights, M. Appleby, *J. Biol. Chem.*, 1969, 244, 3625.
- [99] L. Lineweaver, D. Burk, *J. Am. Chem. Soc.*, 1934, 56 658.
- [100] (a) D. Barham and P. Trinder, *Analyst*, 1972, 97, 142; (b) A. Teuscher, P. Richterich, *Schweiz. Med. Wschr.*, 1971, 101, 345.
- [101] S. Geetha, C. R. K. Rao, M. D. Vijayan, C. Trivedi, *Anal. Chim. Acta*, 2006, 568,119.
- [102] F. Ekiz, M. Yuksel, A. Balan, S. Timur, L. Toppare, *Macromol. Biosci.*, 2010, 10, 1557.
- [103] Q. Fan, D. Shan, H. Xue, Y. He, S. Cosnier, *Biosens. Bioelectron.*, 2007, 22, 816.
- [104] D. Wan, S. Yuan, G. L. Li, K. G. Neoh, E. T. Kang, *ACS Appl. Mater. Interf.*, 2010, 2, 3083.
- [105] E. Turan, T. Caykara, *React. Funct. Polym.*, 2011, 71, 1089.
- [106] C. Chen, Y. Jiang, J. Kan, *Biosens. Bioelectron.*, 2006, 22, 639.
- [107] R. Nathawat, A. Kumar, N. K. Acharya, Y. K. Vijay, *Surf. Coat. Tech.*, 2009, 203, 2600.
- [108] S. Hubert, M. C. Pham, L. H. Dao, B. Piro, Q. A. Nguyen, M. Hedayatullah, *Synth. Met.*, 2002, 128, 67.
- [109] J. Gao, X. Huang, H. Liu, F. Zan, J. Ren, *Langmuir*, 2012, 28, 4464.
- [110] R. Güzel, Z. Üstündag, H. Eksi, S. Keskin, B. Taner, Z.G. Durgun, A. A. I. Turan and A. O. Solak , *J Colloid Interface Sci.*, 2010, 351, 35.
- [111] Z. Tan, J. Liu, *Anal. Chem.*, 2010, 82, 4222.
- [112] T. Luczak, *Electrochim. Acta*, 2009, 54, 586.
- [113] Y.Q. Dang, H.W. Li, B. Wang, L. Li, Y. Wu, *ACS Appl. Mater. Interfaces*. 2009,1, 1533.
- [114] N. German, A. Ramanavicius, J. Voronovic, A. Ramanaviciene, *Colloid Surf. A*, 2012, 413, 224.

- [115] N. German, J. Voronovi, A. Ramanavicius, A. Ramanaviciene, *Procedia Eng.*, 2012,47,482.
- [116] D.R. Paul, L.M. Robeson, *Polymer*, 2008, 49, 3187.
- [117] D. Odaci, M.U. Kahveci, E.L. Sahkulubey, C. Ozdemir, T. Uyar, S. Timur, Y. Yagci, *Bioelectrochemistry*, 2010, 79, 211.
- [118] Y. Xiao, F. Patolsky, E. Katz, J.F. Hainfeld, I. Willner, *Science*, 2003, 299,1877.
- [119] A. Ramanaviciene, G. Nastajute, V. Snitka, A. Kausaite, N. German, D. Barauskas-Memenas, A. Ramanavicius, *Sensor Actuat. B-Chem.*, 137,2009, 483.
- [120] M. Kesik, F. Ekiz Kanik, G. Hızalan, D. Kozanoglu, E. Nalbant Esenturk, S. Timur, L. Toppare, *Polymer*, 54, 2013, 4463.